THE JOURNAL
OF
CHEMICAL PHYSICS

VOLUME 6 MARCH, 1938 NUMBER 3

Fourier Analysis of Liquid Methyl Alcohol*

G. G. HARVEY
George Eastman Laboratory of Physics, Massachusetts Institute of Technology, Cambridge, Massachusetts†

(Received December 20, 1937)

X-ray diffraction curves for liquid methyl alcohol have been obtained at 25°C and −75°C with monochromatic Mo $K\alpha$ radiation out to $(\sin\theta)/\lambda = 1.2$. At −75°C there is much greater detail in the diffraction curve than is observable at the higher temperature. Five diffraction rings are visible on the film. Fourier analyses of these intensity curves lead to radial atom distribution functions which are interpreted in terms of Zachariasen's picture of the molecular arrangement in liquid methyl alcohol. The results are distinctly favorable to Zachariasen's picture.

INTRODUCTION

ZACHARIASEN has recently[1] given an interesting picture of the molecular configuration in liquid methyl alcohol. In support of this picture he uses the x-ray diffraction data of Stewart and Morrow[2] and subjects them to a Fourier analysis. The results obtained, although not too unsatisfactory, leave much to be desired in the way of direct interpretation. There are several reasons for this. First, Stewart and Morrow in their study of the normal alcohols were mainly interested in the position of the principal diffraction peak and the scattering at small angles, and hence did not measure the scattering out to very large angles; further, they did not use strictly monochromatic radiation. Again, the effects of intermolecular interference rapidly decrease in importance except at small angles of scattering as the temperature of the liquid is raised. Although Dželepow[3] has recently measured the scattering from several liquids, including methyl alcohol, with monochromatic radiation, a quantitative interpretation of his results is complicated by his method of measurement and he, too, did not measure the scattering to sufficiently large angles. In the present investigation these defects have been as far as possible remedied.

EXPERIMENTAL

The source of radiation used (Mo $K\alpha$) was a demountable tube with line-focus filament, a simplified modification of the tube described by Dershem.[4] The tube was very compact, occupying a space of only two by two by ten inches and could be run at an input of 1500 watts continuously. The Mo $K\alpha$ lines were reflected from a rocksalt crystal mounted on the camera and

* A preliminary account of some of the results here reported was given at the Washington Meeting of the American Physical Society in April, 1937. See Phys. Rev. **51**, 998 (1937).

† Now at the College of the City of New York.

[1] W. H. Zachariasen, J. Chem. Phys. **3**, 158 (1935).

[2] G. W. Stewart and R. M. Morrow, Phys. Rev. **30**, 232 (1927).

[3] B.S. Dželepow, Physik. Zeits. Sowjetunion **11**, 157 (1937).

[4] E. Dershem, Rev. Sci. Inst. **7**, 86 (1936).

placed close to the tube window. The radiation was quite intense and even after passing through the collimating system of the camera the reflected beam could be seen on a fluorescent screen with the room lights on. A free stream of alcohol was used as a sample, the method being essentially the same as that of Katzoff[5] except that a small "Fountainnette" pump was used to circulate the alcohol. In order to prevent air scattering a stream of hydrogen or helium was passed through the camera continuously throughout the exposures. Fifteen to twenty hour exposures were found to be sufficient if the crystal had been recently polished.

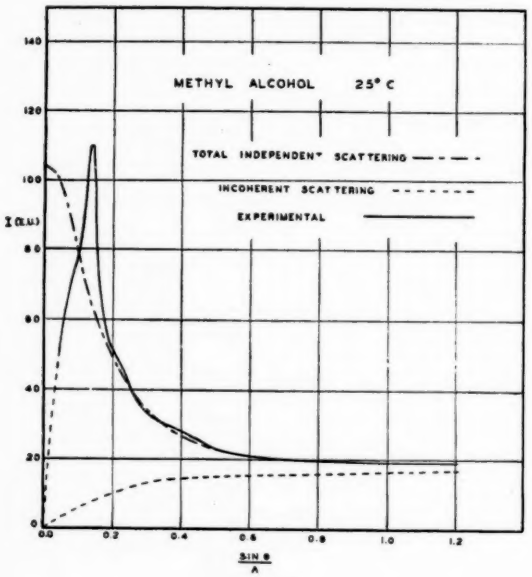

FIG. 1a.

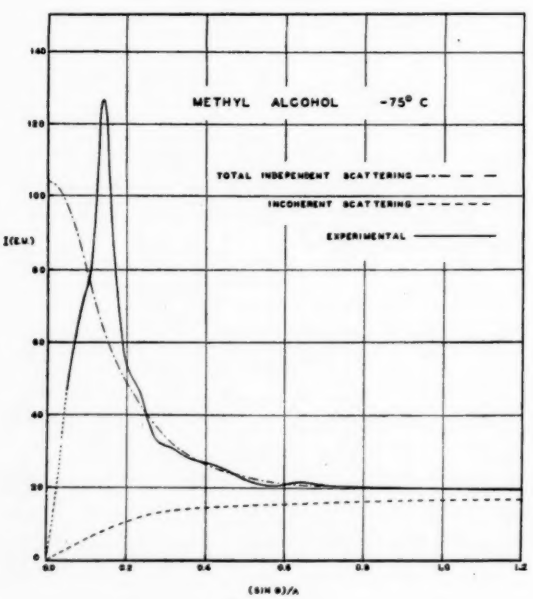

FIG. 1b.

The stream of alcohol flowed from a nozzle accurately centered on the camera (radius 5.43 cm). The radius of the stream was about 0.17 cm and the rate of flow was adjusted so that no turbulence occurred. The stream when observed through a microscope appeared to be a smooth stationary cylinder. The alcohol used was about 99 percent CH_3OH, the remainder being mostly water. A series of pictures was taken at room temperature (25°C). The films were microphotometered and converted to intensities in the usual way. When corrected for polarization and reduced to electron units they give the intensity per molecule as a function of $(\sin\theta)/\lambda$. The absorption factor varied by less than one percent throughout the entire angular range and so was assumed constant. Fig. 1*a* shows the intensity curve so obtained. It will be seen that beyond $(\sin\theta)/\lambda=0.5$ the observed scattering is practically indistinguishable from the independent scattering curve. The observed scattering curve was then subjected to a Fourier analysis. Carbon and oxygen are sufficiently different in scattering power to make it worthwhile to use the theory applied to substances consisting of more than one kind of atom. The method is given in a paper by Warren, Krutter and Morningstar.[6] What one obtains from such an analysis is a weighted distribution of the atoms surrounding any atom in the scattering substance, the weighting factor being practically the effective number of scattering electrons in each atom. The result is

$$\sum 4\pi r^2 K_m \rho_m(r) = 4\pi r^2 \rho_0 \sum Z_m + \frac{2r}{\pi}\int_0^\infty s\, i(s) \sin ks\, ds, \quad (1)$$

where

$\sum$ indicates summation over a molecule
$\rho_m(r)$ = density of atoms of type m about a given atom
ρ_0 = mean electron density of scattering matter
Z_m = atomic number of atom of type m
$K_m = (f_m/f_e)$ average

[5] S. Katzoff, J. Chem. Phys. **2**, 841 (1934).

[6] B. E. Warren, H. M. Krutter and O. Morningstar, J. Am. Ceramic Soc. **19**, 202 (1936).

f_m = scattering factor of atom of type m
$f_e = (\sum f_m)/(\sum Z_m)$ = average f per electron
$s = (4\pi \sin\theta)/\lambda$; 2θ = angle of scattering
$i(s) = (I_e - \sum f_m^2)/f_e^2$
I_e = coherent scattering per molecule in electron units.

The integral in Eq. (1) is evaluated by a harmonic analyzer from a graph of the function $s\,i(s)$. The resulting weighted atom distribution curve is shown in Fig. 2*a*. The first peak corresponds to the intramolecular distance C−O and does not interest us here. The outstanding feature of Zachariasen's picture of liquid methyl alcohol is the existence of hydroxyl bonding between neighboring molecules. This would mean a more or less definite distance of about 2.7A between adjacent oxygen atoms. It is true that the curve in Fig. 2*a* does not drop to zero between 2A and 3A but there is no definite peak. Further, a dip, but not to zero, is typical of all liquid distribution curves.[7] It would be much more convincing evidence of the essential reality of Zachariasen's model if a definite peak could be found at the approximate oxygen-oxygen distance for hydroxyl bonding. As Zachariasen has pointed out,[1] the strength of such bonds should depend on the temperature. At high temperatures the thermal energy of the molecules is sufficient to break up or prevent the formation of bonds. Obviously, a temperature should be considered as "high" if it is near the boiling point of the liquid and as "low" if far removed from that point. Methyl alcohol boils at about 65°C and freezes at about −98°C. Hence 25°C should be considered as a rather high temperature. The availability of a constant and convenient low temperature of about −80°C in the form of solid CO_2 immediately suggests itself. Accordingly the camera and circulating system were thermally insulated so as to permit the circulation of the alcohol at dry ice temperature. A mixture of dry ice and alcohol completely surrounded a reservoir of methyl alcohol just at the point where it flowed into the camera. Since the rate of flow was small it was not difficult to keep the flowing stream at practically dry ice temperature, roughly −75°C. A second series of pictures was taken at this temperature. Five diffraction rings were visible on the films

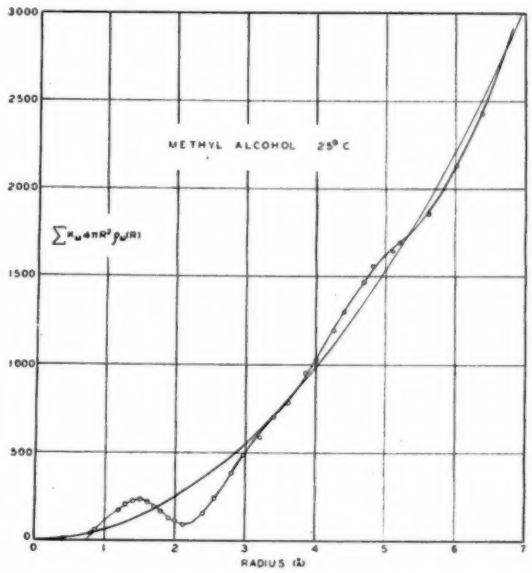

FIG. 2*a*.

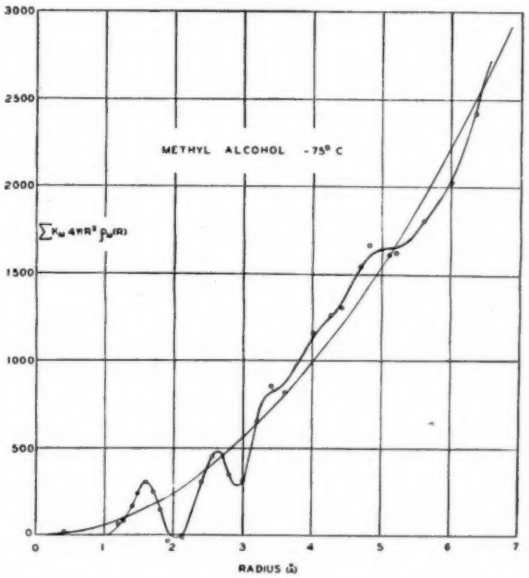

FIG. 2*b*.

whereas at 25°C it was difficult to distinguish a third one. The resulting intensity curve is shown in Fig. 1*b*. Upon analysis this lead to the distribution curve shown in Fig. 2*b*. The well-defined peak at about 2.7A gives immediate and convincing evidence for the existence of hydroxyl bonds.

The area under a peak measures the number of pairs of atoms a given distance apart, each weighted by its effective number of electrons.

[7] E.g., L. P. Tarasov and B. E. Warren, J. Chem. Phys. 4, 236 (1936).

In a molecule such as CH_3OH it is difficult to know how many electrons to assign to the carbon and how many to the oxygen and so one cannot say with certainty just what the area under a peak should be. There are eighteen electrons to be assigned to the molecule; this gives a definite (undoubtedly too large) upper limit to the area under the peak corresponding to C−O of $2\times9^2=162$. The observed area is about 130. If we assign approximately 9 scattering electrons to the oxygen atom then from the measured area under the peak at 2.7A we may calculate the number of oxygen neighbors at this distance: Area$=n\times9^2$. It is hard to know just how much to include in the area under this peak but in any case it is of the order of 200 units. Thus $n\approx2$ in agreement with Zachariasen's picture. The positions of the other peaks are practically the same as Zachariasen obtained from Stewart and Morrow's data and accordingly agree completely with his interpretation. It is felt that the peak in the distribution curve at 2.7A together with its disappearance at high temperatures gives very strong evidence for the truth of Zachariasen's picture of the molecular arrangement in liquid methyl alcohol.

It was planned to carry out a similar analysis on a whole series of the normal alcohols and some work has been completed on ethyl alcohol. Due to unavoidable delay and also to the fact that diffraction patterns from the higher alcohols are not nearly so straightforward of interpretation it is thought worthwhile to record the present results. The author is indebted to Professor B. E. Warren for his encouragement and interest throughout the work.

MARCH, 1938 JOURNAL OF CHEMICAL PHYSICS VOLUME 6

The Isotope Effect in the Vibration Spectrum of CCl_4

C. K. Wu and G. B. B. M. Sutherland
Laboratory of Physical Chemistry, Cambridge, England
(Received October 19, 1937)

The fine structure in certain of the Raman lines of CCl_4 observed by Langseth and interpreted by him as being due to a lack of symmetry in the four carbon valencies has been shown to be accountable for as a purely isotopic effect. Rosenthal's general theory of the isotope effect in molecules of this type has been applied to the case of CCl_4 in an attempt to differentiate between two types of potential function which have been proposed for this molecule. The fine structure patterns predicted on the different theories have been worked out. Unfortunately the existing experimental data are not sufficiently good to allow a decision to be made as to which is the better function.

IN 1931 A. Langseth[1] reported that the Raman lines of carbon tetrachloride possessed a fine structure which he concluded was due to the different varieties of the compound arising from the presence of the two chlorine isotopes. Thus the five isotopic compounds $CCl^{35}{}_4$, $CCl^{35}{}_3Cl^{37}$, $CCl^{35}{}_2Cl^{37}{}_2$, $CCl^{35}Cl^{37}{}_3$, $CCl^{37}{}_4$ should be present in the following relative percentages 31.6, 42.2, 21.1, 4.7 and 0.4. The proportion of $CCl^{35}Cl^{37}{}_3$ and $CCl^{37}{}_4$ being so small it may be taken that the Raman lines from those varieties of tetrachloride will be too weak to be observed; the remaining three varieties should each have their own Raman spectrum differing slightly from one another and so giving rise to an apparent fine structure. The theory of the effect was worked out on very elementary lines by Langseth who found that although he could explain the fine structure in one of the Raman frequencies he could not account for the observed structure in the case of the two other frequencies in which it was observed. It occurred to us that the theory of this effect can be treated much more accurately now since the general equations have been developed by Rosenthal.[2] However in order to make numerical predictions it is necessary to

[1] Langseth, Zeits. f. Physik **72**, 350 (1931).

[2] Rosenthal, Phys. Rev. **45**, 538 and **46**, 730 (1934).

TABLE I.

CX_4	CX_3X'	CX_2X_2'	LANGSETH	
			PREDICTED	OBSERVED
$\nu_1(1)$	$\nu_1'(1)$	$\nu_1''(1)$	$\nu_1-\nu_1'=\nu_1'-\nu_1''=3.15$ cm^{-1}	$\nu_1-\nu_1'=3.10$ cm^{-1} $\nu_1'-\nu_1''=3.20$ cm^{-1}
$\nu_2(2)$	$\nu_2'(2)$	$\nu_{2a}''(1)$ $\nu_{2b}''(1)$	$\nu_2-\nu_2'=1.49$ cm^{-1}	Doublet with spacing $=2.2\pm.2$ cm^{-1}
$\nu_3(3)$	$\nu_{3ab}'(2)$ $\nu_{3c}'(1)$	$\nu_{3a}''(1)$ $\nu_{3b}''(1)$ $\nu_{3c}''(1)$	—	Unresolved
$\nu_4(3)$	$\nu_{4ab}'(2)$ $\nu_{4c}'(1)$	$\nu_{4a}''(1)$ $\nu_{4b}''(1)$ $\nu_{4c}''(1)$	$\nu_4-\nu_4'=2.16$ cm^{-1}	Doublet with spacing $=2.93\pm.2$ cm^{-1}

know the potential constants of CCl_4. Several different sets of those have been proposed by various authors. What we have done then is to compute the isotopic fine structure of the Raman spectrum of CCl_4 using two of the most generally accepted models of this molecule to see whether the predicted isotope effect agrees better with the observations in the one case than in the other. This method of using the isotope effect to discriminate between different force fields is likely to be of great importance in the near future more especially now that methods of concentrating heavy nitrogen have been developed.

The CX_4 molecule in which the X atoms are situated at the corners of a regular tetrahedron possesses nine fundamental modes of vibration. These are not all distinct, falling into groups of 3, 3, 2 and 1 and are conventionally denoted by ν_4, ν_3, ν_2, and ν_1. Suppose now we have the isotopic molecule $CX'X_3$ the nine fundamentals then group themselves into three single frequencies ν_1', ν_{3c}' and ν_{4c}' and three double frequencies ν_2', ν_{3ab}' and ν_{4ab}'. In the case of the isotopic molecule $CX_2'X_2$ all the nine frequencies are distinct. The correspondence between the three cases is illustrated in Table I where the notation of Rosenthal has been used for convenience in reference. From this table it is clear that the effect of the Cl isotopes on the various frequencies will be qualitatively very different. In the case of ν_1 we should expect simply three lines one due to each isotopic variety; in the case of ν_2 there should be four lines while in the case of ν_3 and ν_4 we should expect a sextet. The actual fine structure observed by Langseth is indicated in Table I together with his predicted effect on a very simplified model. For ν_1 Langseth observed the triplet and the separations between the constituents were in good agreement with his calculated value. For ν_2 he observed not a quartet but a doublet having a separation of 2.2 ± 0.2 cm^{-1}; this he interpreted as due to the frequencies ν_2 and ν_2', leaving the nonappearance of ν_{2a}'' and ν_{2b}'' unexplained. The value he calculated for this doublet separation was 1.49 cm^{-1}. In the case of ν_3 he was unable to resolve the fine structure so it was not considered further while for ν_4 he again obtained a doublet having a separation of 2.9 ± 0.2 cm^{-1}. This he interpreted as due to ν_4 and the group ν_{4ab}', ν_{4c}', the separation between which he calculated should be 2.16 cm^{-1}. The fact that the observed separations did not agree with the calculated ones together with the apparent nonappearance of the frequencies due to $CCl^{35}{}_2Cl^{37}{}_2$ led Langseth to conclude that this structure was not due to the isotope effect at all but was due to a lack of tetrahedral symmetry in the molecule of carbon tetrachloride. This result has been quoted and accepted in much of the subsequent literature.[3] Our purpose here is to show that the separations obtained by Langseth are consistent with those due to an isotope effect although exact agreement with calculated values cannot be expected since the dispersion used by Langseth was not suf-

[3] Rousset, Comptes rendus **202**, 654 (1936). Schaefer and Kern, Zeits. f. Physik **78**, 605 (1932).

ficient to reveal all of the fine structure caused by the isotope effect.

The general equations for the isotope effect in a tetrahedral molecule of the type YX_4 have been given by Rosenthal[2] and need not be re-discussed here. In order to apply them to a specific example it is necessary to know the five potential constants of the molecule. Since CCl_4 has only four distinct frequencies it is not possible to determine the five constants without making some additional assumption regarding the nature of the field in the molecule. Several attempts have been made to do this but we shall only concern ourselves with two of them now for reasons which will appear later. The first is that of Voge and Rosenthal[4] who extended the method of independent groups suggested by Sutherland and Dennison[5] and by using the known five constants for methane were able to deduce first the constants of $ClCH_3$ and then those of CCl_4. The assumptions involved are essentially that the CH_3 group is unaltered in going from CH_4 to $ClCH_3$ and secondly that the C−Cl force constant is the same in $ClCH_3$ and in CCl_4. The former assumption is almost certainly correct,[6] the latter is more open to criticism. The second field is that of Urey and Bradley;[7] this assumes

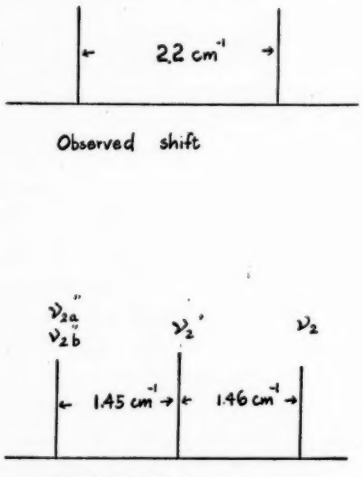

FIG. 1. ν_2 frequency of CCl_4 at 217 cm^{-1}.

[4] Voge and Rosenthal, J. Chem. Phys. **4**, 137 (1936).
[5] Sutherland and Dennison, Proc. Roy. Soc. **A148**, 250 (1935).
[6] Sutherland, Trans. Faraday Soc., February (1938).
[7] Urey and Bradley, Phys. Rev. **38**, 1969 (1931). For convenience we have here used the slightly modified form of this field employed by Rosenthal. See reference 2.

TABLE II.

	Observed	Rosenthal and Voge	Urey and Bradley	
			1	2
$\nu_1-\nu_1'$	3.10	3.2	3.1	3.1
$\nu_1'-\nu_1''$	3.28	3.2	3.1	3.1

that the potential energy is due to central forces plus forces perpendicular to the bond lines and has been found very satisfactory in correlating the four frequencies of molecules of this type although no independent check of its correctness has yet been discovered. The connection of Urey and Bradley's assumptions with the more general treatment has been very fully discussed by Rosenthal.[2] We shall deal with the frequencies individually to avoid unnecessary repetition.

THE FREQUENCY ν_1 AT 458 CM^{-1}

The comparison between the observed triplet separations and the predicted ones is made in Table II. It is clear that either force field gives very good agreement with observation. Actually the slight difference is due solely to the fact that Rosenthal and Voge used "corrected frequencies" which are higher than those observed in an effort to approximate to the values of the frequencies in the gaseous state. It should be explained that the two different fields of Urey and Bradley are due to the two different values of ν_3 which exist. There are actually two different fields on the Voge and Rosenthal theory too but for a different reason since there the two values of ν_3 have simply been averaged. The cause of these two fields is an inherent ambiguity in the determination of the potential constants. It happens however that for ν_1 those two fields give identical isotopic shifts. The figures in Table II are given in the usual frequency units *viz.* cm^{-1}; the exact frequencies of the lines have not been given since these are not important.

THE FREQUENCY ν_2 AT 217 CM^{-1}

The results of the calculations on this frequency are illustrated in Fig. 1 where they are also compared with the observed doublet. First it will be noticed that in each case ν_{2a}'' and ν_{2b}'' are not separated giving a triplet instead of a

quartet. Theoretically there is a separation but it is too small to be shown on the diagram and we shall therefore regard them as coincident. Next it will be observed that the separation of the extreme lines of the triplet is identically 2.9 cm^{-1}, in each case as compared with the observed doublet separation of 2.2 ± 0.2 cm^{-1}. At first this might seem further evidence in favor of Langseth's contention that the doubling is not due to an isotope effect but one must remember that we know nothing of the intensities of ν_{2a}'' and ν_2' relative to ν_2. It may well be that under the resolution of Langseth's instrument two weaker lines due to ν_2'' and ν_2' combine to give the appearance of one line at about 2.2 cm^{-1} from ν_2. A repetition of the observations with higher resolving power is required to make this certain.

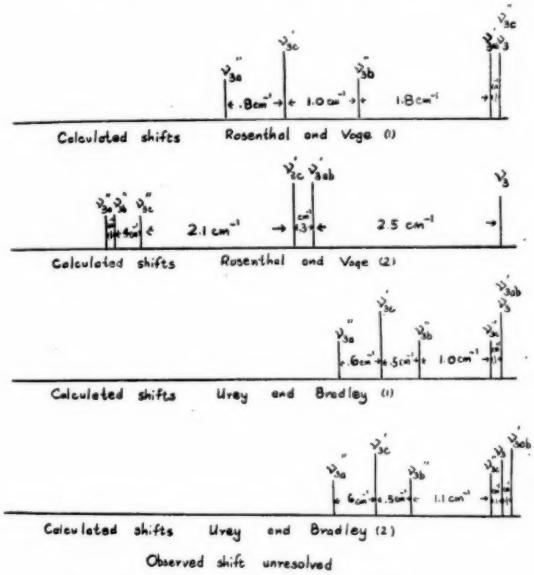

FIG. 2. ν_3 frequency of CCl_4 at 775 cm^{-1}.

THE FREQUENCY ν_3 AT 775 cm^{-1}

In this case the issue is complicated by the fact that the frequency is double, one line being at 762 cm^{-1}, the other at 790 cm^{-1}. This is now known to be due to a resonance between the frequency ν_3 and the combination frequency $\nu_1+\nu_4$. A full treatment of this effect would be very tedious and is not necessary for calculations of the isotope effect for which one may either average the two values as Voge and Rosenthal have done or choose each value in turn as has been done for Urey and Bradley's method. Strictly, this will not give the exact pattern but it is sufficient for our purpose to show that the separations are such that it is understandable that they were not resolved by Langseth. The calculated separations are shown in Fig. 2.

In Figs. 2 and 3 the lines due to the different isotopic species have been shown with heights proportional to the relative abundance of that species. This does not imply that the intensity is proportional to the height shown. When one considers that the intensities of all of those lines may vary relative to one another within wide limits it is understandable except on Voge and Rosenthal (2) that Langseth obtained only broad diffuse lines with the resolving power he employed.

THE FREQUENCY ν_4 AT 311 cm^{-1}

The patterns calculated on the different theories are shown in Fig. 3 on which the observed doublet is plotted on the same scale. It is again difficult to say what this pattern would aggregate into under dispersion too low to resolve it completely but it is fairly likely that the most intense lines would be those due to ν_4 and ν_{4c}'.

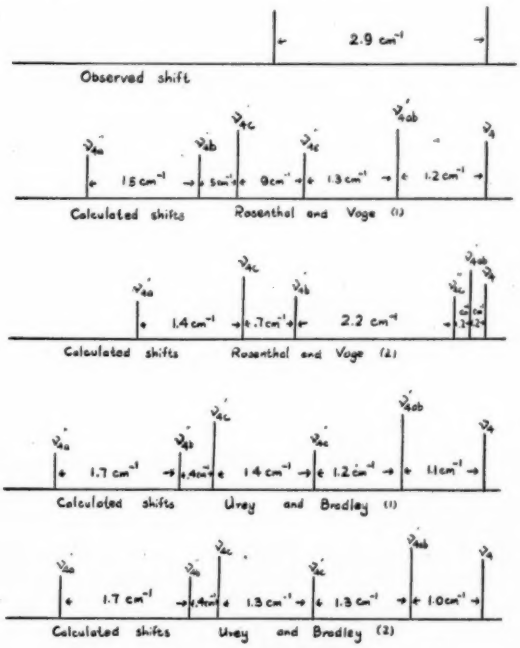

FIG. 3. ν_4 frequency of CCl_4 at 311 cm^{-1}.

The calculated separations between that pair are 3.4 cm^{-1}, 3.3 cm^{-1} (Rosenthal and Voge 1 and 2), 3.7 cm^{-1} and 3.6 cm^{-1} (Urey and Bradley 1 and 2) as compared with the observed doublet separation of 2.9 ± 0.2 cm^{-1}. One must remember that the presence of the other frequencies must modify to some extent the apparent position of ν_4 and ν_{4c}' and so the observation of a doublet is at least compatible with an isotope effect and we may even go so far as to say that the magnitude of the observed separation would here seem to indicate that the potential function of Voge and Rosenthal seems slightly better than that of Urey and Bradley in predicting the order of this effect. The latter conclusion should be accepted with considerable reserve however, as the following discussion will show.

Discussion

Considering the results as a whole, the first conclusion we may draw is that the fine structure observed by Langseth in the Raman lines of CCl_4 can certainly be attributed a purely isotopic origin and there is no need to make any assumption of a lack of symmetry in the molecule from the conventional regular tetrahedral model. Although it has been possible to account for the exact structure observed in only one of the four frequencies the failure in the other cases is almost certainly due to the fact that the fine structure has not been completely resolved. In the case of the frequency (ν_3) where no fine structure at all was observed the theory indicates that the spread of the separate components is probably less in this frequency than in the others. It has not been possible (as had been hoped originally) to use the isotope effect to discriminate between different potential functions which have been proposed for the molecule as the existing data are not yet accurate enough. We would emphasize here that the isotopic shifts in ν_1 and ν_2 are practically independent of the potential function used and it is only from ν_3 and ν_4 that large differences can be expected on the different theories. From the fact that no fine structure was observed for ν_3 it would seem that the field designated as "Rosenthal and Voge (2)" may be ruled out since it predicts three rather widely separated groups of lines. This is interesting in as much as it seems physically less admissible than "Rosenthal and Voge (1)." The considerably closer grouping of all of the components in the Urey and Bradley fields would indicate a slight superiority of this function over the "Rosenthal and Voge (1)" in this frequency. On the other hand for ν_4, as we have remarked, the opposite would appear to be the case. It is clear that a resolving power at least capable of separating frequencies 0.4 cm^{-1} apart will be needed to enable one to decide between the different functions.

One must remember that the intensities of the different isotopic frequencies will not be simply in the ratio of their abundance. When a degenerate frequency is split up by the isotope effect the separate components may possess very different intensities. The work of McWood and Urey[8] on the Raman spectra of the deuteromethanes illustrates this point very well. In the case of chlorine isotopes it is not to be expected that there will be such large differences as in the case of the hydrogen isotopes but there certainly will be differences about which we can as yet say very little. It does seem reasonable to suppose however that the semi-empirical rules which have been found to hold good for molecules of a similar type will again hold good here. For instance in molecules of the ZYX_3 type (e.g. methyl halides) it is generally found that in the Raman spectrum the three single frequencies are more intense than the three doubly degenerate ones. This is why we think it likely that ν_{4c}' may be more intense than ν_{4ab}' in the structure of this frequency. On the other hand this rule does not seem to be completely obeyed in the molecules CH_3D and CD_3H,[8] and so we must not apply it until more data are available by which to judge. It is to be hoped that the isotopic fine structure of the CCl_4 Raman lines will be reinvestigated more minutely in the light of the above calculations in the not too distant future.

[8] McWood and Urey, J. Chem. Phys. **4**, 402 (1936).

The Photolysis of Acetone in Presence of Hydrogen

HUGH S. TAYLOR[1] AND CHARLES ROSENBLUM[2]
Laboratoire de la Chaire Francqui, Université de Louvain, Belgium
(Received December 31, 1937)

The photodecomposition of acetone in presence and absence of hydrogen with light of wave-length >2500A has been studied at temperatures from 70 to 300°C. Up to 160°C acetone alone yields negligible amounts of methane and ethane is the hydrocarbon predominantly produced. The proportion of methane increases rapidly with temperature, the activation energy of its formation in acetone being 8.6 kcal. In presence of hydrogen methane formation is negligible at 70°C, is marked at 160°C and increases rapidly with temperature with an activation energy of this increase equal to 6.4 kcal. At 300°C it represents 75 percent of the ethane-methane product, which shows that photodissociation to methyl radicals is the major, if not exclusive primary process. Analysis of the data indicates that ethane formation is either a wall reaction with zero activation energy or a bimolecular association process of small activation energy. A decrease in ethane formation with increase of temperature is ascribed to a decrease in the stationary state concentration of methyl radicals. An activation energy of the reaction $CH_3+H_2=CH_4+H$ equal to 11 ± 2 kcal. has been deduced. A mechanism to account for quantum yields less than unity in the low temperature range, consistent with primary dissociation into radicals, has been suggested.

RECENT investigations of the photolysis of acetone vapor by ultraviolet light have revealed the decomposition of the molecule into radical fragments and the reorganization of these to yield the observed reaction products. Free methyl radicals are the intermediates postulated in the production of ethane.[3] Spence and Wild[4] have shown that below 60°C the free radical, acetyl, must have a definite lifetime since diacetyl is found in isolable amounts among the reaction products below, but not above, this temperature. We have employed the photolysis of acetone, in the range 70–300°C, as a source of free methyl radicals with which to study the kinetics of the reaction with hydrogen, $CH_3+H_2=CH_4+H$. We have compared the yields of ethane and methane at these temperatures from the photolysis of acetone in presence and absence of hydrogen.

EXPERIMENTAL PROCEDURE

Acetone at approximately 35 mm pressure alone or admixed with hydrogen at 175 mm pressure measured at room temperature could be introduced from reservoirs of the carefully purified materials into a cylindrical quartz vessel, 20 cm long and 2.8 cm in diameter, mounted vertically. This vessel, the volume of which, with dead space, amounted to 131.4 cc, could be enclosed in an aluminum block electric furnace with an even temperature distribution, illumination entering through a quartz tube placed snugly in a cut-away section of the furnace the length of the reaction vessel. Ultraviolet light from a hot mercury arc of the Heraeus type, operated vertically (arc length = 12 cm) at 85 volts and 3.9 amp. hand controlled to constant wattage, entered the reaction vessel through a cylindrical quartz vessel containing a continuously renewed stream of 25 percent acetic acid solution by volume to reduce the intensity of the short wave ultraviolet light. The interposition of two quartz tubes between light source and reaction vessel resulted in a separation of these two latter by about 10 cm.

The reaction vessel was suitably connected to an oil pump-mercury vapor pump high vacuum line, to the reservoirs of reactants, to a mercury manometer and to a gas analysis unit for the analysis of gaseous reaction products, with Töpler pumps for transfer of gases from the reaction zone and to constituent units of the analytical system.

Analytical procedure

The reaction products were separated into two fractions by fractional condensation in liquid air. The noncondensible fraction contained the hydrogen, carbon monoxide and methane. This also comprised all gases removed from the condensible fraction by repeated pumping at liquid-air tem-

[1] Francqui Professor, University of Louvain, 1937.
[2] C.R.B. Fellow, University of Louvain, 1935–1937.
[3] Norrish, Crone and Saltmarsh, J. Chem. Soc. 1456 (1934).
[4] Spence and Wild, J. Chem. Soc. 352 (1937).

peratures. The residual condensate contained undecomposed acetone, any condensible polymeric products and the C_2 hydrocarbons.

An aliquot portion of the measured volume of the noncondensible fraction was introduced into a copper oxide chamber maintained at 310°C, an adjoining U-tube being kept immersed in liquid air. Circulation was maintained by raising and lowering the mercury reservoirs in the Töpler pump system. On completion of the combustion the residual methane was pumped into a Ramsay measuring burette and its volume determined. The liquid air around the U-tube was then replaced by acetone-carbon dioxide mixture. The carbon dioxide in the products of combustion thus vaporized were then transferred to the measuring burette and determined. Special tests on the water vapor obtained in the acetone experiments showed that only negligible amounts of carbon dioxide and methane were not recovered by the procedure used. In the experiments in presence of hydrogen, the final amount of hydrogen and the amount consumed were obtained by difference.

In the condensed fraction, the C_2 gases were obtained by pumping the condensate cooled in an acetone-carbon dioxide mixture. Here also the last fractions of the gas were recovered after vaporisation and condensation. The analysis of this fraction involved a catalytic hydrogenation of unsaturated hydrocarbons on an active copper catalyst. The results obtained by this test indicated negligibly small quantities of unsaturated hydrocarbon, within the error of the determination which was rather high, due to the use of an extremely active copper catalyst,[5] which also possessed a high adsorptive capacity for hydrogen. For this analytical work the less active copper catalyst, used by Morikawa,[6] from copper oxide granules, is to be preferred.

TABLE I. *Photolysis of acetone with and without hydrogen.*

	Moles Reactant $\times 10^4$		Moles Products $\times 10^4$					
			"Me_2CO"					
t°C	Me_2CO	H_2	By Diff.	Meas.	CH_4	CO	H_2	C−C
71	2.52	—	0.81	0.72	0.109	1.305	—	1.524
71	2.57	12.85	0.87	0.82	0.101	1.383	12.79	1.512
160	2.52	—	1.07	1.01	0.079	1.377	—	1.352
160	2.55	12.74	0.90	0.86	0.423	1.582	12.61	1.353
200	2.49	12.44	0.88	0.83	0.933	1.592	12.11	0.949
250	2.52	—	0.76	0.71	0.463	1.753	—	1.213
250	2.50	12.49	0.95	0.89	1.57	1.51	11.96	0.482
300	2.49	—	0.86	0.71	0.802	1.513	—	0.863[a]
300	2.54	12.69	0.77	0.72	2.327	1.728	11.69	0.378

[a] This value may be high by ~8 percent which would yield for the final acetone values ~0.92 by difference and ~0.77 by measurement.

The composition of the saturated fraction resulting after the hydrogenation was determined by the method of catalytic hydrogenation to methane, used in the work of Morikawa on these hydrocarbons. A measured quantity of hydrogen was added to a measured portion of the C_2 fraction ($H_2 : C_2 > 2$) and the mixture transferred to a nickel catalyst at 230–240°. The gases were circulated 10–20 times during an average reaction time of two hours, and then returned to the gas burette to test for gas retention by the nickel. The excess hydrogen was then removed by copper oxide at 270–280° with an adjoining tube in liquid air. The measure of the residual methane, giving by difference the hydrogen unused in the reaction on nickel gave a double check on the composition of the saturated hydrocarbon sample. For pure C_2H_6, the hydrogen consumed on nickel and half the methane formed should and, within experimental error, did coincide. We have therefore recorded the condensible hydrocarbon as C−C.

Experimental Results

The analytical results for the experiments at five temperatures from 70 to 300°C are presented in Table I. Columns 2 and 3 record the initial reactants in moles and the following six columns the moles of products. In each experiment the illumination period was 35±5 minutes, except at 71° where the exposure was 2.5 hours.

An analysis of this table indicates that there is no material increase in the acetone decomposed (CO produced) per unit of illumination over the range of temperature 160–300°C, whether hydrogen is present or absent. The random variations are entirely accounted for by variations in the position of the arc and its intensity. The ethane formed in absence of hydrogen progressively decreases with increase in temperature. The decrease in presence of hydrogen is much more

[5] Taylor and Joris, Bull. Soc. Chim. Belg. **46**, 241 (1937).
[6] Morikawa, Trenner, Taylor, J. Am. Chem. Soc. **59**, 1104 (1937).

TABLE II. C_2H_6 : CO *and* CH_4 : CO *in presence and absence of hydrogen.*

	C_2H_6 : CO RATIO		CH_4 : CO RATIO			$(C_2H_6+\frac{1}{2}CH_4)$: CO RATIO	
t°C	H_2 ABSENT	H_2 PRESENT	H_2 ABSENT	H_2 PRESENT	$\frac{2(-\Delta H_2)}{CO}$	H_2 ABSENT	H_2 PRESENT
71	1.17	1.09	0.083	0.073	0.087	1.21	1.13
160	0.982	0.855	0.057	0.268	0.164	1.01	0.99
200	(0.86)[a]	0.595	(0.11)[a]	0.585	0.414	(0.91)[a]	0.89
250	0.692	0.319	0.264	1.04	0.702	0.82	0.84
300	0.570	0.219	0.530	1.35	1.16	0.83	0.89

[a] Interpolated values.

pronounced. *Vice versa*, methane production increases with temperature with acetone alone and much more rapidly in presence of hydrogen, from 160° upwards. At 70°C the methane production is within experimental error the same in the two conditions. These observations are exhibited by the data in Table II.

In the last two columns are given the ratios $(C_2H_6+\frac{1}{2}CH_4)$: CO, which indicates the relation between total hydrocarbon produced (reckoned as C_2) per unit of carbon monoxide formed. These columns reveal that at low temperatures a carbon monoxide deficiency obtains, whereas, at temperatures above 160°, a hydrocarbon deficiency is observed. We interpret these results most readily on the assumption that at temperatures of 70° and lower there occurs the formation of more complex molecules, as for example, $CH_3COCOCH_3$.[4] At high temperatures these do not form, but polymers of the hydrocarbons are formed as well as ethane and methane. The recent work of Taylor and Jungers[7] has revealed that in presence of free radicals any unsaturated hydrocarbons are rapidly polymerized in the temperature range here under study.

Since methane is formed in the absence of hydrogen it is to be expected that the methane formation in presence of hydrogen should be greater than that calculated from measurements of hydrogen consumed, expressed as a ratio to CO produced in the column of Table II headed $2(-\Delta H_2)/CO$. Comparison of this column with the adjoining column CH_4 : CO indicates that this is consistently the case. The agreement between the two sets of data cannot be very close. The hydrogen consumption involves the small difference of two large quantities. The methane value depends on the efficiency of the fractionation process and on the extent to which methane formation from acetone alone is suppressed in presence of hydrogen.

[7] Taylor and Jungers, Trans. Faraday Soc. **33**, 1353 (1937).

DISCUSSION OF RESULTS

Activation energies

The influence of temperature on methane formation can be deduced from the data on hydrogen consumption and from the actual measurements of methane production. The result in the latter case will be less certain than in the former for the reason just discussed. A plot of the logarithms of the $(-\Delta H_2/CO)$ values, which represent rates of reaction, against the reciprocal of the absolute temperature gives a straight line with slope corresponding to an activation energy of 6.4 kcal. This line passes through the points for $t=250$ and 300°C which are the most accurate and passes below and above the points at 200 and 160°C. The value at 71° is off the line entirely, due to the large experimental error in the determination, consequent, in all probability, on extraneous secondary processes, during the long period of exposure required at this temperature. A straight line through the data from 160–300° for observed methane production (CH_4/CO) in presence of hydrogen is not so satisfactory, tending to curve over at the high temperatures. Such curvature undoubtedly arises from diminishing methane production from acetone due to the competition of the hydrogen reaction. The best straight line through the four points gives a slope with an activation energy of 5.9 kcal.

The activation energy of methane formation from acetone in the absence of hydrogen (CH_4/CO) has a value of 8.6 kcal. in the range 160–300°C, a value which accounts for the increasing effectiveness of the interaction with hydrogen when this is present.

The data on ethane and methane formation can also be represented on a plot log (CH_4/C_2H_6) against $1/T$ giving a good straight line with a slope corresponding to an activation energy of 11.4 kcal. The increase of slope over that of methane formation arises from the decrease in the yield (C_2H_6/CO) with rise in temperature as

set forth in Table II. The straight line obtained implies, however, that the ethane producing process, if represented by a kinetic expression of the form $+d\mathrm{C_2H_6}/dt = Ze^{-E/RT}$, must yield values of Z in the equation *decreasing* exponentially with temperature. The obvious method of interpreting this is in terms of a decreasing stationary state concentration of methyl radicals with increase of temperature, due to the competition, with the reaction which produces ethane, of the reaction of the radicals with hydrogen, or with acetone, producing methane.

We may represent the reaction producing methane in presence of hydrogen by means of the equation

$$+d[\mathrm{CH_4}]/dt = k_1[\mathrm{H_2}][\mathrm{CH_3}]e^{-E_M/RT}.$$

The process producing ethane may be unimolecular at the wall, a bimolecular association of methyl radicals or a three-body combination of two radicals, representable by an equation

$$+d[\mathrm{C_2H_6}]/dt = k_2[\mathrm{CH_3}]^x e^{-E_E/RT},$$

where x may be either 1 or 2 and k_2 in the case of a termolecular reaction would include a concentration of a third body.

Taking the unimolecular case first with $x=1$, $[\mathrm{H_2}]$ constant, and the activation energy $E_E=0$ we obtain

$$+\frac{d[\mathrm{CH_4}]}{d[\mathrm{C_2H_6}]} = \frac{k_1[\mathrm{H_2}][\mathrm{CH_3}]e^{-E_M/RT}}{k_2[\mathrm{CH_3}]} = k_3 e^{-11.4/RT},$$

from the slope of the curve log $([\mathrm{CH_4}]/[\mathrm{C_2H_6}])$ *vs.* $1/T$. On this assumption $E_M=11.4$ kcal. The difference between this value and the observed slope log $[\mathrm{CH_4}]/[\mathrm{CO}]$ *vs.* $1/T=6.4$ kcal., must represent the variation of stationary state concentration of methane with temperature, $[\mathrm{CH_3}]=ke^{5.0/RT}$. In the interval from 160 to 300°C the quantity $e^{5.0/RT}$ changes by the factor $e^{-1.42}$ or approximately 0.24. This is almost exactly the ratio in which ethane production in presence of hydrogen decreases in the same interval. This concordance therefore strongly suggests a unimolecular reaction at the wall with negligible activation energy.

In the bimolecular case, $x=2$ we have

$$+\frac{d[\mathrm{CH_4}]}{d[\mathrm{C_2H_6}]} = \frac{k_1[\mathrm{H_2}][\mathrm{CH_3}]e^{-E_M/RT}}{k_2[\mathrm{CH_3}]^2 e^{-E_E/RT}} = k_3 e^{-11.4/RT}.$$

From this equation we deduce

$$E_{[\mathrm{CH_3}]} - E_M = -11.4 - E_E + 2E_{[\mathrm{CH_3}]}.$$

As before, from the observed slope log $[\mathrm{CH_4}]/[\mathrm{CO}]$ *vs.* $1/T$,

$$E_{[\mathrm{CH_3}]} - E_M = -6.4.$$

By addition,

$$2E_M - E_E = 17.8 \text{ kcal.}$$

This gives a minimum value for E_M when $E_E=0$, in which case $E_M=8.9$ kcal., and $E_{[\mathrm{CH_3}]}$ becomes 2.5 kcal. This also will give the correct variation of ethane formation in presence of hydrogen with temperature. A positive value of E_E would increase E_M by $\frac{1}{2}E_E$; for $E_E=5$ kcal., the value of E_M would be $8.9+2.5=11.4$ kcal., and for $E_E=8$ kcal., $E_M=12.9$ kcal. Recent researches have assigned to E_E a value of zero or at most a few kilocalories.[8]

The analysis therefore does not lead to an unequivocal value for the activation energy of the reaction $\mathrm{CH_3}+\mathrm{H_2}=\mathrm{CH_4}+\mathrm{H}$. The data just cited would indicate that it should lie within the range $E_M=11\pm2$ kcal.

A further observation is possible from an analysis of the data in Table II. At 300°C it is seen that, with hydrogen present, at least 75 percent of the decomposed acetone found in the form of the two hydrocarbons is present as methane, and the percentage is increasing rapidly with rise in temperature. Under our experimental conditions ethane once formed would not be markedly converted to methane. This signifies that, in the photochemical decomposition, under these conditions, the primary absorption process in the diffuse region leads mainly, if not exclusively, to radical fragments and that an intramolecular rearrangement of an activated molecule to yield ethane and carbon monoxide is a minor, if not entirely negligible, mode of decomposition. In processes of thermal decomposition of organic molecules both modes of decomposition appear to be possible, with the relative extent of each still a matter for experimental decision.

Our data on the photolysis of acetone alone overlap those previously obtained by

[8] See, for example, Bawn, Trans. Faraday Soc. **31**, 1542 (1935).

Leermakers.[9] They check these latter in the invariance of quantum yield with temperature over the range 160–300°. At 71° the quantum yield is much smaller since the illumination for 2.5 hours produced approximately the same decomposition as 35 minutes at the higher temperatures. This points to a quantum yield of approximately 0.2 at 70°C a value comparable with those of Damon and Daniels[10] at 56°C. We suggest that the increase in quantum yield from 70 to 160° is to be associated with the suppression in the higher temperature range of diacetyl formation. From room temperatures to 70° the formation of diacetyl might permit, in addition to processes of recombination of the radicals CH_3 and $COCH_3$, a reaction, regenerative of acetone, of the form,

$$CH_3CO\cdot CO\cdot CH_3+CH_3 = CH_3COCH_3+CH_3CO.$$

This would decrease the quantum yield below the value of unity which might be anticipated from the spectroscopic evidence concerning the primary process. This suggestion is analogous to that put forward by Mund and van Tiggelen[11] to account for the low quantum yield in ammonia photodecomposition by the regenerative reaction,

$$N_2H_4+H=NH_3+H_2.$$

The occurrence of diacetyl formation in the low temperature range is probably also responsible for methane formation which is abnormal when compared with that in the higher temperature range, due to secondary reactions during the longer period of illuminations involved.

The value of 11 ± 2 kcal. which we obtain for the activation energy of the reaction $CH_3+H_2=CH_4+H$ is to be compared with the experimental data of Hartel and Polanyi[12] for the same reaction with the methyl radicals from sodium vapor and methyl halides. Their observations are generally quoted as leading to a value of 8 kcal. Examination of their data shows two series of determinations, one of which, at 9 mm hydrogen pressure, leads to the value of 8 kcal., the other at 10 mm hydrogen pressure leading to a "best" value of 5.5 kcal., and 6.3 kcal. as the largest value which can be obtained from the data. Our value is beyond their upper limit and is coincident with the value of 11 kcal. estimated by Morikawa, Trenner and Taylor[6] from their studies of interaction between atomic hydrogen and hydrocarbons.

Acknowledgments

We wish here to express our acknowledgments to all those who, by their assistance, made this work possible. To the Foundation Francqui for the professorship held by one of us (H.S.T.) at Louvain; to the Commission for the Relief of Belgium Educational Foundation Inc. for a fellowship (to C.R.) at the University of Louvain during 1935–1937; to the Fonds National de la Recherche Scientifique for funds for apparatus and equipment; and finally to the Rector, to Professor W. Mund and to our colleague Dr. J. C. Jungers for hospitable reception in the university and chemical laboratory.

[9] Leermakers, J. Am. Chem. Soc. **56**, 1899 (1934).
[10] Damon and Daniels, J. Am. Chem. Soc. **55**, 2363 (1933).
[11] Mund and van Tiggelen, Bull. Soc. Chim. Belg. **46**, 104 (1937).
[12] Hartel and Polanyi, Zeits. f. physik. Chemie **11B**, 97 (1930).

A Simple Method for Determining the Polarization of Raman Lines

JOHN T. EDSALL AND E. BRIGHT WILSON, JR.
Department of Physical Chemistry, Harvard Medical School, Boston, Massachusetts
and the
Mallinckrodt Chemical Laboratory, Harvard University,
(Received December 27, 1937)

A simple method is described for determining qualitatively the polarization of Raman lines. The incident light is polarized by means of "Polaroid." One of the arrangements used permits very high intensity of incident illumination. A brief statement of the theory of the method is given, and experimental data on acetic acid, acetone and ethanol are presented.

THE determination of the polarization of Raman lines is of great importance in assigning these lines to modes of molecular vibration. The usual methods of measuring this polarization are, however, rather difficult and involve the use of expensive apparatus, so that relatively few such measurements have been reported. Ordinarily, unpolarized incident light is used, and the scattered radiation is resolved into two components by a birefringent prism. Now that large sheets of transparent polarizing material ("Polaroid") are available at relatively low cost, we have found it possible to determine qualitatively the polarization of Raman lines with considerable ease. When the spectra are photographed in a suitable manner, it is possible to discriminate sharply between polarized and depolarized frequencies.

EXPERIMENTAL PROCEDURE

Two different experimental arrangements have been used. In one, the cell containing the liquid is illuminated by four vertical mercury lamps[1] equipped with parabolic reflectors. See Fig. 1. A cylinder of Polaroid,[2] made so that it transmits only light polarized with its electric vector parallel to the axis of the cylinder, slips over the Raman tube. Two exposures are made: one with all the lamps operating and the Polaroid in place, and the other with reduced illumination and with no Polaroid. It is necessary to reduce the illumination for the second exposure in order to obtain two pictures of comparable intensity inasmuch as Polaroid absorbs rather strongly the violet light used in these experiments. As will be shown later, all Raman lines arising from unsymmetrical vibrations of the molecule should show the same decrease in intensity when the Polaroid is used, whereas lines associated with completely symmetrical vibrations will usually be attenuated more strongly. Consequently, the most sensitive way to distinguish the symmetrical vibration frequencies is to adjust the light intensity of the second exposure so that all the depolarized lines (unsymmetrical vibrations) have equal intensities on the two plates. The polarized lines should then stand out because of their unequal intensities. Because of the failure of the photographic reciprocity law, it is safest to use the same exposure time for the two pictures, but different intensities of illumination.

We have also made use of a second method, which has the advantage of great simplicity, although the light intensity is relatively low, and long exposures are therefore required. This is based on the experimental arrangement devised by Wood[3] and is shown diagrammatically in Fig. 2, which represents a cross section perpendicular to the axis of the Raman tube. The light from a single mercury arc (A) passes through the cylindrical tube F, which contains a solution which acts as a light filter, and also as a lens, gathering the light from the arc into a concentrated and nearly parallel beam. This light then passes through the plane Polaroid disk (P), which can be so oriented as to transmit light which vibrates either parallel or perpendicular to the axis of the Raman tube (R). An exposure is first taken with the plane of the

[1] The lamps, Raman cell, and several other parts were made by Professor G. B. Kistiakowsky and we are deeply indebted to him for his kindness in placing them at our disposal.

[2] We are indebted to the Polaroid Corporation for supplying us with this cylinder.

[3] R. W. Wood, *Physical Optics*, third edition, 1934, Chapter XIV.

incident light parallel to the axis of R (perpendicular to the plane of the paper); then the Polaroid disk is revolved through a right angle (around the axis indicated by the arrow in Fig. 2) to admit light polarized perpendicular to the plane of the paper, and a second exposure is given for an equal time.

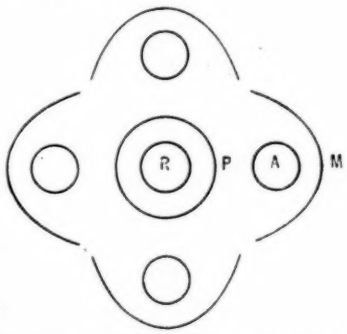

FIG. 1. Diagram of one type of apparatus used (top view). R is Raman tube in cross section; P, Polaroid cylinder; A, mercury arc; M, parabolic reflector.

As with the first method, it is very desirable to adjust the light intensity in the second exposure so that depolarized lines have the same intensity in both exposures. It was found that three plane thin glass sheets[4] placed between the Polaroid disk and the Raman tube during the second exposure accomplished this result quite satisfactorily. (See the photographs reproduced below.) These results were obtained with a Hilger E-439 glass spectrograph; the exact intensity ratio for the two polarized beams will vary somewhat from one spectrograph to another, depending on the degree to which polarized light is reflected from the prisms of the spectrograph.

It is essential, of course, in photographing these spectra, that the axes of the mercury arc, the Raman tube, and the collimator of the spectrograph should all be parallel and in the same plane; also the plane of polarization of the light transmitted by the Polaroid must be carefully adjusted.

Filters

Either of the methods described requires two separate exposures. The intensity of the highly polarized Rayleigh scattering (including the continuous background) will be very much greater in one exposure than in the other. It is desirable, therefore, to reduce the continuous background as nearly as possible to zero in *both* exposures. A filter which nearly achieves this purpose has been devised by Sannié, Amy and Poremsky,[5] and we have used a slight modification of the filter which they recommend. This consists of an alcoholic solution of *p*-nitrotoluene and rhodamine 5GDN Extra.[6] A solution of 2 percent *p*-nitrotoluene, and one part in 50,000 of the rhodamine dye, in a layer 30 mm thick, completely absorbs the ultraviolet, transmits less than 1 percent of λ4047 and about 1 percent of λ4916, while transmitting 70 percent or more of λ4358. Transmission falls rapidly on either side of λ4358, so that the continuous background between 4500 and 5000A is very largely wiped out; furthermore, Raman lines are excited by the 4358 triplet and by this alone,[7] so that there is no difficulty in the assignment of frequencies.

Long exposures are required by the second method here described. We have found it most satisfactory to give 24 hours for each of the two exposures in order to obtain the fainter Raman lines in such substances as acetic acid or ethanol.[8]

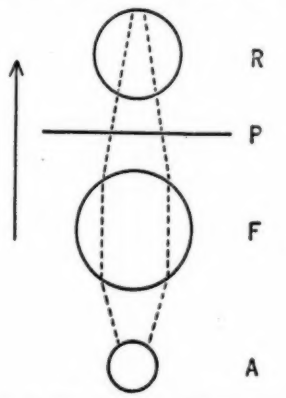

FIG. 2. Diagram of second type of apparatus. R, Raman tube; P, Polaroid disk, F, filter tube; A, mercury arc.

[4] Microscope slides were found very convenient for this purpose.

[5] C. Sannié, L. Amy and V. Poremsky, Bull. Soc. Chim. France **3**, 2018 (1936). These authors used nitrobenzene and rhodamine 5G Extra, dissolved in alcohol. We have not been able to obtain the latter dye, but rhodamine 5GDN Extra appears to give essentially identical results.

[6] This dye was supplied to us through the courtesy of E. I. duPont de Nemours and Co.

[7] The filter completely absorbs the green region of the spectrum, but freely transmits the yellow mercury lines. The presence of the latter, of course, does no harm; in fact it facilitates the focusing of the light from the Raman tube upon the spectrograph.

[8] Substances like carbon tetrachloride, which yield only a few, very intense Raman lines, can be photographed in a very much shorter period.

This is true even with the use of the Hilger E-439 spectrograph (aperture ratio $f:3$). With spectrographs of low light-gathering power, the time involved would be prohibitively long, and only the first method would be worth considering.

A word may be added regarding the advantages and disadvantages of Polaroid, as compared with other polarizers, such as birefringent prisms. The advantages are several: (1) Very high incident illumination may be used, if the first method described here is employed. (2) The technique is relatively simple. (3) The materials are inexpensive. On the other hand, there are two important disadvantages: (1) Polaroid absorbs strongly in the blue-violet region: a nonabsorbing polarizer would probably transmit three or four times as much light of these wavelengths. (2) It is necessary to make two separate exposures in employing either of the techniques described.

Theoretical Considerations

Placzek[9] has shown that for polarized incident light, the radiation scattered in the direction parallel to the electric vector of the incident light has the intensity

$$I_{||}=6\gamma^2_{VV'}kI, \tag{1}$$

for a given vibrational transition VV'. Here k is a constant, I is the intensity of the incident polarized illumination, and $\gamma^2_{VV'}$ is the matrix element between the vibrational states V and V' of the quantity

$$\gamma^2=\tfrac{1}{2}\{(C_1-C_2)^2+(C_2-C_3)^2+(C_3-C_1)^2\}, \tag{2}$$

in which C_1, C_2, C_3 are the principal values of the polarizability tensor of the scattering molecule. The light which is scattered in a direction perpendicular to the direction of the electric vector of the incident illumination has the intensity

$$I_{\perp}=(5A^2_{VV'}+7\gamma^2_{VV'})kI, \tag{3}$$

in which $A^2_{VV'}$ is the matrix element of

$$A^2=(C_1+C_2+C_3)^2. \tag{4}$$

In the experimental arrangement shown in Fig. 2, the incident light is polarized first parallel to the axis of the Raman tube and secondly perpendicular to that axis. In the first case, Eq. (1) applies; in the second, Eq. (3). The ratio of intensities is

$$I_{||}/I_{\perp}=\frac{6\gamma^2_{VV'}}{5A^2_{VV'}+7\gamma^2_{VV'}}, \tag{5}$$

Vibrational transitions can be divided into two classes, those for which $A^2_{VV'}=0$ and those for which $A^2_{VV'}\neq 0$. All fundamentals involving unsymmetrical vibrations belong to the former class; consequently $I_{||}/I_{\perp}=6/7$ for such frequencies when the experimental arrangement of Fig. 2 is used. The symmetrical frequencies may have ratios anywhere between zero and 6/7.

If the illumination comes from all sides as in Fig. 1, exactly the same result is obtained as in Eq. (5). This follows from the theorem that no matter what the distribution of light as a function of angle about the axis of the Raman tube,[10] the equation $I_x+I_y=I_z$ holds, where I_x, I_y and I_z are the intensities of the light polarized in the two directions perpendicular and the direction parallel to the axis of the Raman tube, respectively. This theorem can be proved as follows. Let $I(\varphi)d\varphi$ be the total intensity falling radially on the Raman tube from an angular wedge $d\varphi$. Then the contributions of this intensity to I_x, I_y and I_z are $\frac{1}{2}I(\varphi)\cos^2\varphi d\varphi$, $\frac{1}{2}I(\varphi)\sin^2\varphi d\varphi$, $\frac{1}{2}I(\varphi)d\varphi$, respectively. Integration over φ gives

$$I_z=\tfrac{1}{2}\int_0^{2\pi}I(\varphi)d\varphi=\tfrac{1}{2}\int_0^{2\pi}I(\varphi)\sin^2\varphi d\varphi$$
$$+\tfrac{1}{2}\int_0^{2\pi}I(\varphi)\cos^2\varphi d\varphi=I_x+I_y. \tag{6}$$

Consequently if two cylinders of Polaroid are used, one transmitting I_z only, the other light tangentially polarized, Eq. (5) can be used.

It is possible to replace the exposure with illumination polarized perpendicularly ($I_{\perp}$) by one using unpolarized light. The expression for the ratio of the intensities of the two exposures then becomes

[9] G. Placzek, Marx, *Handbuch der Radiologie*, Vol. VI.

[10] The light is assumed to strike the Raman tube radially. In practice, baffles may be needed to prevent light from falling on the tube nonperpendicularly.

$$\frac{\text{Polarized}\parallel}{\text{Unpolarized}}=\frac{6\gamma^2_{VV'}}{5A^2_{VV'}+13\gamma^2_{VV'}}. \quad (7)$$

This is the method actually used with the apparatus shown in Fig. 1.

Experimental Results

Polarization photographs of acetic acid, acetone and ethanol are shown in Figs. 3, 4 and 5 (obtained by the second method). Note that the only mercury lines appearing in these photographs are those of the 4358A triplet; all other lines are Raman lines. The data are listed in Table I, where numbers in the top row give

Fig. 3. Acetic acid.

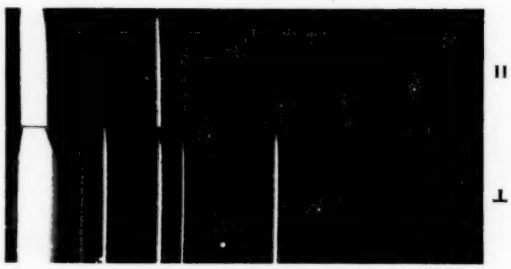

Fig. 4. Acetone.

Fig. 5. Ethanol.

Table I.

Acetic Acid					
446 (1) (0.59) *D* ?	621 (3) 0.89 *D*	893 (5) 0.16 *P*	1024 (1) — *D* ?	1221 (1) — —	
1277 (1) — —	1366 (2) 0.21 *P*	1431 (3*b*) 0.85 *D*	1663 (2*b*) 0.37 *P*	2940 (8) 0.04 *P*	
Acetone					
391 (1) 0.87 *D*	532 (3*b*) 0.70 *D*	788 (8) 0.20 *P*	1067 (2) 0.64 *P*	1122 (2) 0.88 *D*	1350 (½) 0.23 —	1423 (3) 1438 (4) 0.90 *D*
1708 (5*b*) 0.38 *P*	2838 (1) — —		2922 (12*b*) 0.22 *P*	2965 (4*b*) — —		3005 (4*b*) — —
Ethanol						
432 (6) 0.55 *P*	884 (60) 0.31 *P*	1051 (32) 0.59 *P*	1095 — *P*	1274 (17) — *D* ?	1455 (46) 0.90 *D*	
2878 (58) 0.14 *P*	2928 (100) 0.23 *P*		2972 (61) 0.87 *D*		3359 (10*vb*) — ?	

frequency and estimated intensity of each line,[11] the second row gives the value measured by Simons for the depolarization ratio, and the third row indicates whether the line is polarized (*P*) or depolarized (*D*) according to our own measurements. In general there is very good agreement between the two estimates. The line at 1095 in ethanol (on which Simons did not report) is found to be strongly polarized, much more so than the line at 1051. We also find (in agreement with Simons) that the line at 1067 in acetone is strongly polarized, contrary to the suggestion of Kohlrausch and Pongratz[12] that it might be depolarized.

Previous measurements, employing the present technique (method 2), have already been reported by one of us.[13]

[11] Values taken from Landolt-Börnstein, *Tabellen*, fifth edition, 3d Ergänzungsband, Part II. The polarization measurements (by Simons) are taken from the same source.

[12] K. W. F. Kohlrausch and A. Pongratz, Zeits. f. physik. Chemie **27B**, 176 (1934).

[13] J. T. Edsall, J. Chem. Phys. **5**, 225, 508 (1937).

The Influence of Salts on the Absorption Spectra of Aqueous Cobalt Chloride Solutions

J. N. Pearce* and Lyle R. Dawson†
State University of Iowa, Iowa City, Iowa

(Received December 9, 1937)

The effects of equal concentrations of the alkali and alkaline earth chlorides and of hydrogen chloride on the absorption spectra of aqueous cobalt chloride solutions have been studied. Solutions prepared both on the molar and on the molal bases were used. In all cases, the absorption bands widen with an increase in concentration of the added salt. The increase in width of the absorption bands varies directly as the ionic charge and inversely as the ionic volume of the added cation. The inadequacy of existing explanations of the well-known color changes in cobalt chloride solutions is discussed and a new explanation is offered.

THE influence of added salts on the color of cobalt chloride solutions has been studied by several investigators but no completely satisfactory explanation of the observed color changes has been given.

Vogel[1] reported anomalous changes in the absorption bands of cobalt chloride solutions with changes in concentration. Donnan and Bassett[2] suggested the existence of blue $CoCl_4^{--}$ ions and Macwalter and Barratt[3] carried out experiments designed to determine the extent to which conversion to this form can proceed. Jones and Bassett[4] and later Jones and Uhler[5] studied the effects of added dehydrating agents. They attributed the color changes to variations in the degree of hydration of the cobalt ion.

Brdicka's[6] work showed that the addition of anhydrous calcium chloride increases the activity of the cobalt ion. He employed Fajans'[7] theory of ion deformability to explain the color changes.

The object of the work herein reported was to compare the effects of added salts under identical conditions of solvent environment and to investigate the influence of the hydrating power of the cation of the added salt.

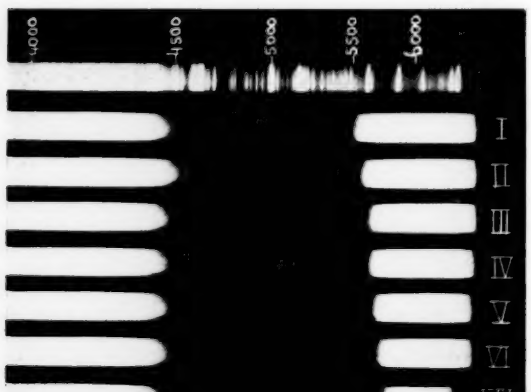

Fig. 1. Influence of salts (3.00 molal) on the absorption spectrum of $CoCl_2$ (0.250 molal). I, $CoCl_2$ alone; II. NH_4Cl; III, KCl; IV, NaCl; V, LiCl; VI, HCl; VII, $CaCl_2$.

Experimental

Cobalt chloride, specified as "analytical reagent," was recrystallized three times for further purification. A fairly concentrated stock solution was prepared and standardized electrolytically.

Alkali and alkaline earth chlorides of "analyzed" grade were further purified by repeated recrystallizations. Constant boiling hydrochloric acid was prepared by the method of Hulett and Bonner.[8] Solutions containing a fixed concentration of cobalt chloride and varying concentrations of these salts and of hydrogen chloride were prepared with conductivity water.

The absorption spectra of the solutions were photographed with a large quartz spectrograph having a dispersion of 30A per mm at 5000A. The instrument was built by Dr. Thomas Poulter[9] and loaned for this investigation. A 150-watt Point-o-Lite lamp served as a light source.

* Deceased November 14, 1936.
† Present address, Universal Atlas Cement Co., Gary, Indiana.
[1] Vogel, Ber. **11**, 913 (1878).
[2] Donnan and Bassett, J. Chem. Soc. **81**, 942 (1902).
[3] Macwalter and Barratt, J. Chem. Soc. **137**, 517–24 (1934).
[4] Jones and Bassett, Am. Chem. J. **34**, 290 (1905).
[5] Jones and Uhler, Am. Chem. J. **37**, 129, 207 (1907).
[6] Brdicka, Coll. Czechoslav. Chem. Comm. **2**, 545–58 (1930).
[7] Fajans and Joos, Physik. Zeits. **23**, 1 (1924).
[8] Hulett and Bonner, J. Am. Chem. Soc. **31**, 390 (1909).
[9] Chief scientist of the Second Byrd Expedition to Little America.

Eastman's spectrographic plates, type III-F, were used. These were developed in Eastman's solution, D-11, and fixed in Eastman's solution, F-I.

The cobalt chloride solutions were held in a Baly adjustable tube equipped with optical quartz ends. Adjustments in length with changes in concentration were made in such a way that the product of the thickness of the solution and the concentration of cobalt chloride per unit volume, remained constant.

Spectra of solutions containing equal concentrations (both 0.25 molal and 0.25 molar) of cobalt chloride and six different concentrations of each ammonium, potassium, sodium, lithium, hydrogen, and calcium chlorides were photographed. Each series of solutions was prepared both on the molal and on the molar bases. Also several series of spectrograms were obtained in which the effects of equimolal and equimolar concentrations of the added salts were compared. Only three of these series of spectrograms are included here.

Discussion of Results

In all cases, absorption in the region from 4500A to 5500A increases with an increase in concentration of the added salt (spectrograms not shown). Comparing equal concentrations of different salts, it may be observed that increased absorption follows the order in which the solutions were photographed (Figs. 1–3). The effect is more pronounced in the solutions prepared on the molar basis than in those prepared on the molal basis. This is to be expected, for on the molar basis, the actual concentration of water molecules varies with the partial molal volume of the added salt. In solutions prepared on the molal basis, the ratio of water molecules to cobalt ions remains constant and the number of variables is reduced to one—the concentration of the added salt only. It is these spectrograms which yield data most applicable to the problem at hand.

Absorption increases with decrease in ionic volume of the added alkali cations. If the cation in hydrochloric acid is considered to be the proton, or hydrogen ion, it fits into the series. It has been shown[10, 11] that the degree of hydration of these cations varies in the same way. Thus, increased absorption of light and the consequent color changes accompany an increase in the degree of hydration of the cation of the added salt. This relationship is further established by the effects of the calcium ion, which has greater hydrating power than any of the alkalies. If the only absorbing mechanism[12] is the cobalt ion, one is forced to conclude that its change in character is associated with a decrease in the number of solvent molecules surrounding it. However, the explanation of this effect must involve some other factors.

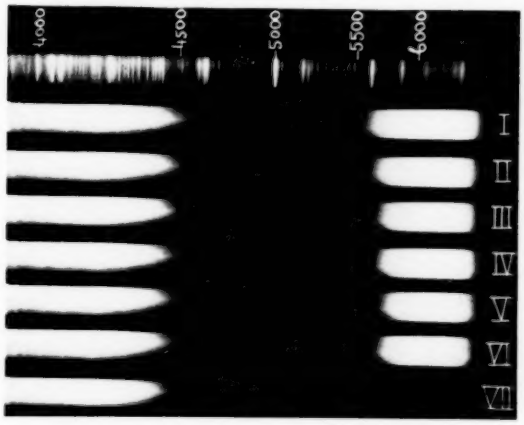

Fig. 2. Influence of salts (4.00 molal) on the absorption spectrum of $CoCl_2$ (0.250 molal). I, $CoCl_2$ alone; II, NH_4Cl; III, KCl; IV, NaCl; V, LiCl; VI, HCl; VII, $CaCl_2$.

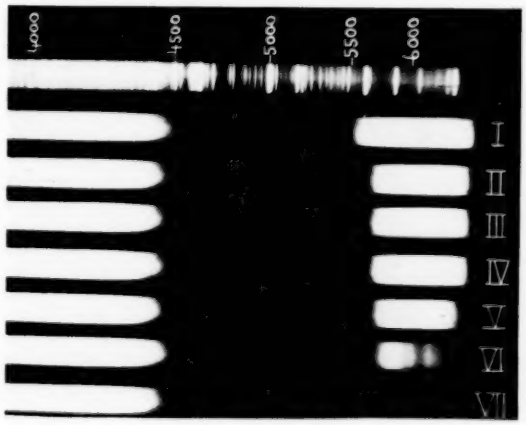

Fig. 3. Influence of salts (4.00 molar) on the absorption spectrum of $CoCl_2$ (0.250 molar). I, $CoCl_2$ alone; II, NH_4Cl; III, KCl; IV, NaCl; V, LiCl; VI, HCl; VII, $CaCl_2$.

[10] Jones and Pearce, Am. Chem. J. **38**, 683 (1907).
[11] Washburn, J. Am. Chem. Soc. **31**, 322 (1909).
[12] Vaillant, Comptes rendus **189**, 747 (1929); **190**, 170 (1930); **173**, 654 (1931).

The fact that equimolal high concentrations of added chlorides do not produce equal color changes serves to cast doubt upon the theory that complex ions, of the type $CoCl_4^{--}$ are formed. That such color changes could be due to deformation of the chloride ions[6] by strongly hydrating cations seems improbable, since pure concentrated solutions of aluminum chloride and of calcium chloride are colorless.

Absorption of energy in the visible region may be accomplished by the electrons[13] within the cobalt atom. The change in color of a dilute aqueous solution of cobalt chloride from red to blue, upon adding strongly hydrating cations, may be explained on this basis. In dilute solutions, the cobalt ion is completely hydrated. Solvent molecules are held tightly bound[14] and the solvent sheath prevents close approach of the cobalt and chloride ions. Electronic transitions in the unfilled third quantum group result from the absorption of green wave-lengths and the solution is red. As strongly hydrating ions are added, they attract and orient solvent molecules. At high concentrations of the added salt, much of the solvent envelope about the cobalt ions is removed. Cobalt and chloride ions are then drawn more closely together by electrostatic attraction.

According to Lewis,[15] the strongly electronegative chloride ion tends to attract electrons of an ion near it. Thus, it is reasonable to assume that chloride ions distort the electronic system of the cobalt ion in such a way that the electrons in the third quantum group are capable of absorbing smaller quanta of energy. Hence, the yellow and red wave-lengths are absorbed and the solution becomes blue.

The blue color of concentrated solutions of pure cobalt chloride as well as of the anhydrous salt may also be explained in this way.

[13] Taylor, *Treatise on Physical Chemistry* (D. Van Nostrand Co., 1931), pp. 1533, 1544.
[14] Webb, J. Am. Chem. Soc. **48**, 2589 (1926).
[15] Lewis, *Valence and the Structure of Atoms and Molecules* (Chemical Catalog Co., 1923), p. 139.

MARCH, 1938 JOURNAL OF CHEMICAL PHYSICS VOLUME 6

Theory of Order for the Copper Gold Alloy System

W. SHOCKLEY
Bell Telephone Laboratories, Inc., New York, N. Y.
(Received December 15, 1937)

The theory of order and disorder, in the form used by Bragg and Williams, is extended to arbitrary composition of the constituent elements. The work is based upon the nearest neighbor interaction assumption of Bethe and the connection between the Bethe and Bragg-Williams theory is shown. In order to extend the Bragg-Williams theory to compositions other than 25 and 50 atomic percent, new definitions of order are developed. The results are presented in terms of phase diagrams and curves showing energy *vs.* temperature, specific heat *vs.* temperature and state order *vs.* temperature. These results are of importance in giving a general picture of the order-disorder transformation for a wide composition range. They are not in detailed accord with experiment due to the rather idealized picture underlying the nearest neighbor assumption.

I. The Nearest Neighbor Assumption

1. Introduction

The phenomenon of order and superlattice formation in alloys is of an energetic nature, being governed by forces which tend to establish atoms in an orderly array. Several theories have been developed based on various assumptions regarding the relationships between the orderliness of the alloy and its energy.

The best known of these is probably that of Bragg and Williams.[1] They gave a quantitative significance to the concept of order by introducing the idea of "right" and "wrong" positions for the atoms. If an alloy in an imperfect state of order is compared with the perfectly ordered alloy, it will be apparent that a certain fraction of the atoms are missing from their "right" positions—those

[1] W. L. Bragg and E. J. Williams, Proc. Roy. Soc. **A145**, 699 (1934); **A151**, 540 (1935); **A152**, 231 (1935).

which are occupied by atoms of their species in the ordered state—and occupy "wrong" positions. Complete disorder will correspond to a random arrangement of atoms so that the fraction of the atoms of a given species which are "right" will be equal to the atomic fraction of that species. The Bragg-Williams order parameter, S, is a linear function of the fraction of "right" atoms of such a form that $S=1$ corresponds to perfect order and $S=0$ to a random arrangement. From an intuitively appealing physical argument, Bragg and Williams concluded that the configurational energy, that is, the energy required to disorder the alloy from perfect order to order S, would be given by the expression $\frac{1}{2}W_0(1-S^2)$.

A weakness of the Bragg-Williams attack was its rather macroscopic character. It would be expected that more adequate theories would be developed by considering the atoms in detail and inquiring into the forces acting between them. Considerable progress in this direction has been made by Bethe,[2] whose work was later extended by Peierls.[3] Bethe assumed that the atoms interacted in pairs, so that every two atoms had a mutual potential energy which, however, fell off rapidly with increasing separation of atoms. Bethe assumed that this falling off was so rapid that potential energies were appreciable only for those pairs of atoms which were nearest neighbors in the lattice.

The alloys of the Cu-Au system possess face-centered lattices—slightly distorted for some conditions of order—and each atom is surrounded by twelve nearest neighbors and hence has twelve non-negligible mutual potential energies. Since each of these is shared between a pair of atoms, there will be in all six potential energies per atom. The value of each potential energy will be V_{AuAu} if the pair of atoms to which it belongs are both Au, V_{CuCu} if both are Cu, and V_{AuCu} if the pair is mixed. In this work it will be assumed that these energy values are characteristic constants of the two elements; and no variations in their magnitudes, caused by change in order, composition, or state of strain, will be considered. This assumption will be referred to as the "nearest neighbor assumption".

In terms of the nearest neighbor assumption a formally simple expression for the energy of the alloy can be obtained. Let the number of pairs of nearest neighbors which are CuCu, CuAu, and AuAu be denoted by Q_{CuCu}, Q_{CuAu}, and Q_{AuAu}, respectively. Then associating with each pair its proper potential energy and summing these for all pairs in the lattice, we obtain

$$E=V_{\mathrm{AuAu}}Q_{\mathrm{AuAu}}+V_{\mathrm{CuCu}}Q_{\mathrm{CuCu}}+V_{\mathrm{CuAu}}Q_{\mathrm{CuAu}}. \quad (1)$$

In spite of the simplicity of the energy form the mathematical difficulties involved in a statistical mechanical treatment of it are so great that approximate and indirect methods are necessary. Bethe[2] has given a very satisfactory statistical mechanical treatment for a 50 atomic percent alloy having a simple type of lattice, but it is somewhat inappropriate to apply his results to CuAu. Peierls[3] has carried out an appropriate extension to Cu_3Au. The improvement of their work over that of Bragg and Williams is considerable in some respects but much is still desired in the way of agreement with experiment.

In this paper we shall give an approximate treatment of the form (1) for all compositions of Cu-Au. It is shown, Part III, that this treatment reduces to that of Bragg and Williams for the compositions 25 and 50 atomic percent so that the latter may be regarded as an approximation to the nearest neighbor theory.

2. Some consequences of the nearest neighbor assumption

For the purposes of this paper it is convenient to use not the actual energy (1) of the lattice but the difference between its energy and the energy of two chemically pure crystals of its components. By methods given in Part III, this energy can be expressed in the very simple form,

$$E=-\tfrac{1}{2}VQ_{\mathrm{CuAu}}. \quad (2)$$

Here
$$V=V_{\mathrm{AuAu}}+V_{\mathrm{CuCu}}-2V_{\mathrm{CuAu}} \quad (3)$$

is a measure of the tendency of the alloy to order itself, giving the reduction in energy obtainable by putting unlike atoms together to form a superstructure rather than putting like atoms together to form pure metals. Two significant features of Eq. (2) should be noted: the replacement of the three potential energies by V, and the obvious symmetry between Au and Cu. The first shows that the nearest neighbor assumption

[2] H. A. Bethe, Proc. Roy. Soc. **A150**, 552 (1935).
[3] R. Peierls, Proc. Roy. Soc. **A154**, 207 (1936).

leads to a theory involving only one adjustable parameter; hence the numerical determination of this parameter on the basis of a single experimental or theoretical item fixes all the quantitative predictions of the theory. The second means that all predictions based upon the nearest neighbor assumption alone will be symmetrical about 50 atomic percent, that is, the same behavior will be expected for any two alloys differing only in interchange of Cu and Au atoms. This prediction is in marked disagreement with experiment, for Cu_3Au readily forms ordered structures, whereas $CuAu_3$ does not. We shall return to this point briefly in Part II, Section 3.

It is not necessary to apply statistical mechanics to determine the limiting energies predicted by (2) for low and high temperatures; these correspond to minimum energy and random arrangement, respectively. These limiting values are shown as functions of the composition in Fig. 1(a), in which, as will be uniformly done in this paper, the composition is expressed in atomic percent. The unit of energy U_0 has been arbitrarily chosen so that,

U_0= Change in configurational energy from perfect order to complete disorder for one gram atom of 50 atomic percent CuAu alloy.

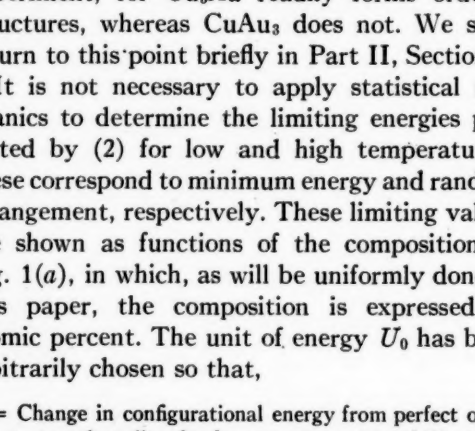

FIG. 1. (a) Energy of formation of one gram atom of best ordered (lower curve) or completely disordered (upper curve) Cu-Au alloy as a function of composition. (b) Difference of curves shows energy, $U_{X\text{ percent}}$, required to transform one gram atom from best order to complete disorder. (The curves in this figure result directly from the "nearest neighbor assumption." They do not depend upon the approximations used in the statistical mechanical equilibrium theory which follows.)

In terms of the Loschmidt number N and the quantity V,

$$U_0=\tfrac{1}{2}NV. \tag{4}$$

(In the notation of Bragg and Williams[4] $U_0=NV_0/8$, and in that of Fowler[5] $U_0=\frac{1}{2}W_0$ per mole.) The curve 1b is the difference between the curves of 1a; it shows the dependence upon composition (denoted by X percent) of the entire change in configurational energy ($U_{X\text{ percent}}$) between best order and complete disorder.

The remainder of this paper is devoted to examining the details of the transition from the state of minimum energy to the state random arrangement.

II. The Approximate Equilibrium Theory

Definitions and approximations

1. Definition of the state of order.—The Bragg-Williams definition of order is given in terms of the number of right and wrong atoms in the lattice—i.e., those which are or are not in positions appropriate to their species in the state of perfect order. This definition, although very convenient for alloys of simple composition, is unsuitable for this problem, because as the composition is varied the lattice points which are right and wrong do not remain the same. Furthermore, it may introduce artificial distinctions: in Cu_3Au one lattice point out of four is right for Au, but the choice of the set of right points is somewhat arbitrary since any one of four possibilities is physically equivalent.

For this case it proves best to define order in terms of the atoms located upon four sublattices. The face-centered lattice can be divided into four simple cubic sublattices which we shall refer to as L_1, L_2, L_3 and L_4 (Fig. 2a). If the fraction of the L_1 lattice points which are occupied by Au atoms is f_{Au} then a, the order parameter of L_1, is defined by the equation $a=2f_{Au}-1$. In terms of a the fractions of Au and Cu in L_1 are $(1+a)/2$ and $(1-a)/2$, respectively; so that $a=+1$ corresponds to a pure Au partial lattice, $a=-1$ to pure Cu, and $a=0$ to a 50 atomic percent mixture. The order parameters b, c and d of L_2,

[4] W. L. Bragg and E. J. Williams, Proc. Roy. Soc. **151**, 540 (1937), p. 556.

[5] R. H. Fowler, *Statistical Mechanics* (Cambridge University Press, 1936), p. 794.

L_3, and L_4 are similarly defined. Giving the values of the four order parameters will be regarded as specifying "the state of order." The total fractions of Au and Cu present, F_{Au} and F_{Cu}, respectively, are, of course, the averages for the sublattices:

$$F_{Au}=\tfrac{1}{2}+\tfrac{1}{8}(a+b+c+d), \qquad (5)$$
$$F_{Cu}=\tfrac{1}{2}-\tfrac{1}{8}(a+b+c+d).$$

It is readily seen from the figure that each atom is surrounded by twelve nearest neighbors. These are divided four to each of the three other sublattices with none in the same sublattice as the central atom. These facts prove of considerable convenience in setting up the energy expressions.

There are five readily distinguishable types of order which can be expressed by these parameters. First, the disorder type, in which no superlattice is detectable, and hence $a=b=c=d$. We denote this by the symbol (4) meaning that all four order parameters have the same value. Next there is a type for which three order parameters have one value and the other has a different value; this is denoted by (31). Examples of it are furnished by Cu_3Au, which has, in the perfectly ordered state, the parameter value -1 thrice (i.e., 3 pure Cu sublattices) and $+1$ once; the somewhat disordered state of Cu_3Au with values -0.8 thrice and $+0.4$ once is also represented by (31). Similarly, there is a type (22) for which ordered CuAu with $+1$ and -1 each twice is an example. When three distinct values of the parameters are allowed there is only one possibility (211), and also for four values—(1111).

The types of order possess different crystallographic symmetries. In Fig. 2 the different types are indicated schematically, sublattices marked in different ways having different order parameters. The order type (4), which would correspond to the same symbol upon every lattice point, is not shown; it will clearly give rise to a macroscopic cubic symmetry. The order type (31), Fig. 2(*b*), has cubic symmetry as is indicated by the presence of three fourfold symmetry axes represented by heavy arrows. Types (22) and (211) have tetragonal symmetry, while (1111) has orthorhombic symmetry. (These are, so to speak, maximum possible symmetries; they will, however, probably occur for the Cu-Au alloys since

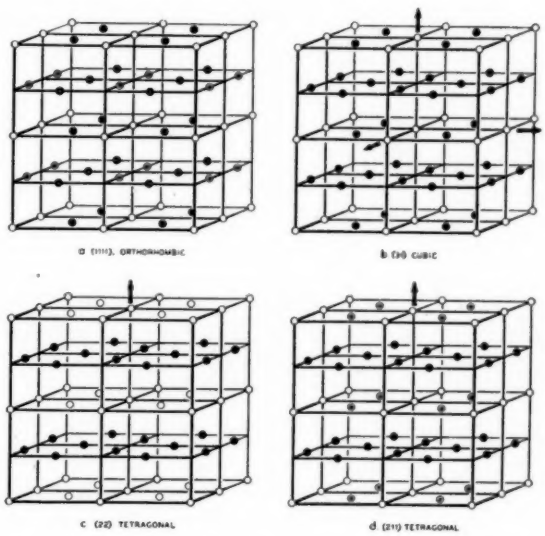

FIG. 2. Diagrams for discussing types of order for Cu-Au alloys. (*a*) Resolution of face-centered lattice into four simple cubic sublattices L_1 ○, L_2 ●, L_3 ⊙, L_4 ○. This also represents the order type (1111) for which all four order parameters have different values. (*b*) Order type (31), with $a\neq b=c=d$ as the example. Heavy arrows indicate fourfold axes. This also represents the known ordered state of Cu_3Au. (*c*) Order type (22), with $a=b\neq c=d$ as the example. This also represents ordered state of CuAu. (*d*) Order type (211), with $a\neq b\neq c=d\neq a$ as the example.

the free ions of these noble metals are known to possess spherical symmetry.) All three symmetry types have been observed in Cu-Au alloys.[6] The theory presented here predicts all but the orthorhombic type; however, there is reason to believe that its absence is due to mathematical approximations.

2. The mathematical approximation: the connection between the configurational energy and the state of order.—There are, of course, a great number of ways of distributing the atoms for a fixed state of order *abcd*. If there are N atoms in the lattice altogether and $n(=N/4)$ on each sublattice, then the number of arrangements is easily shown to be

$$W(abcd)=\frac{n!}{[\tfrac{1}{2}(1+a)n]![\tfrac{1}{2}(1-a)n]!}\cdots\frac{n!}{[\tfrac{1}{2}(1+d)n]![\tfrac{1}{2}(1-d)n]!}. \qquad (6)$$

[6] C. H. Johansson and J. O. Linde, Ann. d. Physik **25**, 1 (1936), who discovered the orthorhombic phase, do not, however, find the (1111) type of order.

Among these many arrangements there will be a great variety of energies depending upon the particular way in which neighboring atoms are placed in the various sublattices. It may readily be shown, however, that for a large number of atoms there is a very narrow range of energy, centered about the average energy, to which all but a very small fraction of the arrangements correspond. The approximation made in this work consists of lumping together all of the arrangements for a given state of order and assigning to them a single definite energy—the average energy. We shall calculate this quantity in Part III and represent it here by the symbol $E(abcd)$.

This approximation is equivalent to that used by Bragg and Williams throughout their work, in which the energy was taken to be a definite function of the long distance order and independent of the particular arrangement. Rather serious errors are produced by this process; in particular no anomalous specific heat occurs above the disordering temperature of the alloy. Methods of improving it have been devised by various writers. The work of Bethe and of Peierls in which the basic concept is that of the arrangement of nearest neighbors—short distance order—has been mentioned. Another method has been developed by Kirkwood[7] which appears very promising. In the first approximation Kirkwood's method reduces to that used here; however, it can readily be formulated in terms of higher approximations, the second of which apparently has an accuracy comparable to that of Bethe while the third should be somewhat better. Due to the mathematical difficulties involved in getting solutions to Kirkwood's second approximation, the first has been used here. However, in view of the possibility of its predicting the appearance of an orthorhombic phase, it would be very interesting to carry out the calculations.

3. The condition for thermodynamic equilibrium.—The condition for thermodynamic equilibrium state of an alloy at a given temperature is that the free energy F must be a minimum. (The effect of the pv term, which is small for a solid, is neglected.) The free energy may conveniently be thought of as arising from three sources: the lattice vibrations, whose energy may be expressed in terms of the Debye temperature; the electrons, whose free energy is related to the degeneracy temperature of the electron gas; and the state of order, which gives rise to the "configurational free energy." In all treatments of order and disorder, it has been assumed that the contributions from the first two sources are independent of the state of order. If this is true, then they can be disregarded, and the equilibrium state of order will be found by minimizing the configurational free energy.

Some preliminary work by F. C. Nix and the writer has shown that the dependence of vibrational free energy upon the state of order may be quite important in the Cu-Au system and has an influence in the right direction to explain the difference in behavior of Cu_3Au and $CuAu_3$. We shall neglect this effect here and consider only the configurational free energy.

The approximation introduced in the last section enables us to give a simple expression for the configurational free energy. Both the energy $E(abcd)$ and the entropy $S(abcd)(=k \ln W(abcd))$ are known functions of the state of order. We must therefore minimize $F=E-TS$ while holding the temperature and composition constant.[8] The resultant values of $abcd$ will then specify the equilibrium state of order.

Results

4. Phase diagram.—When the equilibrium state problem described above is solved (the details of the solution are given in Section III), it is found that the free energy depends upon composition in a distinct way for three different kinds of order. We may conveniently think of these as phases. They are the (4) type cubic disordered phase ξ, the (31) type cubic ordered phase η, and the tetragonal phase ζ, which consists of two distinguishable types ζ_1 and ζ_2 corresponding to (211) and (22) respectively. ζ_1 and ζ_2 join continuously as regards state of order to each other, and for most purposes can be lumped into the single phase ζ. Due to the

[7] J. G. Kirkwood, remarks made at the Symposium on the Structure of Metallic Phases, Cornell University, July, 1937. J. Chem. Phys. **6**, 70 (1938.)

[8] G. Borelius, Ann. d. Physik **20**, 57 (1934) and **24**, 489 (1935), has discussed in a general way the order-disorder phenomenon in these thermodynamic terms. Our work is of a much more specific and detailed nature.

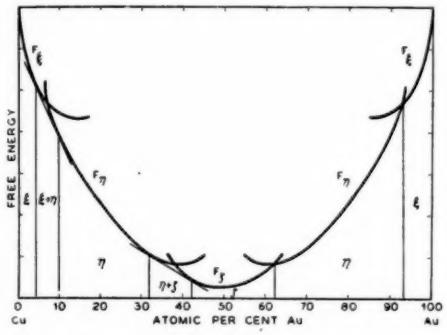

FIG. 3. Schematic representation of free energy *vs.* composition, showing the difference in free energy for the different phases, the crossing points, and the method of finding phase boundaries.

intrinsic symmetry resulting from the nearest neighbor assumption, the same symbols have been used for phases which differ only by interchange of Cu and Au.

The dependence of free energy upon composition for a typical temperature is shown in Fig. 3. (This curve is schematic; in an exact plot the reentrant portions near the crossing points are much less prominent.) It is seen that in different composition ranges different phases are stable. In the neighborhood of the intersection points of the free energy curves, common tangents can be drawn. For compositions between the points of tangency the most stable state of the alloy will be a mixture of two phases having compositions corresponding to the points of tangency.[9] After similar calculations are made for different temperatures a phase diagram can be constructed (Fig. 4). For convenience phase boundaries have been shown on the left while crossing points of the free energy curves are shown on the right. This explains the apparent lack of symmetry. (The extra division of the η phase is not significant and is included for use with Part III.) The temperature T_0, chosen as the unit of temperature in this work, is defined as follows:

T_0 = Temperature above which the 50 percent CuAu alloy is completely disordered.

The relationship between T_0 and U_0, derived in Part III, is

$$RT_0 = 2U_0. \qquad (7)$$

[9] For a discussion of this point see N. F. Mott and H. Jones *The Theory of the Properties of Metals and Alloys* (Oxford University Press, New York, 1936), p. 24.

($T_0 = T_c$ in the notations of Bragg and Williams[4] and of Fowler.[5] The equations analogous to (7) are $T_c = V_0/4k$ and $T_c = W_0/Nk$, respectively.)

If an alloy of, say, 40 percent Au is cooled from the disorder phase ξ so slowly that it is in the equilibrium state, it will at a certain temperature commence to acquire a second phase of the η type with a composition of more than 40 percent Au. As it is cooled through the two-phase region the η phase becomes more abundant and its composition approaches 40 percent until at the lower boundary a phase of pure η results. A similar transition from η to ζ will occur at lower temperature.

In actual experiments, the times required to produce equilibrium are frequently very long. For this reason certain experimental effects were at first considered to be hysteresis whereas they really represented a nonequilibrium behavior.[10] These effects depended mainly upon establishing an equilibrium state in a single phase. The process of producing two phases of different composition, requiring first of all the formation of nuclei for growth of the new phase and involving the transport of an appreciable fraction of the atoms across phase boundaries, will, of course, be much slower; and for this reason will be very difficult to observe.

If the formation of two phases with different compositions does not have time to occur, then the behavior of the alloy is to be predicted from the right side of Fig. 4. Here an alloy of 40 percent Cu when cooled from the ξ phase passes abruptly into the η phase with the production of

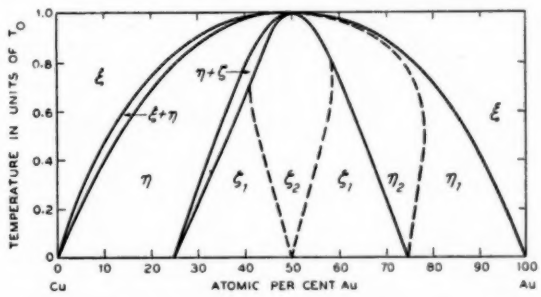

FIG. 4. Phase diagram: Left half conventional; right half alloy restrained to one phase of prescribed composition. Both diagrams when shown in full are symmetrical about 50 atomic percent.

[10] G. Borelius, Proc. Phys. Soc. **49**, 77 (1937), however, refers to some experimental effects which are apparently true hysteresis.

a latent heat. Further cooling again produces an abrupt transition to the ζ phase with another latent heat.

Even the single phase type of transition may be prevented from taking place due to the effective freezing out of atomic interchange at low enough temperatures. Anomalous specific heat, attributable to ordering processes, has been observed by Sykes and Jones[11] at temperatures as low as 60°C. However, at this temperature only changes in the degree of order in a phase take place and apparently no change of order type is possible. It is probable that only for temperatures in the top third of Fig. 3 (above 200°C in the actual case) will the ordering process be rapid enough to allow realization of changes of phase.

The latent heats per gram atom in making the transitions from ξ to η and η to ζ are represented by the upper and lower curves, respectively, of Fig. 5.

5. Behavior of various fixed compositions with temperature.—The behavior of a given composition as a function of temperature is of particular interest as it has close correspondence with experimental work. In this treatment, the possibility of two phase regions is disregarded for the reasons given previously.

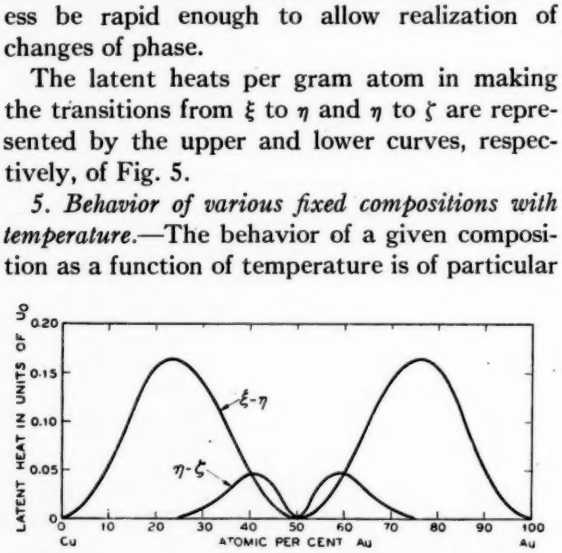

FIG. 5. The latent heats of transformation per gram atom from ξ to η and η to ζ as functions of composition.

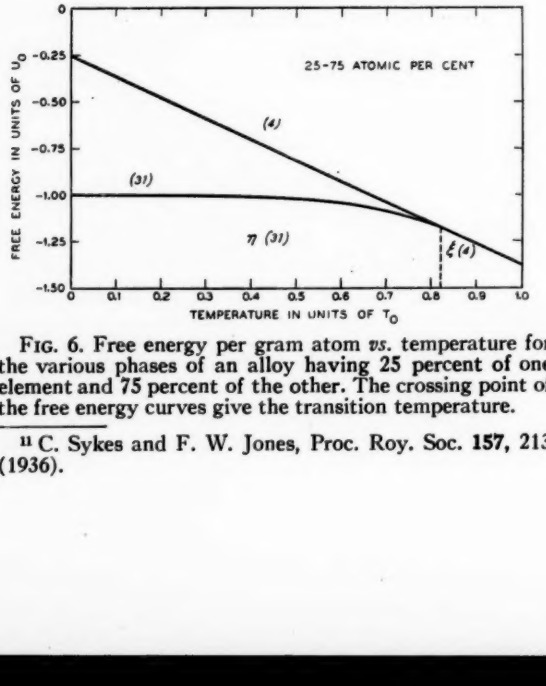

FIG. 6. Free energy per gram atom *vs.* temperature for the various phases of an alloy having 25 percent of one element and 75 percent of the other. The crossing point of the free energy curves give the transition temperature.

Figure 6 shows the dependence of the free energy upon temperature for an atomic ratio of 1 : 3 (either Cu_3Au or $CuAu_3$ being implied since the symmetry about 50 atomic percent makes them equivalent). We see that at low temperatures the free energy is less for the (31) or η phase than for the (4) ξ phase. At $T=0.82T_0$, the curves cross and (4) is less than (31); hence at this temperature there is a transition from the η to the ξ phase. Since the slope of the free energy curve is minus the entropy, the latent heat is T times the difference in the slopes of the two curves at the crossing point.[12] Similar curves have been analyzed for other compositions. (The free energies of Fig. 6 differ from F by additive constants; they are actually $\psi/4$ as defined in Part III.)

As pointed out previously, these curves should be modified by adding to them the order-dependent part of the other free energies, such as that of lattice vibrations. Near the crossing points there is very little difference between the various free energy curves like those of Fig. 6. For this reason, we may expect a consideration of vibrational free energy to modify considerably the results presented here.

The behavior of the configurational energy as a function of temperature is shown for several compositions in Fig. 7. Of the two percentages on each figure, either may refer to the Cu and the other to the Au. The energies are given in terms of $U_{x\ \text{percent}}$, the entire difference in energy between order and disorder. The actual change in terms of U_0, as determined from Fig. 1(*b*), is also indicated. We note that all compositions except 50 percent show a latent heat. Both 37.5 and 45 percent show two latent heats, which are very small for 45 percent.

The absence of a latent heat at 50 atomic percent is due mathematically to the smooth joining of the free energy curves, like those of Fig. 6. If we include the dependence of vibrational free energy upon order, there is no reason to suppose that the curves will still join without a break in slope.

[11] C. Sykes and F. W. Jones, Proc. Roy. Soc. **157**, 213 (1936).

[12] $dF/dT=dE/dT-TdS/dT-S=C_v-TC_v/T-S=-S$. $\Delta E=T\Delta S$.

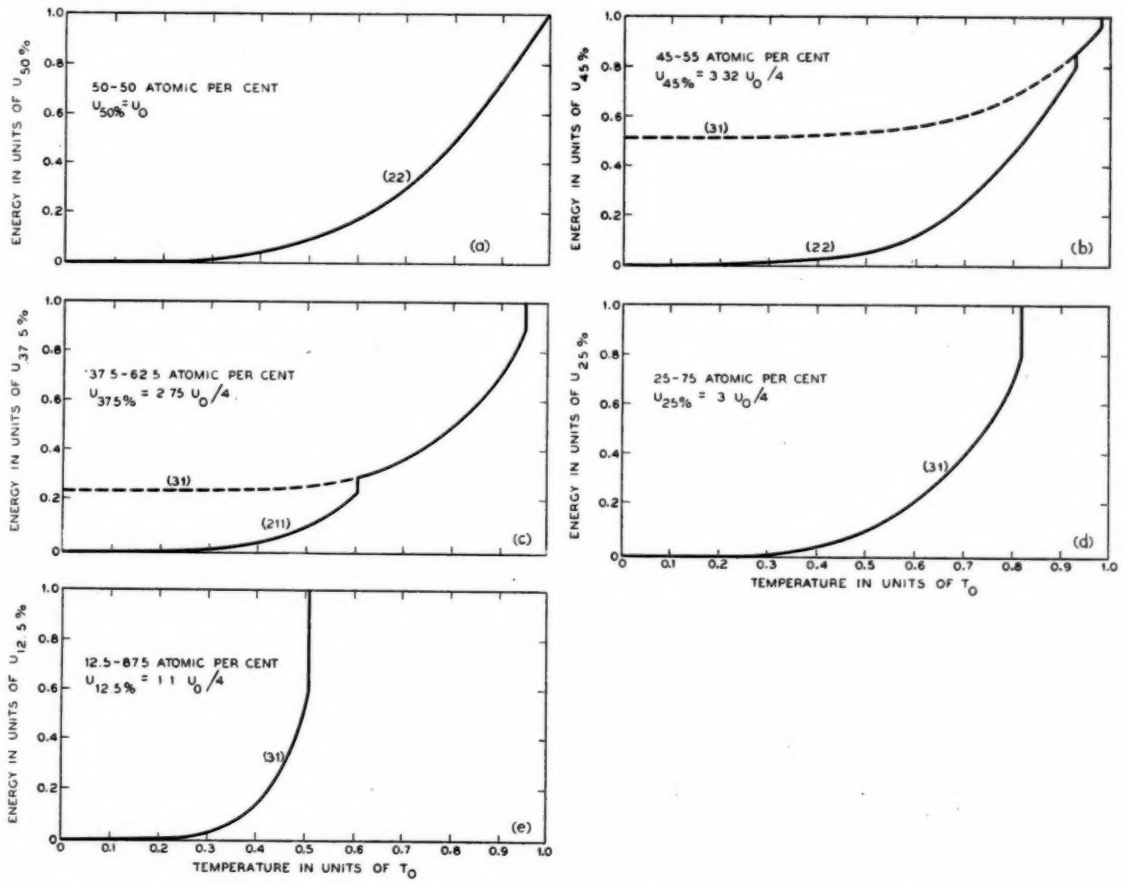

FIG. 7. Energy per gram atom due to disordering *vs.* temperature for fixed compositions. The unit on the energy scale has been chosen as the energy necessary to disorder completely the alloy. The value of this quantity in terms of U_0 is also shown.

For CuAu it is observed experimentally that there is a discontinuity in lattice constants at the critical temperature[6] and it is natural to expect an associated energy discontinuity and latent heat.

Figure 8 shows the specific heat per gram atom for the same set of compositions.

Figure 9 shows the change in order as a function of temperature. The number next to each curve indicates the number of order parameters which have the value corresponding to the ordinate of the curve. The larger atomic percentages refer to Cu in this case. For corresponding Au percentages, the vertical scale should be reversed in sign.

The compositions 25 percent and 50 percent have been previously treated by Bragg and Williams and the results here are repetitions except for correlation of the respective critical temperatures and energy changes.

6. Dependence of state of order upon composition at fixed temperature.—For temperatures above T_0 the behavior of the order parameters as functions of composition is very simple. Fig. 4(*d*) shows that each sublattice has the same composition as the whole sample. A calculation of energy for this case leads to the upper curve of Fig. 1(*a*).

At absolute zero the behavior, shown in Fig. 10*a*, is also fairly simple. Starting with pure Cu and adding Au, the process consists of converting first one entire sublattice to Au. This is complete at 25 percent Au, and during the process the order type is (31), the η phase. Next another sublattice is converted to Au ending at 50 percent Au; during this the order type is (211), ζ_1 phase.

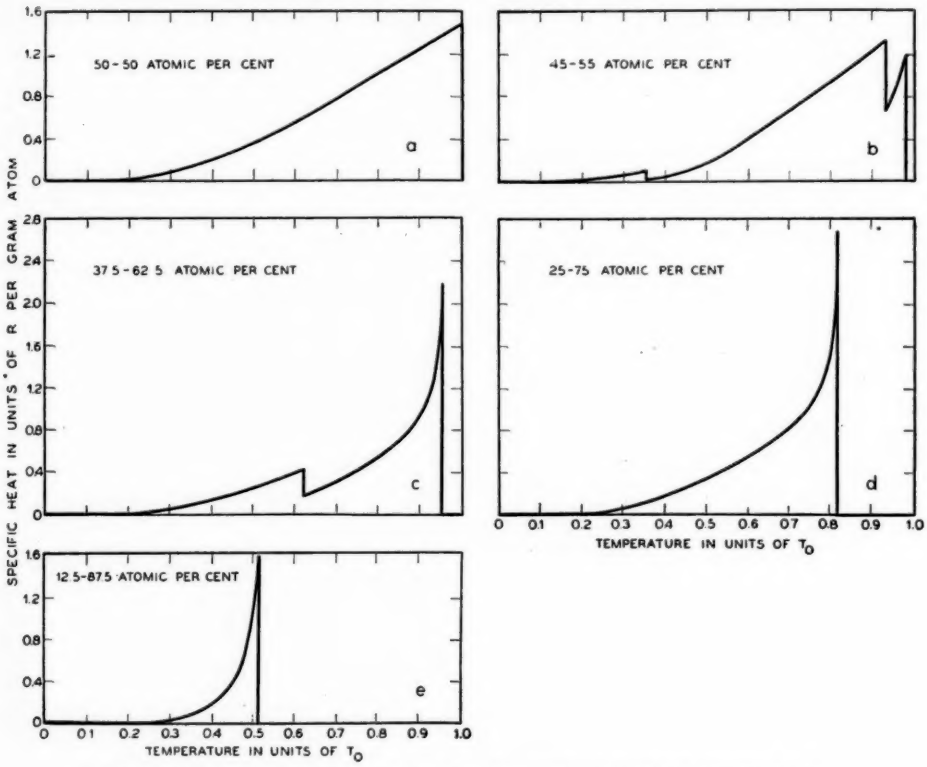

FIG. 8. Heat capacity per gram atom *vs.* temperature for fixed compositions.

Two more such processes result in pure Au. At any stage in the process three of the sublattices are purely Au or else Cu, while the fourth is in an intermediate stage. These situations lead to the lower curve of Fig. 1(*a*). (See III, 2 for a proof that this is the lowest possible curve.) It is realized that some of the aspects of this description are too detailed and result only from the mathematical approximation. Thus for composition less than 25 percent, the state of lowest energy can be realized without any long distance order.

For an intermediate temperature $T=0.4T_c$, for example, the behavior is more complicated. From the phase diagram, neglecting the two-phase possibility, Fig. 4, we see that from 0 percent to 10 percent Au we have the disordered ξ phase, hence the state of order is the same as for $T>T_0$. Between 10 percent and 33 percent the alloy is in the η or (31) state; hence three order parameters have one value and one a different value. It is seen in Fig. 10*b* which shows quantitatively the effects discussed above, that for the η phase up to 25 percent Au the equilibrium order differs only slightly from the $T=0$ state of order. Above 25 percent instead of going at once to (211) order, ζ_1 type, which corresponds to $T=0$, the η type persists considerably modified up to 33 percent, when a shift over to (211) order takes place. The (211) order holds only up to 44 percent, when it is replaced, without any break in state of order, by (22).

At $T=0.8T_c$ the behavior is generally similar. The difference from $T=0$ order is more marked and the (211) region, ζ_1, has been swallowed up by (31), η, which has moved to higher compositions, and (22), ζ_2, which has widened its range.

For still higher temperatures the η and ζ regions move closer about 50 percent and nearer to the line of complete disorder, until at last at T_c only the latter remains.

III. Mathematical Details

1. Simplification of the energy expression

Since the results derived in this section depend only on the nearest neighbor assumption and

apply to any binary alloy, we shall substitute A and B for Cu and Au. Consider a lattice containing N atomic sites each surrounded by z nearest neighbors; the total number of pairs will then be

$$Q=\tfrac{1}{2}zN. \tag{8}$$

Let Q be made up of Q_{AA}, Q_{BB}, and Q_{AB} pairs of the different types. Next imagine that a model of the alloy, consisting of wooden balls and wooden rods representing the atoms and the lines between pairs, is pulled apart into pairs, each pair carrying with it $1/z$th of a ball at either end. Each AA pair then has the fraction $(2/z)$ of a A ball, etc. If the total numbers of A and B balls in the model are F_AN and F_BN then we must have

$$F_AN=(2/z)Q_{AA}+(1/z)Q_{AB}, \tag{9a}$$

$$F_BN=(2/z)Q_{BB}+(1/z)Q_{AB}. \tag{9b}$$

We can solve these for the like neighbor pairs:

$$Q_{AA}=F_AQ-\tfrac{1}{2}Q_{AB}, \tag{10a}$$

$$Q_{BB}=F_BQ-\tfrac{1}{2}Q_{AB}. \tag{10b}$$

Let us next consider the energy of the alloy as compared to the energy of two pure crystals of A and B from which it could be made. The energy of a crystal of pure A with F_AN atoms will be V_{AA} times the number of pairs, which is $(z/2)F_AN=F_AQ$. Hence the energy in question is

$$E=V_{AA}Q_{AA}+V_{BB}Q_{BB}+V_{AB}Q_{AB}-F_AV_{AA}Q-F_BV_{BB}Q, \tag{11}$$

which reduces to

$$E=[V_{AB}-\tfrac{1}{2}(V_{AA}+V_{BB})]Q_{AB}. \tag{12}$$

It is best to define a new quantity

$$V=V_{AA}+V_{BB}-2V_{AB}. \tag{13}$$

In terms of V the energy is

$$E=-\tfrac{1}{2}VQ_{AB}. \tag{14}$$

The meaning of V is indicated in the diagram below:

A A A–B A–B A A		A A A–A B–B A A
lesser energy	difference V	greater energy

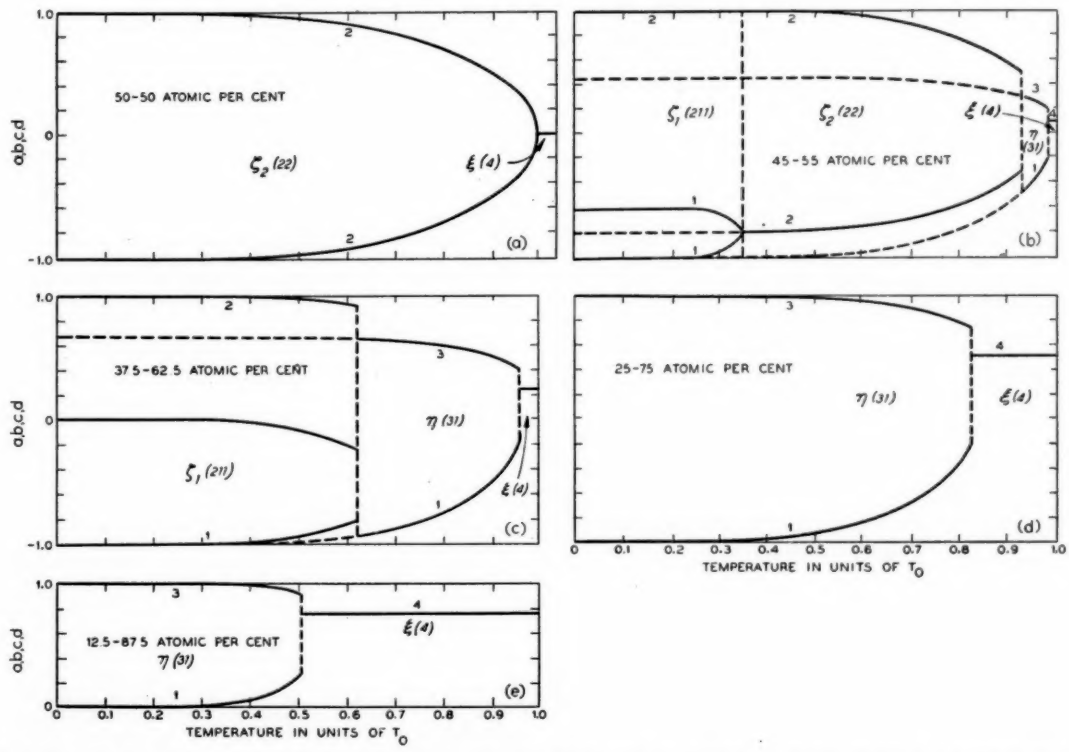

FIG. 9. State of order *vs.* temperature for fixed compositions. The number near each curve shows the number of order parameters whose common value is given by the ordinate. (The larger percentages refer to Cu.)

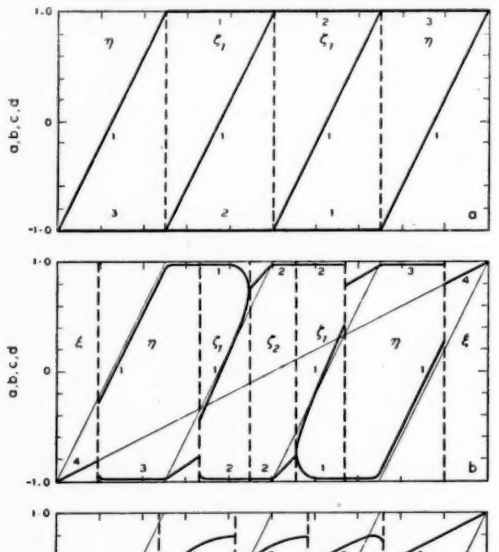

FIG. 10. Dependence of state of order upon composition for several fixed temperatures: *a*, $T=0$; *b*, $T=0.4T_0$; *c*, $T=0.8T_0$; d, $T>T_0$. The numbers next to the heavy lines indicate the number of order parameters whose values are given by the ordinates.

We see that V must be positive or else there will be a tendency at low temperature for the alloy to separate into two components of pure A and B, contrary to the assumption that we are dealing with an alloy which forms a superlattice at low temperatures.

2. Determination of the curves of Fig. 1

The determination of the high temperature curve of Fig. 1(*a*), which corresponds to random arrangements and hence to the state of order represented by Fig. 10*d*, is postponed to the next section where $E(abcd)$ is treated. There is no difficulty in connection with it since random order can be clearly defined and the average energy readily calculated. The situation is quite different for the lowest energy curve, for in its case we must prove that the best possible arrangement can only give a certain number of CuAu pairs, namely that indicated by the lowest curve of Fig. 1(*a*).

Consider again a wooden model of the alloy in which for the moment nothing is specified about the arrangement of the balls. Let this be divided into cubes the corners of which are the midpoint of balls upon one of the sublattices. Every one of these cubes will have one-eighth of a ball at each of its eight corners and one-half a ball on each of its faces—4 balls in all—there will be twelve rods in its body and twenty-four half rods lying in its faces—24 rods in all. One may easily show that Eqs. (9) and (10) apply to this case with $N=4$ and $Q=24$. There are $N/4$ of these cubes and we number them with integers $1, 2, \cdots, i, \cdots N/4$. Now let the number of Cu balls in cube i be n_i, where n_i, may have any value from 0 to 4 in steps of $\frac{1}{8}$. Let the number of CuAu rods be q_i. Then we have

$$F_{\mathrm{Cu}}N=\Sigma n_i, \tag{15}$$

$$Q_{\mathrm{CuAu}}=\Sigma q_i. \tag{16}$$

Next we consider a particular cube having n Cu's. By actual trial (rearranging the n Cu's, divided into half balls and eighth balls among all the corners and faces) we find that there is a certain maximum possible number of CuAu pairs, $q(n)$, for each value of n. This number is shown in Fig. 11 as a function of n. Since q_i must

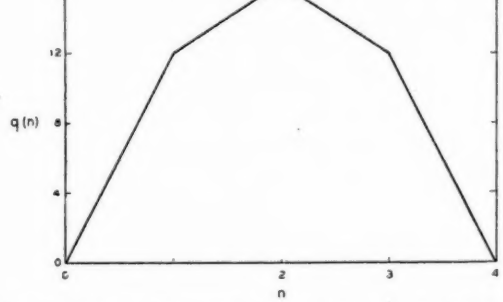

FIG. 11. Plot of the maximum possible number of AuCu pairs, $q(n)$, for one of the cubic cells as a function of the number of Cu atoms in the cell n. This function is defined only for values of n which are integer multiples of $\frac{1}{8}$; the straight lines are drawn through such points.

be less than or equal to $q(n_i)$ we may write

$$Q_{\mathrm{CuAu}} \leqq \Sigma q(n_i). \tag{17}$$

Suppose now that two cubes have different numbers n_i and n_j. If n_i and n_j lie on different sides of a kink in Fig. 11, then bringing them nearer together while keeping n_i+n_j constant (thus preserving (15)) will increase $q(n_i)+q(n_j)$. The maximum value of $\Sigma q(n_i)$ will then be obtained by choosing all n_i in the same range between two of the kinks. This will give

$$Q_{\mathrm{CuAu}} \leqq (N/4)q(\bar{n}), \tag{18}$$

where $\bar{n}=4F_{\mathrm{Cu}}$.

This argument does not show that such a high value of Q_{CuAu} can be obtained. However, the type of order given in Fig. 10*a* leads to just this optimum result and hence the curve of Fig. 1*a*, drawn on that basis, is the true minimum.

3. Calculation of the energy, E ($abcd$)

We shall now specialize upon a face-centered lattice containing N atoms in all of mixed Au and Cu and in a state of order *abcd*. We wish to know the average value of the energy E when we average over all arrangements of the atoms keeping *abcd* fixed. Consider a pair consisting of atoms in L_1 and L_2. During the averaging process, the atom of L_1 is Au in a fraction $\frac{1}{2}(1+a)$ of the arrangements and the atom of L_2 is Cu in a fraction $\frac{1}{2}(1-b)$ of the arrangements. Hence this pair is $L_1\mathrm{Au}L_2\mathrm{Cu}$ in a fraction $(1+a-b-ab)/4$ of the arrangements. Similarly the situation $L_1\mathrm{Cu}L_2\mathrm{Au}$ occurs in a fraction $(1-a+b-ab)/4$. Hence an L_1L_2 pair is of AuCu type in $(1-ab)/2$ of the arrangements. Of the entire Q pairs in the lattice, $\frac{1}{6}$ are between L_1 and L_2. Hence in the average the contribution of L_1L_2 to Q_{CuAu} will be

$$(1/12)(1-ab)Q \tag{19}$$

and the average value of Q_{CuAu} will be

$$\bar{Q}_{\mathrm{CuAu}}=(1/12)[6-(ab+ac+ad+bc+bd+cd)]Q. \tag{20}$$

This expression can be simplified by introducing the quantity

$$C=a+b+c+d. \tag{21}$$

C is a parameter which represents the composition of the alloy. In terms of C

$$F_{\mathrm{Au}}=(4+C)/8, \tag{22a}$$

$$F_{\mathrm{Cu}}=(4-C)/8. \tag{22b}$$

and

$$\bar{Q}_{\mathrm{CuAu}}=(1/24)[12-C^2+(a^2+b^2+c^2+d^2)]6N. \tag{23}$$

Hence the energy is given by

$$E=-\tfrac{1}{2}V\bar{Q}_{\mathrm{CuAu}}$$
$$=(NV/8)[-(a^2+b^2+c^2+d^2)+C^2-12]. \tag{24}$$

4. Calculation of the entropy, S ($abcd$)

The logarithm of one term in the entropy expression is

$$ln\frac{n!}{[\frac{1}{2}(1+a)n!\frac{1}{2}(1-a)n]!}$$

$$=\frac{n}{2}[2ln2-(1+a)ln(1+a)-(1-a)ln(1-a)]$$

$$=(N/8)\eta(a), \tag{25}$$

where $\eta(a)$ is the quantity in the square brackets. Hence the entropy is

$$S=\tfrac{1}{8}kN[\eta(a)+\eta(b)+\eta(c)+\eta(d)]. \tag{26}$$

5. New units and the free energy

Before dealing with free energy we shall introduce some convenient units of temperature, energy, and entropy. The new temperature, t, is measured in units of V/k and from (4) and (7), which can be regarded as definitions of U_0 and T_0 at present, we obtain

$$t=T/(V/k)=T/(NV/R)=T/T_0. \tag{27}$$

We next restrict N to mean Loschmidt's number so that we have to do with one gram atom. A new energy, u, and free energy, f, measured in units of $V/8$ per atom are related to E and F as follows:

$$u=8E/NV=4E/U_0, \tag{28}$$

$$f=8F/NV=4F/U_0. \tag{29}$$

Hence quarter units on energy scales measured in units of V_0 are now units for u and f.

The value of entropy in units of $k/8$ per atom is s so that

$$s=8S/R. \tag{30}$$

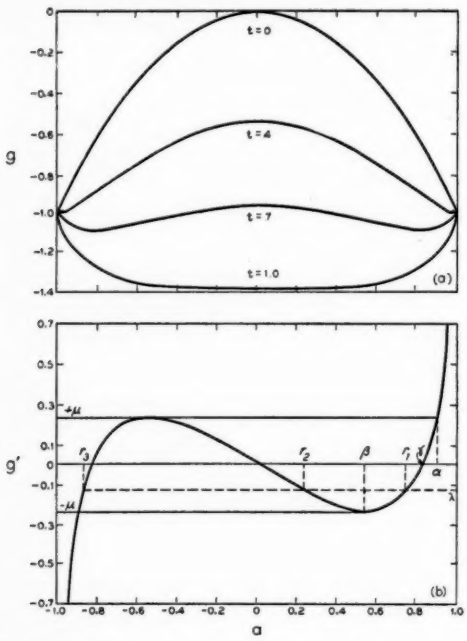

FIG. 12. (a) Plot of $g(a)=-a^2-t\eta(a)$ *vs.* a with t as a parameter for four values of t. (b) Plot of $g'(a)=dg/da$ for $t=0.7$ showing the meaning of α, β, γ, μ, λ, r_1, r_2, r_3.

The values of u, f and s are found to be

$$u=-(a^2+b^2+c^2+d^2)+C^2-12, \tag{31}$$

$$f=u-t(\eta(a)+\eta(b)+\eta(c)+\eta(d)), \tag{32}$$

$$s=\eta(a)+\eta(b)+\eta(c)+\eta(d). \tag{33}$$

6. Minimization of the free energy

Our problem is therefore to minimize f while keeping C constant. For this purpose we may omit the C^2-12 from f. Writing

$$g(a)=-a^2-t\eta(a), \tag{34}$$

we have

$$\psi=f-C^2+12=g(a)+g(b)+g(c)+g(d). \tag{35}$$

The method of La Grange multipliers at once yields the equations

$$g'(a)=g'(b)=g'(c)=g'(d)=\lambda. \tag{36}$$

Figure 12 shows the behavior of $g(x)$ with t as a parameter and also the shape of the derivative $g'(x)$ for $t=0.7$.

We see that for $\mu>\lambda>-\mu$, there are three roots $r_1r_2r_3$ of the equation

$$g'(x)=\lambda. \tag{37}$$

The La Grange equations unfortunately do not show which order parameters have which roots. They show merely that for the minimum conditions the values of the four-order parameters must be chosen from the three roots of Eq. (37). There are in all 15 distinct ways of assigning three different values to a set of four numbers. Let the number of order parameters assigned to value r_1 be n_1, to r_2 be n_2, to r_3 be n_3. Then each distinct set of values of the triplet $n_1n_2n_3$ corresponds to one of the 15 ways of satisfying Eq. (36). In Table I the 15 different triplets are classified according to the type of order. For example, the triplet 202 means that two order parameters are equal, having value r_1, and are different from the other two which are also equal, having value r_3; this situation corresponds to the type of order (22). There appears to be no way of telling *a priori* which triplet gives the lowest free energy for a given C. Hence we proceed by calculating the functions

$$\psi(n_1n_2n_3\lambda)=n_1g(r_1(\lambda))+n_2g(r_2(\lambda))+n_3g(r_3(\lambda)), \tag{38}$$

$$C(n_1n_2n_3\lambda)=n_1r_1(\lambda)+n_2r_2(\lambda)+n_3r_3(\lambda), \tag{39}$$

which give the values of ψ and corresponding values of C when the order parameters are chosen according to the possibilities shown in the table. The values of ψ are then plotted *versus* C; the lowest ψ for a given C represents the true minimum for that composition, while the other curves represent only virtual minima, for which $\delta\psi=0$ for small changes in order satisfying $\delta C=0$.

The results of plotting all fifteen realizations of the 4 kinds of orders are shown in Fig. 13.

Certain features of this figure should be pointed out. For $\lambda=-\mu$, $r_1=r_2=\beta$ and $r_3=-\alpha$, and hence the curves 400, 310, 220, 130, and 040 have the common values $\psi=4g(\beta)$, $C=4\beta$. Similarly 301, 211, 121, 031 meet at $\psi=3g(\beta)+g(\alpha)$, $C=3\beta-\alpha$; 202, 112, 022 at $\psi=2g(\beta)+2g(\alpha)$, $C=2\beta-2\alpha$; 103 and 013 at $\psi=g(\beta)+3g(\alpha)$, $C=\beta-3\alpha$; the curve 004 is at $\psi=4g(\alpha)$, $C=-4\alpha$. This set of branch points are

TABLE I.

TYPE OF ORDER	CORRESPONDING TRIPLETS
(4)	400, 040, 004
(31)	310, 301, 130, 031, 103, 013
(22)	220,202, 022
(211)	211, 121, 122
(1111)	Impossible

colinear and will be referred to as the $-\mu$ series. When λ equal $+\mu$, the $+\mu$ series of branch points is obtained for which triplets $n_1n_2n_3$ with a common value of n_1 meet.

The slope $d\psi/dC$ along the curves is equal to λ, as may be verified at once:

$$\frac{d\psi(n_1n_2n_3\lambda)}{d\lambda}=n_1g'(r_1)\frac{dr_1}{d\lambda}+n_2g'(r_2)\frac{dr_2}{d\lambda}+n_3g'(r_3)\frac{dr_3}{d\lambda}$$
$$=\lambda\left[n_1\frac{dr_1}{d\lambda}+n_2\frac{dr_2}{d\lambda}+n_3\frac{dr_3}{3\lambda}\right]$$
$$=\lambda(d/d\lambda)[n_1r_1+n_2r_2+n_3r_3]$$
$$=\lambda(d/d\lambda)C(n_1n_2n_3\lambda). \quad (40)$$

Hence

$$d\psi/dC=(d\psi/d\lambda)/(dC/d\lambda)=\lambda. \quad (41)$$

This accounts for the fact that all curves have the same slope $-\mu$ on the $-\mu$ series and $+\mu$ on the $+\mu$ series.

Another regular array of points is produced by $\lambda=0$. For these points

$$\psi(n_1n_2n_3)=(n_1+n_3)g(\gamma)+n_2g(0), \quad (42)$$

$$C(n_1n_2n_3)=(n_1-n_3)\gamma. \quad (43)$$

At them $d\psi/dC=\lambda$ is 0. These are called the $\lambda=0$ array.

As a curve goes from a point of the $-\mu$ array the slope $d\psi/dC$ increases from $-\mu$ to a value zero, at a point of the $\lambda=0$ array, and then to $+\mu$ when the curve reaches the $+\mu$ series. Next suppose C attains values not between those of its end points on the $\pm\mu$ series; then if we follow the curve in the sense of continually increasing λ, we reach a point where C is an extremum. At this point $d\psi/dC$ must lie between $+\mu$ and $-\mu$, and when the curve turns back it does so with a finite slope, thus producing a sharp point on the curve.

Investigations can also be carried out to determine the direction of the curves as they pass through points of the $\lambda=0$ array, and also to see which leave with greater curvature at points of the $\pm\mu$ series. With this information, reasonably accurate plots like that of Fig. 13 can be drawn using only these limiting values of λ. This has been the procedure adopted for values of t except 0.7, for which quite complete calculations were made.

The curves of Fig. 13 are symmetrical about $C=0$, that is 50 atomic percent. The division

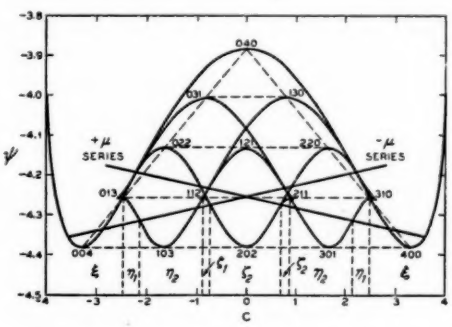

FIG. 13. Plot of ψ *vs.* C, showing the phases having lowest free energy for each composition.

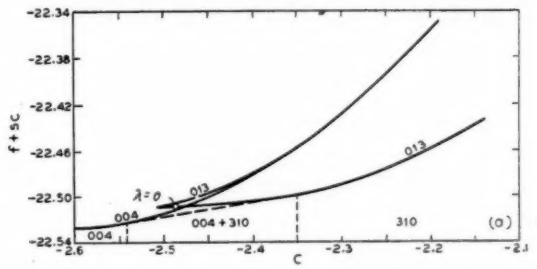

FIG. 14. Free energy f plus a linear term in composition *vs.* composition, showing the method of determining phase boundaries and two phase regions.

into stable states is indicated in the same notation as is used in connection with the phase diagram.

7. Calculation of the phase boundaries

Figure 13 cannot conveniently be used to find phase boundaries. A tangent to the minimum points of the ψ curves, being a parabola in the f *vs.* composition plane, does not give phase boundaries. Fig. 14 shows an enlargement of the region including $\xi+\eta$; the linear term in C added to f has been chosen so as to facilitate plotting and does not, as does the C^2 term by which ψ differs from f, distort the relations derived from the tangency. For values of t other than 0.7 the width of the two-phase region has been estimated roughly. The behavior near $t=0$ and $t=1$ is generally correct.

8. Behavior of various fixed compositions with the temperature

The work with the fixed compositions was carried out somewhat differently. For points in the $\xi(4)$, $\eta(31)$, and $\xi(22)$ regions there is only one independent order parameter, the second being determined in terms of the first and the composition. Thus for $\eta(31)$ we have *abbb* for the state of order. For composition value C we can derive the equations

$$b=(C-a)/3 \quad (44)$$

and

$$\psi(31)=-a^2-3b^2-t[\eta(a)+3\eta(b)]. \quad (45)$$

Hence for equilibrium

$$d\psi/da=0$$

or

$$t=-\frac{2}{3}\frac{C-4a}{\ln[(1-a)(1+b)/(1+a)(1-b)]}. \quad (46)$$

From this relationship t was found as a function of a and then ψ was computed and plotted *versus* t. The intersection with

$$\psi(4) = -\tfrac{1}{4}C^2 - 4t\eta(C/4) \tag{47}$$

gives the critical temperature. The energy content, $\mu = -(a^2+3b^2)$, and the state of order were also plotted.

The specific heat was found by differentiating (46), obtaining

$$\frac{dt}{da} = +\left[\frac{8-2a^2-6b^2}{(1-a^2)(1-b^2)}t - 8\right] \div 3\ln\frac{(1-a)(1+b)}{(1+a)(1-b)}. \tag{48}$$

Combining this with

$$du/da = 2(b-a) \tag{49}$$

and transforming to E and T, we obtain

$$C_v = \frac{dE}{dT} = \frac{(\dot{N}V/8)du}{(V/k)dt} = \frac{R}{8}\frac{(du/da)}{(dt/da)}. \tag{50}$$

Similar calculations applied to $\xi(22)$ yield

$$b = C/2 - a, \tag{51}$$

$$\psi(22) = -2(a^2+b^2) - 2t[\eta(a)+\eta(b)], \tag{52}$$

$$t = \frac{C-4a}{\ln[(1-a)(1+b)/(1+a)(1-b)]}, \tag{53}$$

$$dt/da = [4 - t(4-2a^2-2b^2)/(1-a^2)(1-b^2)] \div \ln[(1+a)(1-b)/(1-a)(1+b)], \tag{54}$$

$$du/da = 4(b-a). \tag{55}$$

This method when applied to Cu_3Au and CuAu is mathematically identical with the work of Bragg and Williams and the results are in harmony with theirs.

The values needed for (211) with compositions 37.5 percent and 45 percent were estimated from the ψ *vs.* C curves for various temperatures. They are not very accurate, but since the entire set of calculations must be viewed with regard to suggested trends rather than high accuracy, they are probably quite good enough.

9. Latent heat curves

The latent heats for the $\xi-\eta$ transformation were taken from the work at constant C. The regions near $C=4$ and $C=0$ were obtained, respectively, from Fig. 1*b* and from an analytic expansion of $\psi(4)$ and $\psi(31)$. Two values for the $\eta-\zeta$ transformation were found from detailed work at $t=0.7$ and 0.6. The behavior near $C=0$ was found analytically.

IV. Conclusions

The "nearest neighbor assumption" is capable of giving a coherent description of the Cu–Au alloy system showing how the ordered structures of Cu_3Au and CuAu are related by an intermediate series of phases. It cannot possibly describe the behavior in correct detail because it requires symmetry about 50 atomic percent which does not actually exist. One simple modification which will effect improvement (inclusion of vibrational free energy) is mentioned.

Two new features are brought out by this work: a definition of the "state of order" which is applicable to a wide composition range; and the theoretical possibility of two transition temperatures with two latent heats.

The writer is indebted to Professor J. G. Kirkwood, Dr. F. Seitz, and Dr. L. P. Bouckaert for several interesting discussions which were helpful in crystallizing the ideas presented here, and to Drs. C. J. Davisson and F. C. Nix for their continued interest and encouragement in the progress of this work. Sincere thanks are due also to Miss E. C. Kempfer who carried out the computational work and Mr. H. M. Yates who furnished the figures.

The Unimolecular Decomposition of Gaseous Chloropicrin

E. W. R. STEACIE AND W. McF. SMITH*
Physical Chemistry Laboratory, McGill University, Montreal, Canada
(Received December 6, 1937)

The decomposition of gaseous chloropicrin has been investigated in the temperature range 138 to 170°C at pressures from 6 to 20 cm. The reaction is homogeneous and unimolecular, the rate constants being expressed by the equation

$$k = 4.90 \times 10^{15} e^{-37670/RT} \text{ sec.}^{-1}.$$

The products of the reaction are phosgene, nitrosyl chloride, nitric oxide, and chlorine, as represented stoichiometrically by the equation

$$\begin{array}{c} CCl_3NO_2 = COCl_2 + NOCl \\ \qquad\qquad\quad \downarrow\uparrow \\ \qquad\qquad\quad NO + \tfrac{1}{2}Cl_2. \end{array}$$

There is, however, evidence to show that at least part of the nitric oxide and chlorine are formed otherwise than by the decomposition of nitrosyl chloride.

INTRODUCTION

REACTIONS of simple inorganic molecules have the advantage that they are often more clear-cut and free from secondary changes than are organic reactions. From this point of view completely substituted organic molecules are also advantageous. Recent work in this laboratory on the decomposition of the alkyl nitrites has furnished considerable information on the effect of chemical constitution on the reaction rate. Unfortunately, however, the effect of substituents cannot be investigated since practically all substituted aliphatic nitrites are impossible to prepare. A search has therefore been made for a suitable simple molecule in which it should be possible to vary the substituents. Chloropicrin has been chosen, since it should be feasible to replace successively the chlorine atoms by other halogens.

The decomposition of chloropicrin has been previously investigated in a purely qualitative way by Gardner and Fox,[1] who found that it decomposes slowly at its boiling point into phosgene and nitrosyl chloride. A brief investigation of the kinetics of the process has also been made by Radulescu and Zamfirescu.[2] They heated weighed amounts of chloropicrin in sealed ampules in an oil bath, and after the lapse of different intervals of time removed the tubes and analyzed for undecomposed chloropicrin by titration with permanganate. No analysis of the products of the reaction was made. Also, no statement is made of the pressure existing in the sealed tubes, or whether the reaction was investigated in the liquid or in the vapor phase. They found the reaction to be first order, but made no test of its homogeneity. Their velocity constants were very reproducible, typical values given by them being

$$k_{131.1} = 0.11 \times 10^{-3} \text{ sec.}^{-1},$$
$$k_{141.2} = 0.32 \times 10^{-3} \text{ sec.}^{-1},$$
$$k_{151.1} = 0.97 \times 10^{-3} \text{ sec.}^{-1},$$
$$k_{161.2} = 3.27 \times 10^{-3} \text{ sec.}^{-1}.$$

From these results we may estimate the activation energy to be about 40,000 cal.

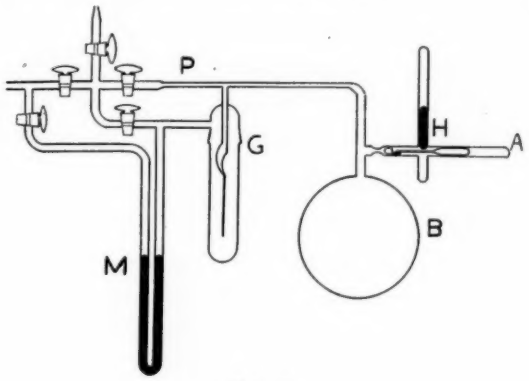

FIG. 1.

* Holder of a Studentship from the National Research Council of Canada.

[1] Gardner and Fox, J. Chem. Soc. (London) **115**, 1188 (1919).

[2] Radulescu and Zamfirescu, Bull. Soc. Chim. Romania **17**, 87 (1935).

Experimental

The reaction was followed by observing the rate of pressure change in an all-glass system of constant volume. A diagram of the apparatus is given in Fig. 1. The entire reaction system was constructed of Pyrex glass. The reaction vessel *B* had a capacity of about 1 liter, and was immersed in an electrically heated oil bath. The temperature was controlled manually to within ±0.15°C, and was measured by standard mercury thermometers. The reaction vessel was connected to the magnetic hammer *H* and to the glass manometer *G*, which was of the spoon type. The tip of the glass manometer was illuminated with blue light (Corning blue green filter no. 430) and viewed through a telescope with an adjustable cross hair in the eyepiece. A number of gauges of different sensitivity were employed at various times, but in no case was the sensitivity less than 0.5 mm. The outside jacket of the glass manometer was connected to the mercury manometer *M* and to an air-pressure regulating system, the glass gauge being used as a null instrument and balanced by air pressure in the jacket. All the tubing in the reaction system, including the jacket of the glass gauge and the magnetic hammer, was wound with Nichrome wire and heated electrically to 110°C during a run.

Prior to an experiment the desired amount of chloropicrin, sealed in a glass tube with a fine drawn-out tip, was placed in position under the magnetic hammer through the open end of the tube *A*, which was then sealed off. The oil bath was brought to the required temperature and the apparatus evacuated, all the tubing outside the bath being heated electrically to 110°C during the evacuation with the exception of that immediately surrounding the tube of chloropicrin. Finally this part of the tubing was also heated for a short time, and the reaction system was then isolated by sealing off the connecting tubing at *P*. The tip of the tube containing the chloropicrin was then broken off with the magnetic hammer, and the variation of pressure with time was followed by means of the glass manometer.

For purposes of analysis the reaction vessel in the oil bath was replaced by a cylindrical vessel heated by a removable electric furnace. The cylindrical vessel carried a narrowed portion at its base for the condensation of reaction products, and a small tip in which they could be sealed off.

Chloropicrin was obtained from the Eastman Kodak Co. It was fractionated before use, and was then sealed off in vacuum in small tubes.

The Course of the Reaction

As pointed out above, Gardner and Fox found that chloropicrin decomposes at its boiling point into phosgene and nitrosyl chloride. In the temperature range of the present investigation, 138° to 170°C, NOCl decomposes slowly into nitric oxide and chlorine. We would therefore expect that the final products of the reaction would be phosgene and an equilibrium mixture of NOCl, NO, and Cl_2. This equilibrium has been investigated by Dixon.[3] The total pressure increases at completion obtained in the present investigation are in excellent agreement with values calculated from Dixon's results. Thus, for example, at 160°C and initial pressures of 9 and 12 cm of chloropicrin, the assumption of equilibrium amounts of NOCl, NO, and Cl_2 leads to predicted pressure increases at completion of 111 and 110 percent. Experimental values at the end of 15 hours reaction time were 111 and 112 percent, respectively.

In order to check the reaction products, however, they were examined by an analytical method which has been previously described.[4] This method depends on the action of the gases on mercury, phosgene being unaffected, NOCl replaced by an equimolecular amount of NO, and chlorine entirely removed. The amount of NOCl is thus equal to the NO formed, and the amount of chlorine to the decrease in pressure. The method is capable of considerable accuracy in the absence of NO_2. NO_2 reacts with mercury yielding half its molecular amount of NO. Consequently when NO_2 is present the decrease in pressure on reaction with mercury indicates the amounts of NO_2 and chlorine only within the limits consistent with this decrease. Moreover, the amount of NO formed will also be indefinite as a measure of the NOCl present to the extent of the amount of NO_2.

Two analyses of the products of the reaction at completion gave the results shown in Table I.

[3] Dixon, "Bodenstein Festband," Zeits. f. physik. Chemie, 479 (1931).

[4] Steacie and Smith, Can. J. Research, in press.

TABLE I. *Products of the reaction at completion. Reaction time—approximately 3 hours.*

Temperature, °C	Initial Pressure, cm	Products, moles/mole of CCl_3NO_2			
		$COCl_2$	NOCl	Cl_2	NO
160	12.3	0.91	0.83	0.08	0.19
170	8.1	0.91	0.81	0.12	0.27

These results are calculated on the assumption that NO_2 is absent at this stage of the reaction, as will be shown later. The fraction recorded as phosgene exhibited the vapor pressure of this substance when condensed. It will be seen that the amount of phosgene is lower than that required by the mechanism given above. However, the amount of NO is somewhat high, and considering the difficulty of condensation it is possible that some of the NO recorded is really uncondensed phosgene. If we assume that 0.04 cm and 0.08 cm of the recorded NO are really phosgene, respectively, the products balance in a quite satisfactory manner, as shown by Table II. It should be pointed out that the extent of dissociation of NOCl reported in the tables is not necessarily the actual amount existing at the temperature of the reaction, since NO and chlorine combine at an appreciable rate even at room temperature.

The condensed products at liquid-air temperature showed a slight green coloration, indicating the presence of some NO_2, which would combine with NO to form blue N_2O_3, which in the presence of NOCl yields a green coloration. A consideration of the pressure change accompanying the chloropicrin decomposition shows that there cannot have been much nitrogen dioxide present. This was confirmed by adding small amounts of NO and NO_2 to NOCl and observing the color at liquid air temperature. One percent of NO_2, combined as N_2O_3, gave a definite green color to the mixture. NO_2 is therefore not an important product of the reaction. It appears to result from purely secondary changes, since the longer the time allowed for an experiment to go to completion the more NO_2 appeared to be formed. During the early stages of the decomposition no evidence of the presence of NO_2 was found. Moreover, a number of runs were carried on for 15 hours, and partial recombination of the NO and chlorine was accelerated by several condensations and evaporations. These indicated only a small pressure drop on reaction with mercury, as shown by the data of Table III. Considering that recombination is not complete, so that some chlorine is certainly present, the amount of NO_2 formed during 15 hours cannot be great.

TABLE II. *Products of the reaction (corrected).*

Temperature, °C	Initial Pressure, cm	Products, moles/mole of CCl_3NO_2			
		$COCl_2$	NOCl	Cl_2	NO
160	12.3	0.95	0.83	0.08	0.15
170	8.1	0.99	0.81	0.12	0.19

The products of the reaction are thus essentially $COCl_2$, NOCl, NO, and Cl_2. There is, however, some evidence that all the NO and Cl_2 do not result from a simple secondary decomposition of NOCl. From the rate constants of the NOCl decomposition throughout the temperature range of our investigation[5] calculations show that when 50 percent of the chloropicrin has been decomposed less than 1 percent of the NOCl formed will have dissociated into NO and Cl_2. Actual experiments were made by cooling the reaction vessel as quickly as possible after 25 or 50 percent of the chloropicrin had decomposed, and measuring the residual pressure at −103°C (at which temperature NO is all in the vapor phase, while the other products have a negligible vapor pressure). These measurements are only approximate, since the residual pressures are small, but they should give the order of magnitude of the partial pressure of NO. The results are given in Table IV.

Although these measurements are very rough, they indicate unequivocally that more NO is present than can be accounted for by the known rate of decomposition of NOCl. Furthermore, the

TABLE III. *Products of reaction after recombination.*

Temperature, °C	Products, in Arbitrary Units		
	$COCl_2$	NOCl	Cl_2
160	10.8	10.5	0.4
160	11.7	11.2	0.35
160	10.5	10.6	0.2
160	9.45	8.85	1.1

[5] Waddington and Tolman, J. Am. Chem. Soc. **52**, 689 (1930).

TABLE IV. *Decomposition of* NOCl *during the intermediate stages of the reaction.*

Temperature, °C	Initial Chloropicrin Pressure, cm	Approximate Percent Decomposition of Chloropicrin	P_{NO}, cm	Percent Decomposition of NOCl
160	15.5	48	0.8	15
	15.2	21	0.3	14
140	14.0	48	0.55	11
	19.0	26.5	0.15	5

TABLE V. *Data for typical experiments.*

Temperature	145.2°C		161.7°C			170.2°C		
Initial Pressure	10.8 cm		11.5 cm			11.3 cm		
Time, Min.	% Reaction	$k\times10^5$, sec.$^{-1}$	Time, Min.	% Reaction	$k\times10^4$, sec.$^{-1}$	Time, Min.	% Reaction	$k\times10^4$, sec.$^{-1}$
10	4.5	7.7	2	5.2	4.5	2	9.3	7.9
20	9.0	7.9	4	10.4	4.6	4	18.2	7.8
30	12.3	7.3	6	14.3	4.3	6	27.4	8.2
40	17.3	7.9	10	23.5	4.5	8	35.4	8.4
50	20.4	7.7	15	33.0	4.5	10	42.0	8.3
60	24.0	7.6	20	41.0	4.4	12	49.0	8.5
70	26.8	7.7	25	49.5	4.6	14	54.5	8.5
90	33.2	7.5	30	56.0	4.0	16	59.0	8.3
110	38.4	7.3	40	65.0	4.4	18	64.5	8.6
130	45.0	7.7	50	74.0	4.5	20	69.0	8.6
150	50.0	7.7	60	81.0	4.6			

form of the pressure-time curves, and the agreement of the unimolecular constants throughout a run indicate that the reaction cannot be a rapid decomposition into phosgene and NOCl, followed by a slow decomposition of NOCl. The rate of recombination of NO and Cl_2 to NOCl is also slow, so that it cannot be assumed that we have

$$CCl_3NO_2 = COCl_2 + NO + \tfrac{1}{2}Cl_2,$$

followed by recombination of NO and Cl_2. The only alternatives seem to be, therefore, (a) NOCl and $NO+Cl_2$ are produced independently,

$$CCl_3NO_2 \begin{cases} \nearrow COCl_2 + NOCl \\ \searrow COCl_2 + Cl_2 + NO, \end{cases}$$

followed by a later slow establishment of the equilibrium. (b) Some sort of "hot molecule" mechanism, such as

$$CCl_3NO_2 = COCl_2 + NOCl^*,$$
$$NOCl^* + M = NOCl + M,$$
$$NOCl^* = NO + Cl,$$
$$2Cl = Cl_2.$$

(c) Some complex mechanism involving atoms or radicals which leads ultimately to the formation of NOCl, NO, and Cl_2.

In any case, secondary changes do not seem to be of any importance in the early stages of the reaction, and it appears to be justifiable to use the pressure change as a measure of the progress of the reaction.

The Rate of Reaction

Data for typical experiments are given in Table V. In calculating the percentage reaction from the pressure change, the effect of a 10 to 15 percent decomposition of NOCl is practically cancelled by the correction for 5 percent dead space, so that the percentage pressure increase is a direct measure of the percentage reaction. (Actually completion corresponds to a few percent more than 100 pressure increase, but this is almost entirely due to the very slow secondary decomposition of NOCl.) It will be seen from

TABLE VI. *Summarized rate data.*

Initial Pressure, cm	t_{25}, sec.	t_{50}, sec.	Initial Pressure, cm	t_{25}, sec.	t_{50}, sec.
Temperature 170.2°C					
20.7	300	710	7.2	310	744
16.75	310	710	7.1	321	760
11.3	324	750	4.3	310	744
9.1	335	792			
Temperature 161.7°C					
18.4	600	1510	11.5	645	1584
17.3	618	1518	11.2	612	1650
16.5	690	1584	9.2	660	1560
16.1	642	1530	7.8	690	1548
13.1	600	1590	7.5	672	1698
11.8	678	1602	6.6	690	1680
Temperature 153.5°C					
18.0	1440	3600	10.5	1560	3900
17.7	1452	3540	9.2	1560	3510
13.0	1524	3600	8.75	1548	3900
12.5	1518	3900			
Temperature 145.2°C					
18.2	3660	9300	11.0	3840	9300
16.8	3720	9360	10.8	3900	9000
Temperature 138.0°C					
19.6	7980	—	12.3	8040	—
16.0	8100	—			
Temperature 170.2°C—Packed Bulb					
16.0	337	780	6.65	300	740
9.6	320	680			
Temperature 161.7°C—Packed Bulb					
20.7	610	1800	8.35	655	1680
11.0	633	1780			

Table V that satisfactory unimolecular constants are obtained.

Summarized data for all runs are given in Table VI. The packed bulb had a surface-volume ratio 15 times that of the empty vessel, so that it is evident that the surface has no appreciable effect on the rate of reaction.

The results may perhaps indicate a slight falling-off in rate at low pressures. The effect, however, is too small to establish with certainty. The rate of reaction at low pressures is at present under investigation. Since the high pressure rate appears to have been practically attained in the experiments given in Table VI, the temperature coefficient of the reaction has been calculated merely from the average values of t_{25} and t_{50}, without attempting an extrapolation to infinite pressure rates. These average values are given in Table VII. It will be seen that the average ratio of t_{50} to t_{25} over the whole temperature range is 2.42, as compared with the theoretical value of 2.41 for a unimolecular reaction.

In Fig. 2 the logarithms of t_{25} and t_{50} are plotted against $1/T$. From the slopes of the lines we obtain 37,450 and 37,900 cal., respectively, for the activation energy. Whence, taking the mean of these, and making a rough extrapolation to infinite pressure of the results at 153.5,° we obtain

$$k = 4.90 \times 10^{15} e^{-37670/RT} \text{ sec.}^{-1}.$$

This is a rather high value for the nonexponential factor.

The above value of the activation energy is in fairly good agreement with that calculated from Radulescu and Zamfirescu's results, *viz.* approximately 40,000 cal. Our velocity constants are, however, higher than theirs by a factor of about 2. They make no definite statement of the

TABLE VII. *Mean values of rate data.*

TEMPERATURE, °C	t_{25}, sec.	t_{50}, sec.	t_{50}/t_{25}
170.2	315	744	2.36
161.7	650	1587	2.44
153.5	1525	3701	2.43
145.2	3780	9315	2.46
138.0	8040	mean = 2.42	

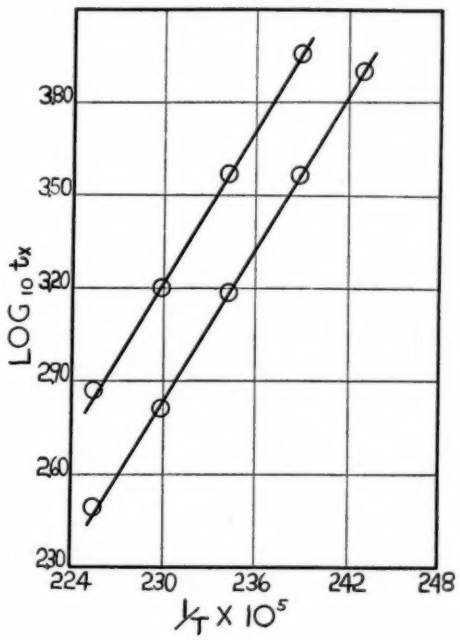

FIG. 2.

conditions of pressure, etc. during their experiments. It appears probable, however, that their runs were really made with the chloropicrin almost entirely in the liquid phase. (They merely state that the chloropicrin was heated in an oil bath "*en ampoules scellées a la lampe.*") This would appear to be the cause of the difference in the rates.

It was hoped at the outset that it would be possible to compare the decomposition of chloropicrin with that of the analogous nonhalogenated compound, nitromethane. The decomposition of this substance has been investigated by Taylor and Vesselovsky,[6] but the mechanism of the decomposition appears to be entirely different from that of chloropicrin, and no comparison of activation energies, etc. is possible. The difference in behavior is perhaps due to the higher strength of the C−H bond relative to that of C−Cl. In the case of nitromethane C−H splits are thus forbidden, and only the NO_2 group can participate in the primary step. With chloropicrin, however, C−Cl bonds presumably break as well.

[6] H. A. Taylor and Vesselovsky, J. Phys. Chem. **39**, 1095 (1935).

Interpretation of the Properties of Alkali Halide-Thallium Phosphors

FREDERICK SEITZ
General Electric Company, Schenectady, New York
(Received November 16, 1937)

An attempt is made to interpret the properties of alkali halide-thallium phosphors. The experimental basis of this interpretation is the work of Pohl and his numerous collaborators on these substances. It is concluded that the long wave-length absorption peaks of the phosphors which are not contained in the pure alkali halides are to be attributed to the excitation of the thallium ions. These are assumed to be distributed throughout the crystal, replacing alkali metal ions. The structure of the observed peaks is interpreted in terms of the details of the spectrum of Tl^+ and the probable effects of crystalline perturbations. The nature of the fluorescent and phosphorescent spectra is then correlated with the behavior of the normal and excited levels during the time after absorption and before optical radiation in which the crystal again comes to mechanical equilibrium. Distinction is drawn between two cases: That in which the excited Tl ion has no thallium ions among its twelve positive ion neighbors and that in which it has one. It is concluded tentatively that excitation to the lowest excited levels, associated with a triplet in the free ion, will give rise to fluorescence in either case, and that excitation to the higher, singlet level will lead to the alternative possibility of phosphorescence in the second case, but not in the first. The theoretical justification of these tentative conclusions involves assuming that the homopolar forces between the excited ion and its neighbors depress singlet excited levels more than triplet excited levels, and that singlets are depressed more when one of the neighbors of a Tl ion is another Tl ion than when none are.

I. SURVEY AND INTRODUCTION

MANY kinds of crystals, when they contain suitable impurities, are fluorescent and phosphorescent. Such impure crystals are called phosphors, and the effective impurity element is termed the activator. Phosphors have been extensively investigated during the past forty years, and much experimental data on their properties is available.[1] A large part of this accumulated information is, unfortunately, not very useful to one who is trying to form a fairly complete picture of the mechanism of crystal fluorescence and phosphorescence. Most of the measurements have concerned only a particular phase of the behavior of a particular phosphor, such as its decay characteristic, and most of the materials studied have been intricate in composition and properties. Attention has been given, quite naturally, to those phosphors which are technically important, and these without exception are so complex as to discourage theoretical attack, as long as a detailed mechanism has not been established for simpler cases.

There is, however, one group of phosphors which are relatively simple and for which the data are fairly complete. These are the alkali halides, activated with thallium. They have been studied by Pohl[5, 7] and his collaborators Hilsch,[2, 5] Smakula,[3] Lorenz,[4] MacMahon,[6] Koch,[7, 9] Fórro,[8] von Meyeren,[10] Bünger,[11, 12] and Flechsig.[11, 12]

These phosphors can be obtained as large single crystals, on which unambiguous absorption measurements are possible. The light which is absorbed by the activated halide, exciting it to fluorescence and phosphorescence, is in bands fairly distinct from the absorption bands of the pure substance. Hence, the dependence of these exciting bands on such variables as temperature and concentration of activator can be conveniently studied, and the quantum efficiency of the fluorescent processes can be measured with comparative ease. Finally, since these phosphors show many characteristics common to phosphors in general, there is some reason for the hope that they may furnish a key to the understanding of the more complicated substances.

The present paper proposes a picture, based on the modern theory of the solid state, which appears to correlate practically all of the observed facts about the behavior of these thallium-activated alkali halide phosphors. The treatment is similar in some ways to that of Muto,[14] which came to the author's notice while this paper was being written. We shall comment upon the differences between our picture and his in the last section.

II. PREPARATION OF THE PHOSPHORS

The experimental samples are made by dissolving a small quantity of thallous halide in a

melt of the corresponding alkali halide, and growing a crystal by the well-known Kyropolous method. The crystal contains a smaller mole percentage of Tl than the liquid. Koch,[9] using an optical absorption method, finds that in KCl +TlCl the ratio between the concentration in the crystal and in the melt varies from 0.5 to 0.05, depending upon unknown factors, and is not the same for all parts of the same crystal. Since most of the workers quote only the mole percentage of thallous salt added to the melt, we shall have to estimate the concentration of Tl in the final crystal. Koch shows that the absorption coefficient for one of the exciting bands, in KCl+TlCl, is practically proportional to the Tl concentration. We shall use this linear relation in estimating the Tl content in KCl+TlCl, whenever this absorption coefficient is stated.

We shall assume that the Tl is present in the lattice in the thallous (monovalent) state, since this form of the thallium salt is most stable at the high temperatures at which the crystals are grown. In addition, we shall assume that the Tl ion replaces an alkali ion of the lattice and that the Tl ions are dispersed uniformly throughout the lattice in cases in which the concentration of Tl in the crystal is small (less than 0.1 percent). Koch[9] has presented good evidence for this in a paper which deals with the investigation of the number of dispersion electrons that are associated with the near ultraviolet absorption spectra of the phosphors. He found that for small concentrations this number is strictly proportional to the number of Tl ions present in the crystal and that the ratio of the two numbers, which is the f factor, is of the order of 0.1. This proportionality is not generally valid in other types of alkali halide phosphors, such as those containing Cu or Pb, but we shall not be concerned with these here.[15]

III. Absorption Spectra

The absorption spectrum of an alkali halide phosphor consists of two parts, one part characteristic of the pure substance, the other part characteristic of the activator impurity. The latter component is weaker, and lies on the long wave-length side of the former (see Table I). We shall discuss these two parts separately.

(a) Characteristic absorption of pure alkali halides

These absorption spectra were initially studied by Hilsch and Pohl,[5] and have recently been measured farther into the ultraviolet, to about 1050A, by Schneider and O'Bryan.[16] Hilsch and Pohl interpreted the structure of the bands by supposing that when a quantum is absorbed an electron is transferred from a halogen ion to a nearby alkali ion. Using the classical theory of ionic crystals, they were able to account semi-quantitatively for the positions of the peaks. Von Hippel,[17] also using classical methods, has refined these computations.

At first sight, this interpretation seemed to be at variance with the zone theory of solids. On this theory, the absorption of a quantum should raise an electron from a lower filled band of energy levels to an upper band in which it would be free to move throughout the crystal, not localized in the vicinity of any particular alkali ion. However, recent treatments[19–22] of the quantum-mechanical equations for nonconducting crystals, more accurate than the Bloch-Wilson approximation which yields the zone scheme, have shown that the original interpretation probably is largely correct.

The more precise energy diagram contains, in addition to the quasi-continuous bands of the Bloch-Wilson treatment, some narrow continuous bands lying in the forbidden region between the Bloch-Wilson bands. These additional levels are a contribution from the Heitler-London

Table I. *Position of the absorption peaks in various alkali halide-thallium phosphors in electron volts. (A, B, and C refer to the peaks of Fig. 3.)*

	First Fundamental Peak	*A*	*B*	*C*
NaCl	7.82 ev	4.87	5.80	6.20
KCl	7.60	4.92	5.90	6.30
RbCl	7.39	4.98	5.94	6.40
CsCl	7.63	4.90	5.90	6.30
LiBr	6.68			
NaBr	6.49	4.63		5.72
KBr	6.58	4.73		5.88
RbBr	6.43	4.77		5.82
CsBr	6.61	4.69		5.76
LiI	5.59			
NaI	5.38	4.22		5.28
KI	5.63	4.30		5.23
RbI	5.55	4.32		5.15

approximation which is used along with the Bloch approximation to give a picture that is more exact than is possible with either alone. In these states the excited electron and the hole it leaves in the filled band are closely coupled and move together. As one might expect, the electron and hole do not transport charge during this motion, so that the crystal is not made photoconducting. Because of the analogy to excited states of atoms, Frenkel has termed the states of these bands "excitation states" in contrast to "ionization states" of the Bloch-Wilson theory.

In the alkali halide crystals, the excitation state corresponds quite well with the case imagined by Hilsch and Pohl: an electron in one of them has, effectively, left a halogen ion and attached itself to neighboring alkali ions. The excited electron does not remain fixed, at least at first, but moves through the lattice with its hole.

How many such bands may be expected? Wannier[22] concludes, from an approximate theoretical solution, that there will be an infinite number of them underlying the continuum of the first unfilled band, just as there are infinitely many discrete levels for a free atom, below the continuum of ionization. Wannier treats the "hole," which an excited electron leaves in the highest filled zone, practically like a point positive charge. The problem is then analogous to that of the free hydrogen atom, and an infinity of states is found to each of which corresponds a band. This view seems completely justifiable in the case of the alkali halides. The energy of attraction between the hole and the excited electron may be identified with the sum of the electron affinity of the halogen atom and the electrostatic field of the rest of the lattice. The first term, as Bethe has shown[23] in the case of H^-, is a correlation effect and falls off more rapidly with distance than a Coulomb force. Hence, there are not an infinite number of discrete levels in the free halogen ion. Beyond a few atomic distances from the neutral halogen atom, the other term varies as e^2/r plus a periodic potential, which is the potential of the normal lattice. The Coulomb term will give enough "assistance" to the halogen atom in holding an electron so that we may expect an infinite number of excitation bands.

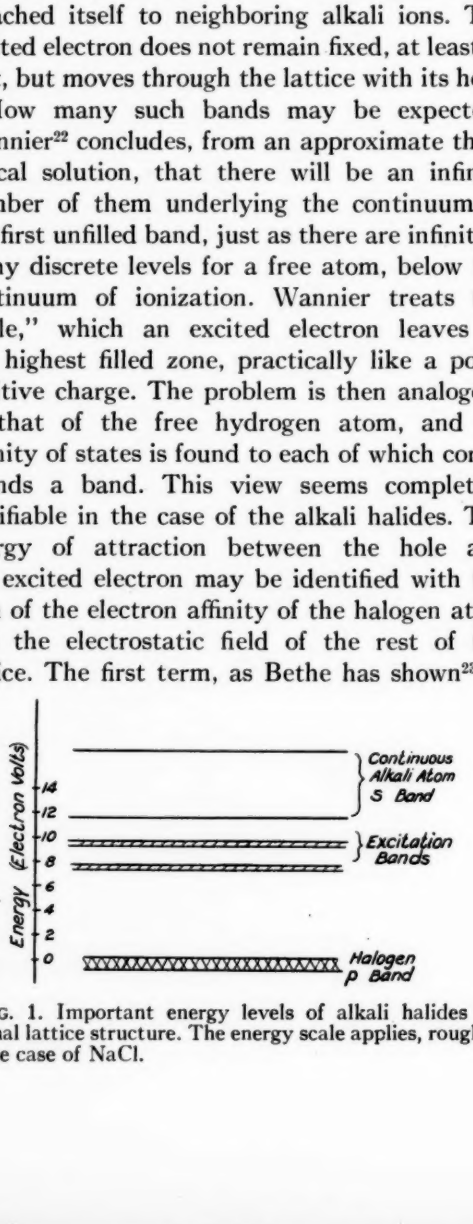

FIG. 1. Important energy levels of alkali halides for normal lattice structure. The energy scale applies, roughly, to the case of NaCl.

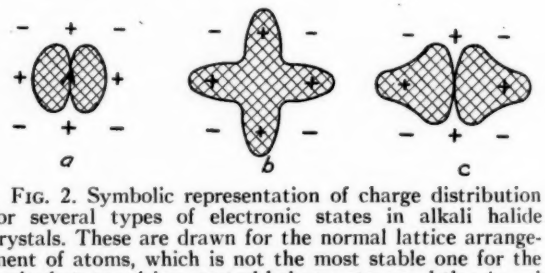

FIG. 2. Symbolic representation of charge distribution for several types of electronic states in alkali halide crystals. These are drawn for the normal lattice arrangement of atoms, which is not the most stable one for the excited states. A is a neutral halogen atom and the + and − correspond to alkali and halogen ions. The shaded region is that in which the electronic distribution of an additional valence electron is appreciable. (a) Distribution of additional valence electron in a normal halogen ion in the lattice. This is a p electron, hence the vertical node passing through A along which the charge distribution is zero. This p electron combines with the five others to form a closed-shell p^6 configuration. (b) Lowest excited electronic state in which the electron is distributed among the six neighboring alkali ions (only four shown). This is analogous to an atomic s function, so that the result is, effectively, a halogen ion with a p^5s configuration. (c) A higher excited electronic state having p-like character.

For the present, then, we shall deal with an energy spectrum such as is shown in Fig. 1. The lowest band, normally completely occupied, arises from the p valence levels of the halogen ion. The upper band, normally empty, arises from the s state of the alkali atom and is an ionization band. The levels between these bands are states in which an electron has been excited from one of the halogen ions, leaving a hole in the lower band, and is localized on the alkali ions neighboring the halogen atom which remains. The charge distribution of an electron relative to the hole in one of these states is shown symbolically in Fig. 2.[24] These two figures were sketched on the assumption that the ions have the same position after excitation as before. This will be true as long as the excited electron and hole are in motion, but, as Frenkel[19] has pointed out, the most stable state will be one in which the electron and hole are localized at one

spot and the lattice is distorted there. Eventually the system will fall into this state.

An electron excited to the upper (ionization) band will have a charge distribution similar to that of a free electron in an alkali metal. If the excitation is by absorption of light, the crystal should be photoconducting. Experimentally, no photoconductivity is observed when the crystal absorbs light in the long wave-length end of the absorption spectrum, covered by the measurements of Hilsch and Pohl—this in itself is evidence that the excitation is to excitation levels. Absorption of quanta of greater energy should raise the electrons to the upper continuum of ionization levels. It is reasonable to expect photoconductivity in the far ultraviolet absorption region investigated by Schneider and O'Bryan. Experiments on this question have yet to be done.

We mention, incidentally, the position of the *F* centers in an energy level diagram such as Fig. 1. One current interpretation[25] is that these are discrete levels in which the electron is localized about a particular alkali ion, and the surrounding lattice is deformed. They are permitted only to "extra" electrons—that is, electrons which have come from a distance of many lattice spacings into a part of the lattice where all the halogens are still ions. Another hypothesis,[25] perhaps in better agreement with the observations, is that *F* centers are electrons trapped in vacant negative ion sites in the lattice, the lattice being supposed to contain, in its equilibrium condition, a certain concentration of sites not occupied by ions. We shall not be concerned further with *F* centers in the present paper.

(b) Absorption associated with the presence of thallium

The additional long wave-length absorption in the phosphors has been carefully measured by several investigators.[2, 4, 8] Through all the alkali halides runs a characteristic pattern of three peaks (Fig. 3). Nearest the visible is a small peak *A*, and about 1 ev beyond this are two peaks *B* and *C*, incompletely resolved. Table I lists, for several halides, the positions of these and of the first peak characteristic of the pure substance. The positions of the three peaks shift only slightly as the alkali or halogen ions are changed. For example, the shift is only about 0.7 ev, toward the red, in passing from chlorides to iodides. In contrast, the fundamental absorption peak shifts by about 2.1 ev.

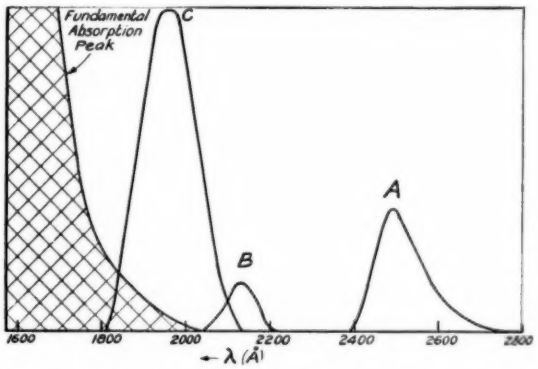

FIG. 3. Typical absorption bands of phosphors. These are adaptations of those obtained by Fórro for KCl. The doublet *B–C* is actually only partly resolved.

This invariance almost dictates the view that these three peaks correspond to absorption by the thallous ion, and this is the hypothesis we shall use. A possible alternative is that the absorption causes the transfer of an electron from a halogen ion to a neighboring thallous ion. We reject this hypothesis, for the following reasons: (1) The peaks show none of the doublet structure which Hilsch and Pohl have associated with the doublet state of the halogen atom.[24] This doublet separation is 0.3 ev in Br and 0.9 ev in I, so it should be fairly conspicuous in these cases. (2) The absorption corresponding to a halogen-thallium transition should lie farther in the ultraviolet. Consider, for example, the rubidium halides. The radii of Rb^+ and Tl^+ are nearly the same, as may be seen from the table of halides in Hermann and Ewald's *Strukturberichte*, and thus a Tl ion can replace a Rb ion in the lattice without causing much distortion. The Madelung potential field, which arises from the neighboring ions, will therefore be practically unchanged; hence, in comparing the energy necessary to transfer an electron from a halogen ion to a Rb ion with the energy necessary for transfer to a Tl ion, the Madelung term can be neglected. This leaves the electron affinities of the two ions for comparison, and these can be estimated, in first approximation, from the ionization potentials of the two atoms. The ionization potential of Tl is 1.9 ev higher than

that of Rb. In the actual case, an even smaller energy difference is to be expected, for in the excited state associated with the fundamental absorption of the pure rubidium halide, six Rb ions cooperate in holding the electron, whereas only the one Tl ion will be effective in a halogen-Tl transfer. In the latter case, the electron is more localized and therefore has a greater kinetic energy. All these considerations tend to the conclusion that the halogen-thallium transition should require about the same energy as the fundamental halogen-rubidium transition. Table I shows, however, that the actual energy gap between the A peak and the fundamental absorption peak is nearly 2.5 ev in the case of RbCl, even higher than the estimated limit of 1.9 ev. This argument is not as conclusive as the first, but, in the writer's opinion, it does carry some weight.

The characteristic absorption of pure thallous halides has been measured in the near ultraviolet by Hilsch and Pohl. They find peaks at the same region of the spectrum as the low energy absorption peaks of the phosphors. If we do not associate these peaks with halogen-Tl transitions

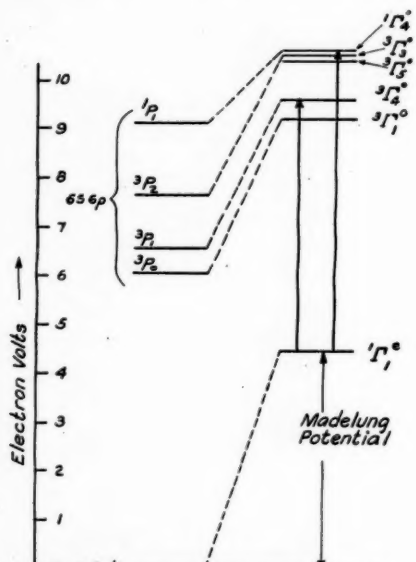

FIG. 4. (a) The energy level diagram of Tl^+ referred to the lowest state. (b) The relative disposition of levels of the ion in the solid. The position of the ground state has been adjusted relative to that of the free atom by means of the Madelung potential for a chloride and that of the upper levels as determined by use of the absorption spectra of the KCl phosphor in the manner described in the text.

in the phosphor, it is scarcely consistent to make this association in the case of the bulk thallous halide. On the other hand, halogen gas is evolved when this absorption occurs in the thallous

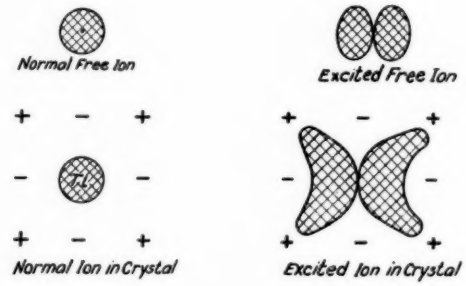

FIG. 5. Schematic representation of charge distributions of normal and excited valence electron on the Tl ion. We have assumed that the fields of the neighboring positive ions will distort the charge in such a way as to spread it in the region between the Tl and alkali ion.

halide. We hope to discuss this observation in another place; for the present we shall only state that it seems possible to reconcile it with the viewpoint adopted here.

Assuming, for these reasons, that the absorption in the three long wave-length peaks is by the Tl^+ ion, and does not correspond to the transfer of an electron from a halogen ion to the Tl^+, we shall next ask about the structure of this absorption. Since the position and nature of excited Tl^+ levels in the crystal must be estimated, it is necessary to inquire how the states of a free Tl^+ ion are modified when this ion is brought into the lattice, replacing an alkali ion (see Fig. 4(a)).[26]

In the first excited state (corresponding to $6s6p$ in the free ion) the electron will be partially removed from the neighborhood of the Tl nucleus and will be shared with the neighboring alkali ions. The charge distribution of this electron about the alkali ions will, however, be nothing like the distribution in free alkali atoms. This may be seen as follows: The Madelung fields about Tl^+ and alkali ions are practically equal, so we can get a rough estimate of the positions of levels in the solid from the levels in the free atoms and ions. The Tl^+ $6s6p$ state lies about 9 ev below the normal state of an alkali atom: this energy would be required in taking an electron from the excited Tl^+ to a distant alkali ion. When the nuclei are a distance r apart,

this energy is diminished by e^2/r, roughly 3 ev for the thallium-alkali distance in the lattice. A net gap of 6 ev remains, and because of this energy difference we should not expect the wave function of the lowest excited state to contain any large atomic alkali component. We may expect some perturbation in spite of this and the charge distribution will be drawn near the positive ion to some extent. The Madelung field of the six neighbors nearest to a Tl^+ ion will be negative, and all the levels of the ion in the solid will therefore be raised above their positions in the free ion. This raising should be most pronounced for the lowest level, and should become less important as the electron goes to higher levels where it comes more and more into the field of the next-nearest positive neighbors.

In addition to this raising of the Tl^+ levels as the ion is brought into the lattice, some splitting of the levels and some changes in the distances between levels is to be expected. The splitting may be predicted qualitatively on the basis of symmetry considerations. The crystalline equivalent of the atomic p functions will not split so long as the crystalline field is cubic, as it will be during absorption. We picture the form of the s and p functions in gas and in solid as in Fig. 5. On the other hand, when these are combined to form multiplets, we may not expect any states of higher than threefold degeneracy; that is, states with $j=2$ will split. We shall not attempt to discuss this splitting quantitatively; Van Vleck and his co-workers[27] have done this for rare earth and iron group atoms in a number of salts.

The mean inner multiplet distances and mean intermultiplet distances may be changed for two reasons. First, the inner atomic energy terms which determine these distances in the free ion may be altered; that is, the spin orbit coupling and the electrostatic interaction terms of the Tl^+ electrons may be altered in passing from the free ion to the bound ion, because the electronic wave functions are distorted as the ion is brought into the crystal. Second, the interaction energy of the Tl ion with its neighbors will be different for states of different quantum numbers.

It is difficult to say in which way the type of inner atomic coupling will change as the ion is brought into the crystal. We mentioned in reference 24 that the excited states of the halogen ions will probably show rather advanced $j-j$ coupling and that there is good experimental evidence to support this. Unfortunately, these excited states are not stable for the free halogen ions; hence, we have no good basis on which to make a comparison. We shall defer further comment on this matter until later in this section (see reference 28).

The interaction of the normal ion with the halogen ions is a combination of electrostatic attraction of ions and homopolar repulsion between closed-shell configurations of electrons (neglecting van der Waals forces). The electrostatic term remains unchanged for the excited states, but the homopolar term will contain an attractive minimum such as that shown in Fig. 6. These minima are sufficient to account for a depression of the excited states of the ion in the solid relative to the normal state.

In connection with the effects of interatomic interaction, it is worthwhile to estimate the difference in position of the levels of the normal halogen ion and excited thallium ion. This difference is between 10 and 11 ev for the ions in free space, because the ionization energy of a thallium ion in its first excited state is about 14 ev and the electron affinities of the halogens range between 3 and 4 ev. The halogen levels are lowered and those of the thallium ion are raised, when these ions are brought into the lattice, because of the Madelung potential. Thus, this difference is decreased by roughly 3.5 (e^2/r) which is about 16 ev for a crystal such as NaCl. This will bring the excited levels of the thallium ion and the normal levels of the halogen ion rather

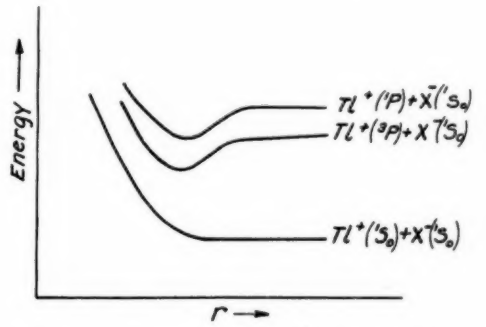

FIG. 6. Schematic representation of the homopolar part of the interaction between thallous ion and a halogen ion.

close together, and will lead to an appreciable resonance interaction. This closeness of approach is shown also by our previous estimate of the difference between the energy of an absorption process in which an electron is transferred from the halogen ion to the thallium ion, and the energy of the process in which the thallium ion is excited. We postulate that this interaction lowers the first singlet excited states of Tl more than it lowers the first triplets. One good reason for expecting this is the following.[28] Singlet states are usually more stable than triplets derived from the same configuration in ordinary valence or homopolar compounds in which valence conditions are satisfied. This, for example, is true of a host of diatomic molecules. The exceptions are molecules, such as O_2, in which the interacting atoms have nearly closed p shell and with which we are not concerned. For this reason, we may expect that the states which correspond to a neutral thallium atom and a neutral halogen atom, and which lie immediately above the states of the excited thallium ion plus normal halogen ion, will have a low lying singlet level. This singlet level presumably will connect adiabatically with the normal nonpolar $^1\Sigma$ state of the free diatomic thallium halide molecule. This singlet interacts with the upper singlet of the excited thallium ion and will depress this level relative to the triplets.

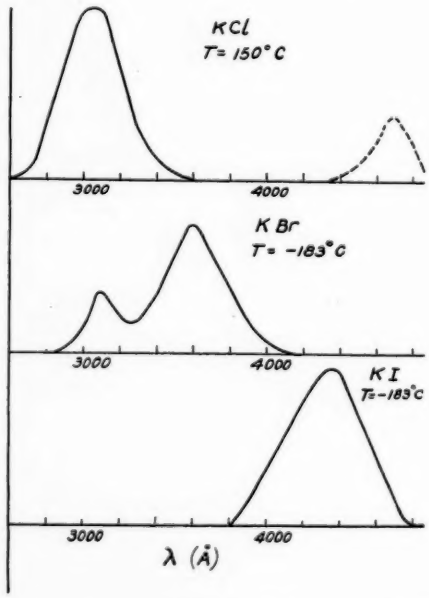

FIG. 7. Typical emission curves of phosphors (after von Meyeren). The dashed peak in KCl is qualitative.

By means of these considerations we arrive at a disposition of levels in the solid such as is shown in Fig. 4(b). The term notation follows that of Bethe;[29] the superscripts e and o correspond to evenness and oddness in the usual spectroscopic sense; the anterior superscript, as usual, denotes the multiplicity. We have adjusted the absolute positions of the levels in this diagram to correspond with our interpretation of the transitions in the KCl phosphor. For the other alkali halide phosphors the positions will be slightly different.

The two most probable absorption transitions, indicated with heavy arrows, are from $^1\Gamma_1^e$ to the two Γ_4^0 states. We shall identify these with the two strong absorption peaks A and C of Fig. 3. The $^3\Gamma_4$ state will have some strong residual triplet character, while the $^1\Gamma_4$ will be mainly singlet. Since pure singlet-triplet transitions are forbidden, C should be a stronger absorption line than A, and this difference in intensity is observed.

If the cubic symmetry is perfect, the other transitions are forbidden. They may be expected to appear with small intensity when there is any local dissymmetry, such as thermal agitation would cause. We shall attribute the peak B to a transition of this sort from the lowest state to either $^3\Gamma_3$ or $^3\Gamma_5$. The peak C is broad enough so it may possibly conceal another small peak arising from the forbidden transition to the other member of this pair. This interpretation is supported by the measurements of Lorenz[4] and Fórro.[8] They find that the peak B is negligible at low temperatures and increases strongly as the temperature is raised (to 550°C). C, on the other hand, broadens and becomes weaker with increasing temperature. This is to be expected, since the changes in the state $^3\Gamma_5$ which are brought about by thermal agitation would tend to add to the wave function elements for which the transition matrix components vanish.

The separation between the $^3\Gamma_4^0$ state and $^3\Gamma_1^0$ is 0.37 ev in the free atom and remains about the same in the crystal, according to our interpretation, because this separation arises from spin

orbit interaction, and we have not assumed that this interaction changes in going from free to bound ions. Any "forbidden" absorption from ${}^1\Gamma_1{}^e$ to ${}^3\Gamma_1{}^0$ must be under the peak A, if the present interpretation is correct. This peak, as measured by Fórro, does in fact show decided asymmetry at high temperatures where forbidden transitions would become prominent. (See reference 28 for discussion of an alternative possibility.)

Additional excited states appear several volts above those shown in Fig. 4(a). In the absorption spectrum, transitions to these would be masked by the much stronger fundamental absorption bands of the halides.

IV. Emission Spectra

The emission spectra have been measured quantitatively[10, 11, 12] by von Meyeren, Bünger, and Flechsig. KCl has received most attention, and for this reason we shall consider it most fully, remarking here that it seems to be typical of the whole group of phosphors. Fluorescence and phosphorescence will be discussed separately.

(a) Fluorescence

The following seem to be the salient experimental facts:

(1) At low concentration of the activator (e.g., less than 0.0015 mole percent in the crystal) only fluorescence, without phosphorescence, is observed. The time constant of the decay of fluorescent light is shorter than 5×10^{-5} sec.

(2) The spectra in the ultraviolet, investigated by von Meyeren between -183°C and 15°C, consist of broad bands which can be resolved into one, two, or (NaBr is the only example) three peaks. These all lie on the long wave-length side on the exciting absorption bands (see Fig. 7). KCl has only one peak in the ultraviolet, but Bünger observed another in the visible (yellow) beyond the range of von Meyeren's apparatus, so it is posisble that others, such as NaCl, which have but one ultraviolet peak may also have peaks in the visible or infra-red.

(3) The entire emission spectrum is stimulated by light in any part of the induced absorption region—the peaks A, B, and C of Fig. 3. The relative intensities of the different emission bands, where more than one has been observed, do not depend on the wave-length of the exciting light.

(4) The quantum efficiency of the fluorescence in KCl was measured by Bünger. He found that about 50 percent of the quanta absorbed in any part of the exciting region reappear in the ultraviolet emission band, and he estimated from a qualitative observation that the other emission band, in the yellow, accounts for most of the remaining 50 percent. The total quantum efficiency is thus close to unity.

These are the data which we wish to fit with our previous interpretation of the absorption spectra.

First, it is necessary to recognize a point emphasized by von Hippel[17] in his discussion of the photoelectronic properties of pure alkali halides: the lattice in the neighborhood of an excited Tl^+ ion will not be in equilibrium immediately after the quantum has been absorbed. The redistribution of electronic charge causes a change in the interatomic forces and the atoms will shift about to new equilibrium positions in the new force field, radiating away the excess energy in the form of elastic waves. A complete description of this rearrangement would obviously require energy contours in a configuration space having three times as many coordinates as there are atoms involved in the change. For a crude qualitative picture, we shall symbolize these many coordinates by a single "configuration parameter." As a convenience, the Tl ion and the group of neighboring ions which are involved in the changes following absorption of a light quantum, and whose coordinates are specified by the configuration parameter, will be called a "center." (Lenard has used this term in a similar but less precisely defined way.) The center is, in effect, a large molecule containing fifty or a hundred ions. The energy states to be discussed can conveniently be called energy states of the center.

According to a general theorem,[30] all degeneracy of each of the levels is removed in the equilibrium position. The neighbors of the Tl ion will not be distributed about it with cubical symmetry: some of the twelve neighboring alkali ions will be nearer than others to the Tl ion. The equilibrium configurations will be different

for the different excited states, of course—the minima of the energy curves will lie at different values of the configurational parameter.

It is not possible to give a precise description of the stable arrangement of atoms for the excited states without more experimental or theoretical work than is available. Fig. 8 shows, however, what we may plausibly expect for the behavior of the various levels as functions of the configurational parameter. The minimum of the lowest curve is the normal energy state of the center. The point a represents the normal configuration of the ions in the center. The positions of the upper energy surfaces at a are as illustrated in Fig. 4(b). As we go away from this point,[30] the state $^3\Gamma_1^0$ remains singly degenerate; the $^3\Gamma_4^0$ and $^3\Gamma_5^0$ split into three states each; and Γ_3^0 breaks into a doublet. We assume that the states arising from $^3\Gamma_4$ and $^3\Gamma_1$ have their minima inside the valley of the lowest state, while those arising from $^1\Gamma_4$ do not have minima before they cross the rising portion of "progeny" of $^3\Gamma_4$. Actually, there will be no true crossing, but two cusps, more or less as shown in Fig. 8, will be formed. The progeny of $^3\Gamma_3$ and $^3\Gamma_5$ are omitted for simplicity. It is assumed that they (figuratively speaking) "cross" $^1\Gamma_4$ and rise. This, of course, will not be true crossing.

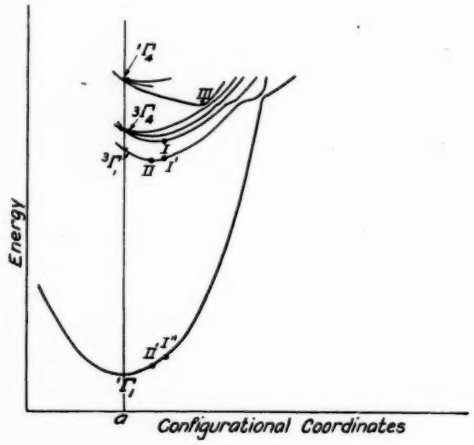

FIG. 8. Diagrammatic representation of behavior of the energy levels of Tl ion in crystal as a function of atomic coordinates. For clarity, the upper triplet states are omitted. The point going with the minimum of the lowest curve corresponds to the normal lattice arrangement.

It seems reasonable to suppose that the energy terms which displace the minima of the excited states from a are connected with the difference in the homopolar term of the interaction of the normal and excited Tl ion with the halogen ion. We referred to this in the preceding section when discussing the change in relative position of excited and normal states at a (see Fig. 6).

In order to explain the comparatively large depression of the singlet state, we apparently must invoke once again the influence of the higher singlet which corresponds to the neutral atomic states. It is possible that this higher singlet actually drops and "crosses" the progeny of this $^1\Gamma_4$ and that the lower singlet curves of Fig. 8 correspond to the offspring of the upper singlet. We cannot decide between these alternatives on the basis of available work.

Absorption in the A band, on this view, excites a center to the $^3\Gamma_4$ state. The system then passes, in about 10^{-13} sec., to the minimum I of the lowest member of the triplet, meanwhile losing the excess energy as elastic waves. If the system initially runs along one of the higher members of the triplet into which $^3\Gamma_4$ splits, it will fall to the lowest level, with elastic radiation, in a time short compared with the 10^{-8} sec. required for optical radiation. This sort of transition will be very probable[20] when the energy to be dissipated is of the order of the energy of lattice vibrational quanta.

From I the system may proceed by an optical transition either to I' in the next lowest state or to I'' in the ground state. These transitions occur vertically, in accordance with the Franck-Condon principle. The transition $I \rightarrow I'$ presumably gives light in the infra-red (possibly this transition also occurs with radiation of elastic waves, since the time required is of the same order as for radiation of a light quantum). From I' the system goes to the minimum II and radiates optically to reach II'—this radiation will be identified with one of the peaks in the fluorescent spectrum. The optical transition $I \rightarrow I''$ will be assumed to account for another emission peak. Without additional experimental evidence or refined computations, it cannot be predicted which of these quanta has the longer wave-length.

If the absorption takes place in either B or C, we shall assume that the system shifts to III, which is at the upper cusp associated with the crossing of the singlet and the lower levels of the

triplet. From here it proceeds to I by a sequence of non-optical transitions. Since the two Γ_4 states are only 1 ev apart at a and draw together, all the energy gaps between cusps in the crossing region will be of the order of fractions of volts, and non-optical transitions will be probable. Having arrived in the state I, the system goes on to the ground state by the course outlined above. The optical emission spectrum is thus independent of which of the three peaks is used for excitation.

Von Meyeren seems to find three emission peaks for the NaBr phosphor. The third peak might be explained by assuming that some of the centers which are excited to the lowest Γ_4 manage to stay in one of the higher levels of the three into which this splits, long enough to radiate a light quantum. There is an obvious difficulty, however, with this interpretation. The transition from III to I, as we have outlined it, involves several jumps through the upper states of the progeny of $^3\Gamma_3$. If the third emission peak in NaBr arises because the center can exist in one of the higher levels of $^3\Gamma_4$ long enough to radiate, we should expect the relative intensity of this peak to depend on the wave-length of the exciting light, since there is no *a priori* reason for supposing that absorption in the peak A will populate the three states of $^3\Gamma_4$ in the same way as an absorption in $B-C$. This point will require additional experimental work.

(b) Phosphorescence

The phosphorescent properties of the phosphors have been examined by Bünger and Flechsig. Most of the work was done on KCl, but some experiments were made with other phosphors in the group. The characteristics listed below seem to be common to the group:

(1) Phosphorescence is stimulated only in the region of the absorption bands B and C of Fig. 3, not by the long wave-length band A. The ratio of phosphorescent light (total light sum) to absorption in this region is roughly proportional to the concentration of Tl for brief illumination with light that is not too intense. Since the absorption itself, from Koch's work, is proportional to the concentration, it follows that the absorption leading to phosphorescence varies as the square of the concentration. In Bünger's measurements of efficiency, the Tl content of the melt is given. Assuming that the concentration in the crystal is 10 percent of this, the phosphorescent quantum efficiency turns out to be of the order of twenty times the mole fraction of Tl in the phosphor.

(2) The phosphorescent emission spectrum is identical with the fluorescent spectrum.

(3) The natural decay follows the same simple law as a radioactive disintegration:

$$dN/dt = -\alpha N,$$

where N is the number of quanta yet to be emitted, and α is a constant which varies[11] with temperature according to the relation

$$\alpha = se^{-\epsilon/(kT)}.$$

For KCl, s is 2.9×10^9 sec.$^{-1}$ and ϵ is 0.67 ev. The value of α is the same for all parts and peaks of the emission spectrum—the "color" does not change during decay.

(4) The release of the phosphorescent light can be accelerated, at a given temperature, by irradiating the crystal with additional light of suitable wave-length. The total yield is not altered by this process, and the stimulating light has no observed enduring effect, being influential only during the exposure. The effectiveness of the stimulating light varies with wave-length (Fig. 9); quanta with less energy than about 0.67 ev are not effective.

The quadratic dependence of the phosphorescent yield on Tl concentration shows that two Tl ions are involved in the phosphorescence process, and the most plausible assumption is that they lie in adjacent positive ion sites. If the Tl ions are randomly distributed among positive ion sites, the probability that another Tl ion will

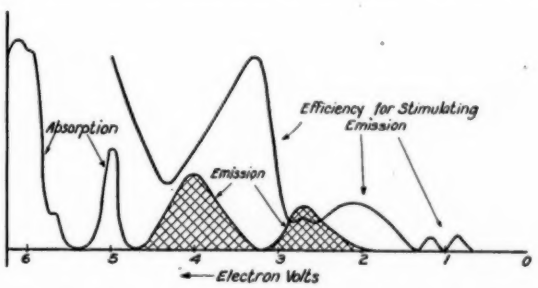

FIG. 9. Curves showing absorption and emission bands along with curve of relative efficiency for stimulating emission of phosphorescent light (after Bünger and Flechsig).

be beside a given one is 12 times the ratio of Tl to alkali metal ions. This is in fair agreement with the phosphorescent efficiency estimated from Bünger's data. The difference is in a direction

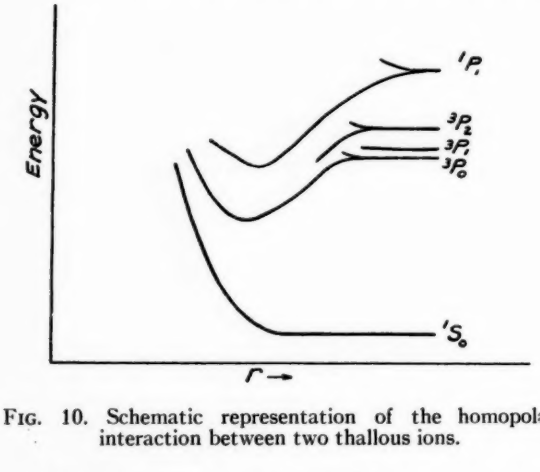

FIG. 10. Schematic representation of the homopolar interaction between two thallous ions.

which indicates that the probability of occurrence of pairs is somewhat higher than for a random distribution.

The presence of another Tl ion among the neighbors of a given one will alter the energy surfaces in the configuration space of the center. In particular, the homopolar interaction term of these two ions will be attractve in the excited state, as shown in Fig. 10, because of resonance phenomena. Fig. 10 is actually based on Finkelnburg's[31] diagram for the interaction of normal and excited mercury atoms, which have the same configuration as Tl^+ ions. There is no evidence which would lead one to conclude that the excited singlet level crosses the lowest level for a diatomic molecule of this type, and it is very unlikely that it does. This does not rule out the possibility that crossing will occur in the solid however. It must be remembered that the excited Tl^+ ion also has an attractive interaction with the neighboring halogen ions of the solid, and we shall assume that the total combination of attractive terms gives the center a metastable state in some region of configuration space. This region will undoubtedly be considerably different from that in which the minima of Fig. 8 occurred, of course, and probably corresponds to an arrangement in which the two Tl^+ ions have drawn closer together than in the normal arrangement.

In connection with these views, one should bear in mind the fact that nonpolar states are believed to be lower than ionic states in diatomic molecules of the type InCl, TlCl, AlH, etc., in contrast with alkali halide molecules. If this be true, the ionic state must "cross" the nonpolar state as one forms the crystal of TlCl adiabatically from molecules. It is not unreasonable to suppose that the metastable center of which we are speaking is analogous to the nonpolar state of the diatomic molecule.

We shall assume, in addition, that there is no great shift in the level for the normal configuration (*a* of Fig. 8), and that the minima in the lowest excited levels in Fig. 8 are preserved. Absorption in the band *A* of Fig. 3 will then have the same consequences for a center containing two Tl ions as for a center containing but one. That is, the same fluorescent spectrum will be produced, and there will be no phosphorescence.

When the center containing two Tl ions absorbs in the band *C* or *B*, however, there enters the possibility of trapping the electron in a metastable level, at the minimum of the singlet

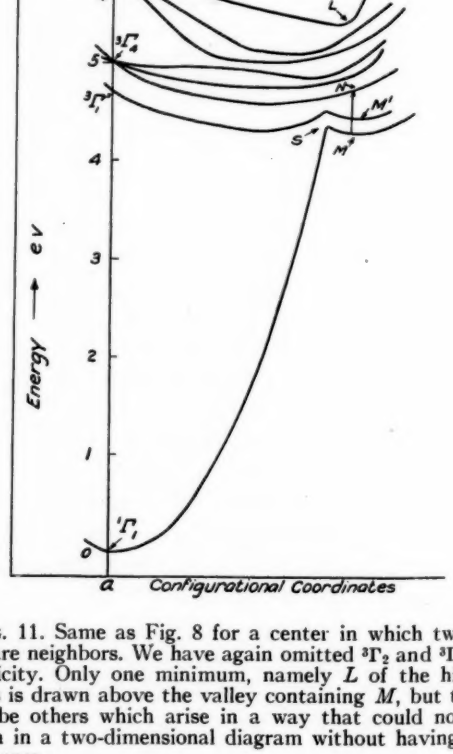

FIG. 11. Same as Fig. 8 for a center in which two Tl ions are neighbors. We have again omitted $^3\Gamma_2$ and $^3\Gamma_5$ for simplicity. Only one minimum, namely *L* of the higher states is drawn above the valley containing *M*, but there may be others which arise in a way that could not be drawn in a two-dimensional diagram without having the lines cross.

state which we have postulated as a characteristic property of these double-thallium centers. In some region of configuration space the three singlet levels will attempt to cut through the lower excited levels in some such way as is sketched in Fig. 11. Since the levels do not actually cross, the state $^1\Gamma_4$ of Fig. 9, which will be the state directly after absorption in $B-C$, does not lead directly into M, the metastable state. We assume, however, that some of the higher states have minima such as L which overlie the valley containing M, so that some of the excited centers, after shifting from I to L, may make a transition which finally places them at M. As there are three singlet levels, it does not seem unreasonable to suppose that the state immediately overlying M, which connects with $^3\Gamma_1{}^0$, will be a singlet with a minimum M'.

These centers which arrive in the state M must now wait for some activation process before they can return to the equilibrium configuration a. The activation energy may be furnished either by thermal fluctuations or by optical radiation. In the former case there are two possibilities:

(a) The system may pass adiabatically over the saddle point S and reach a without emission of an optical quantum.

(b) There may be electronic excitation to a state such as N, after which the system runs downhill to I of Fig. 8, and proceeds to the ground state with the emission of the same spectrum as in fluorescence. We assume, as stated above, that the system will not pass adiabatically from M' to II of Fig. 8 before jumping to M, because M' is a relative minimum. Thus, the system will return to M after excitation to the second level.

We wish to compare the relative probabilities of the two processes (a) and (b). The rates will be given by expressions of the type $A_a e^{-(\epsilon_a)/(kT)}$ and $A_b e^{-(\epsilon_b)/(kT)}$, respectively, where A_a and A_b are practically independent of temperature. The activation energy ϵ_a, equal to the energy difference between M and the saddle point S, will obviously be appreciably less than ϵ_b, the energy difference between M and N. However, the coefficient A_a may be expected to be much smaller than A_b. This expectation follows in part from the theory of reaction rates developed by Pelzer and Wigner[32] and Eyring;[33] the system, even when it has sufficient energy to reach the saddle point S, will have a small probability of finding this point out of a large region in a multidimensional space. Hence, we shall assume that at ordinary temperatures the electronic excitation is much more probable. This implies that the activation energy of 0.67 ev found by Bünger and Flechsig is the energy gap between M and N. At low temperatures, where the exponential factor will dominate in determining the statistical probability, the two rates should be reversed in relative magnitude, and the quantum efficiency of phosphorescence should be less than at room temperature. This prediction would probably be hard to check, since the decay rate at low temperatures is so low.

Suppose the metastable centers are activated by optical absorption. The energy of the lowest frequency quantum that is effective should be

$$\epsilon_b = N - M,$$

and, in fact, from the data of Bünger and Flechsig, the energy associated with long wavelength limit of the light which accelerates decay agrees well with the activation energy of 0.67 ev deduced from the natural decay rate. The stimulating bands at higher energies (Fig. 9) correspond, on this view, to transitions from M to states above N.

V. General Remarks

Muto,[14] in discussing the behavior of phosphors, has recognized the part played in the absorption process by both the continuous and nearly discrete states, but has neglected to include the effect of atomic rearrangement after absorption. For this reason, he finds it necessary to assume that the metastable state involved in phosphorescence owes its life to ordinary atomic selection rules. This view seems scarcely plausible, for the phosphorescent light can remain trapped for hours or days, whereas, under the perturbing conditions that exist in solids, the emission time even for quadrupole radiation should not be longer than seconds.

It may be remarked that the exponential form of the decay curve for these phosphors is that characteristic of a monomolecular reaction. This is in agreement with the basic assumption of our

picture, that the absorption which produces fluorescence and phosphorescence does not result in dissociation or ionization. We should not expect any photoconductivity to accompany this absorption. On the other hand, many phosphors have a decay curve of the type

$$(1/\sqrt{I}) \sim at+b,$$

where I is the intensity, a and b are constants, and t is the time. It has been pointed out elsewhere[34] that such a decay rate, characteristic of a bimolecular reaction, can be explained on the basis of a recombination of dissociated electrons and holes. Absorption resulting in phosphorescence having this sort of decay should, therefore, give rise to photoconductivity. The experimental data on photoconductivity of phosphors are too meager to allow a test of this prediction.

In addition to the thallium-activated alkali halides, halides activated with Hg, Cu, and Pb have been investigated to some extent by the Göttingen school. So far as can be judged from the less complete data presented for these phosphors, their behavior will also fit into a picture of the general type outlined here.

In conclusion I wish to express my indebtedness to Dr. S. Dushman, Mr. C. G. Found, and, especially, to Dr. R. P. Johnson for many helpful discussions and suggestions during the course of preparation of this paper. In addition I wish to thank Dr. Mulliken, who refereed this paper, for a number of comments and suggestions (cf. reference 28).

References

1. A general survey of results may be found in the following books and periodicals: Lenard and Tomaschek, *Handbuch der Exp. Physik*, Vol. 13, 1 and 2 (1928). Pringsheim, *Fluoreszenz und Phosphorenzens* (Berlin, 1928). Riehl, Ann. d. Physik. **29**, 637 (1937). Zener, J. Frank. Inst. To appear shortly.
2. Hilsch, Zeits. f. Physik **44**, 860 (1927).
3. Smakula, Zeits. f. Physik **45**, 1 (1927).
4. Lorenz, Zeits. f. Physik **46**, 558 (1928).
5. Hilsch and Pohl, Zeits. f. Physik **48**, 384 (1928); **57**, 145 (1929); **59**, 812 (1930).
6. MacMahon, Zeits. f. Physik **52**, 336 (1928).
7. Koch and Pohl, Nachr. Gott. (1929).
8. Fórro, Zeits. f. Physik **56**, 235 (1929); **56**, 534 (1929); **58**, 613 (1930).
9. Koch, Zeits. f. Physik **57**, 638 (1929); **59**, 378 (1930).
10. Von Meyeren, Zeits. f. Physik **61**, 321 (1930).
11. Bünger, Zeits. f. Physik **66**, 311 (1930).
12. Bünger and Flechsig, Zeits. f. Physik **67**, 42 (1931); **69**, 637 (1932).
13. Hilsch, Proc. Phys. Soc. **49**, 40 (1937).
14. Muto, Sci. Pap. Inst. Phys. and Chem. Research (Tokyo), **28**, 171 (1935); **32**, 5 (1937).
15. Hilsch (reference 13) has presented good evidence to show that most of the silver atoms in phosphors, obtained by dissolving AgI in alkali iodides, are not dispersed but are concentrated in clumps of AgI.
16. Schneider and O'Bryan, Phys. Rev. **51**, 293 (1937).
17. Von Hippel, Zeits. f. Physik **101**, 680 (1936).
18. Details of the zone treatment have been worked out by Shockley, Phys. Rev. **50**, 754 (1936) and by Ewing and Seitz, Phys. Rev. **50**, 760 (1936). This type of work gives a satisfactory discussion of the continuous bands of levels for the undistorted lattice, but lacks any trace of the discrete levels.
19. Frenkel, Phys. Rev. **37**, 17 (1931); **37**, 1276 (1931); Physik. Zeits. Sowjetunion **9**, 158 (1936).
20. Peierls, Ann. d. Physik **13**, 905 (1932).
21. Slater and Shockley, Phys. Rev. **50**, 105 (1936).
22. Wannier, Phys. Rev. **52**, 191 (1937).
23. Bethe, Zeits. f. Physik **57**, 815 (1930).
24. We have remarked in connection with Fig. 2b, that the resulting configuration is effectively p^5s while that for 2a is p^6. This analogy to atomic states should apply beyond this point and allow us to say that the configuration 2b will lead to a singlet and a triplet multiplet when spin-orbit action is taken into account. The levels are ^1P and $^3P_0$, $^3P_1$, $^3P_2$ in the free atom, this being the order of decreasing energies. The $^3P_2$ will split into a doublet in the crystal, and we should have five levels in all. By analogy with the rare gases, we may conclude that the positions of these will be determined by rather advanced j–j coupling, so that the five levels tend to form two groups which are separated by the distance between the $j=\frac{1}{2}$ and $j=\frac{3}{2}$ levels of the halogen atom doublet. Only these two peaks appear in the high temperature absorption bands of the halides, as Hilsch and Pohl have pointed out, but the low temperature results show additional structure.
25. See "Report of Conference on the Conduction of Electricity in Solids (Bristol 1937)," Proc. Phys. Soc. **49**, 3 (1937).
26. Bacher and Goudsmit, p. 481. The experimental work is by Smith, Phys. Rev. **35**, 235 (1930).
27. Van Vleck, *The Theory of Electric and Magnetic Susceptibilities* (Oxford Press); Penney and Schlapp, Phys. Rev. **41**, 194 (1932); et. seq.
28. Professor Mulliken who refereed this paper has suggested that the thallium ion in the crystal has strong j–j coupling. This assumption is sufficient to account for the closeness of the singlet and higher triplet levels in Fig. 4. Moreover, one may say, on the basis of this assumption, that $^3\Gamma_4^0$ and $^3\Gamma_1^0$ are practically coincident because the corresponding triplet levels are nearly coincident in strong j–j coupling. This assumption is consistent with all of the experimental results and stands as a good alternative to the scheme suggested above. It is also possible that both processes occur together.
29. Bethe, Ann. d. Physik **3**, 133 (1929).
30. Jahn and Teller, Proc. Roy. Soc. **161**, 220 (1937).
31. Finkelnburg, Physik. Zeits. **34**, 529 (1933). The curves referred to are based on the accumulated evidence of a number of workers.
32. Pelzer and Wigner, Zeits. f. physik. Chemie **B15**, 445 (1932).
33. Eyring, Chem. Rev. **17**, 65 (1935). (Survey)
34. Seitz and Johnson, J. App. Phys. **8**, 246 (1937).

Solvent Action on Optical Rotatory Power.

II. The Quadrupole Field of the CS_2 Type Molecule*

KARL COHEN AND CHARLES O. BECKMANN
Department of Chemistry, Columbia University, New York City

(Received December 18, 1937)

The applications of the general expression for the vectorial solvent field in organic liquids are further extended by detailed consideration of quadrupole molecules of the types CS_2. The results of the computation are found satisfying from a theoretical standpoint. The experimental control is undertaken with the aid of a previously developed theory of optical rotatory power in solution. The results are found to be in accord with the existing data.

§1.

IT WAS shown in a previous paper[1] that the average electrostatic field exerted on one molecule (designated as an α-molecule) by a small concentration of other molecules (γ-molecules) in a solution of nonpolar β-molecules, or in a mixed gas of α-, β-, and γ-molecules is given by the expression

$$[F_{(\gamma)\delta}]_{Av}{}^2=\frac{n_\gamma}{8\pi^2}\int \vartheta^{E_{\alpha\gamma}} F_{(\gamma)\delta}\, d\omega_\gamma,$$

where n_γ is the number of γ-molecules per cc, $E_{\alpha\gamma}$ is the interaction energy of one α-molecule and one γ-molecule, $F_{(\gamma)\delta}$ is the δ-component ($\delta=1, 2, 3$ corresponding to three Cartesian coordinates in the chosen α-molecule) of the field of a γ-molecule at the center of the α-molecule and $d\omega_\gamma$ is the differential element of the 6-space of relative coordinates of the two molecules.

Integrating under the assumptions (i) that both molecules are uniformly polarizable spheres with dipoles at the center, (ii) that the effective radii of the spheres are such that $kT>5E_{\alpha\gamma}$, and (iii) that the γ-molecules act independently of one another[3] gave the result

$$[F_{(\gamma)\delta}]_{Av}=\frac{2\mu_\alpha}{d_{\alpha\gamma}{}^3}\cdot\frac{4\pi}{3}n_\gamma\left[C+\frac{\mu_\gamma{}^2}{3kT}\right](3\delta)$$

$$=\frac{2\mu_\alpha}{d_{\alpha\gamma}{}^3}\cdot\frac{n_\gamma}{N}P_\gamma(3\delta), \quad (1)$$

where μ_α (parallel to the 3 axis) and μ_γ are the dipole moments of the α- and γ-molecules, respectively, C is the optical polarizability of the γ-molecule, $d_{\alpha\gamma}$ is the minimum distance of approach of the two molecules, N is Avogadro's number, P_γ the molar polarization of γ and (3δ) is the "conversion operator" denoting zero when 3 and δ are different and unity when they are the same. On the further assumptions that the α- and β-molecules also satisfy assumptions (i), (ii), and (iii)[3] and that $d_{\alpha\alpha}=d_{\alpha\beta}=d_{\alpha\gamma}=d$, it was found that

$$[F_\delta]_{Av}=[F_{(\alpha)\delta}]_{Av}+[F_{(\beta)\delta}]_{Av}+[F_{(\gamma)\delta}]_{Av}$$
$$=(2\mu_\alpha/d^3)\cdot[(\epsilon-1)/(\epsilon+2)](3\delta), \quad (2)$$

where ϵ is the dielectric constant of the medium.

This expression is almost identical with that obtained by assuming the solvent to be a continuous medium, namely

$$[F_\delta]_{Av}=(2\mu_\alpha/d^3)\cdot[(\epsilon-1)/(2\epsilon+1)](3\delta). \quad (3)$$

It was pointed out that without assumption (i), this coincidence of form of the equations (2) and (3) would not exist, and that, in general, Eqs. (2) and *a forteriori* (3) are incorrect. On these grounds, it is clear why classifications of solvent action in terms of the macroscopic quantity ϵ are not possible.

In addition to showing at once the necessary limitations of the continuous medium theory and the justification of it within these limitations, this development makes possible the treatment of those classes of molecules for which the continuous medium theory must necessarily—and has empirically—failed.

This paper concerns itself with the evaluation of $[F_{(\gamma)\delta}]_{Av}$ for solvent molecules of one such

* Publication assisted by the Ernest Kempton Adams Fund for Physical Research of Columbia University.

[1] C. O. Beckmann and K. Cohen, J. Chem. Phys. **4**, 784 (1936).

[2] $F_{(\beta)\delta}$ in the notation of the previous paper.

[3] These assumptions are unnecessarily restrictive (see reference 1) but no greater generality is required for the present purely illustrative purposes.

class; namely, those molecules with a quadrupole of the CS_2-type (CO_2, CSe_2, C_2N_2). Such compounds, as we can see from the data on CS_2, are strongly polar but have a zero dipole moment. CS_2 is of particular interest.

§2.

We assume the linear CS_2 molecule to be of such a shape that the surface of nearest approach of the center of a spherical α-molecule is an ellipsoid of revolution with semi-minor axis b and semi-major axis a (Fig. 1). The dipole of one C→S link, $\mathfrak{y}_\gamma$, is supposed localized at a point Q whose position vector is $\mathbf{q}$ with center of coordinates at the center of the molecule. Correspondingly, the other dipole is located at $-\mathbf{q}$ and can be denoted by $-\mathfrak{y}_\gamma$. The dipole moment of the α-molecule, $\mathfrak{y}_\alpha$, is localized at the center of a spherical molecule. Both the α- and the γ-molecules are considered isotropic with optical polarizabilities A and C, respectively. The external field extending over a molecule is, as before, assumed to be homogeneous.

The equation of the ellipsoid in polar coordinates referred to the center of the carbon atom as origin, with $\mathbf{q}$ taken as the prime directrix is

$$r=b/(1+e^2\cos^2\theta_1)^{\frac{1}{2}},\quad e^2=(a^2-b^2)/a^2.$$

One system of axes ($\mathbf{i}$, $\mathbf{j}$, $\mathbf{k}$) is taken fixed in the CS_2 molecule such that $\mathbf{q}=q\mathbf{k}$ and the other ($\mathbf{i}'$, $\mathbf{j}'$, $\mathbf{k}'$) fixed in the α-molecule such that $\mathfrak{y}_\alpha=\mu_\alpha\mathbf{k}'$. The position of the α-molecule with respect to the center of the γ-molecule is given by the polar coordinates r, θ_1, ϕ_1 and the orientation of μ_α is given by the Eulerian coordinates θ_2, ϕ_2, ψ_2 all taken in the conventional manner.[4]

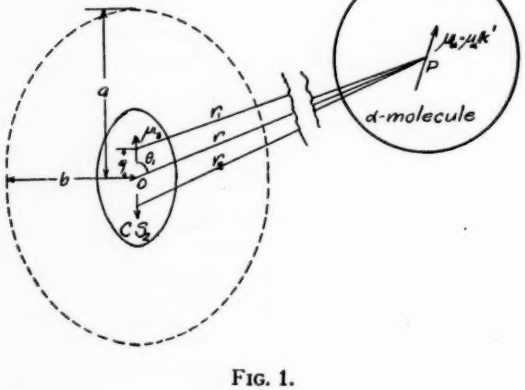

FIG. 1.

Let $\mathbf{r}_1$ be the radius vector from the dipole at $\mathbf{q}$ to the center of the α-molecule P, $\mathbf{r}_2$ the radius vector from the dipole at $-\mathbf{q}$ to P and $\mathbf{r}$ the radius vector from the center of the CS_2 molecule to P. Then $\mathbf{r}_1$ and $\mathbf{r}_2$ are given in terms of $\mathbf{r}$ and $\mathbf{q}$ by

$$\mathbf{r}_1=\mathbf{r}-\mathbf{q},\quad \mathbf{r}_2=\mathbf{r}+\mathbf{q}$$

or

$$r_1=r[1-2(q/r)\cos\theta_1+(q/r)^2]^{\frac{1}{2}},$$
$$r_2=r[1+2(q/r)\cos\theta_1+(q/r)^2]^{\frac{1}{2}}.$$

Since $q<r$ we may expand r_1 and r_2 in terms of q/r. Reciprocal powers of r_1 and r_2 may be expressed by

$$r_1^{-\nu}=r^{-\nu}\sum_{n=0}^{\infty}(q/r)^n C_n^{\nu/2}(\cos\theta_1),$$
$$r_2^{-\nu}=r^{-\nu}\sum_{n=0}^{\infty}(-q/r)^n C_n^{\nu/2}(\cos\theta_1), \tag{4}$$

where $C_n^{\nu/2}(\cos\theta_1)$ are Gegenbauer functions.[5] The two used here may be calculated from the Legendre polynomials by the relations

$$C_{n-1}^{3/2}(z)=(d/dz)P_n(z)$$

and

$$C_{n-2}^{5/2}(z)=\tfrac{1}{3}(d^2/dz^2)P_n(z).$$

The field of the CS_2 molecule is given by

$$\mathbf{F}_\gamma=-\frac{\mathbf{p}_\gamma}{r^3}+\frac{3\mathbf{r}(\mathbf{r}\cdot\mathbf{p}_\gamma)}{r^5}-\frac{\mathfrak{y}_\gamma}{r_1^3}+\frac{3\mathbf{r}_1(\mathbf{r}_1\cdot\mathfrak{y}_\gamma)}{r_1^5}+\frac{\mathfrak{y}_\gamma}{r_2^3}-\frac{3\mathbf{r}_2(\mathbf{r}_2\cdot\mathfrak{y}_\gamma)}{r_2^5}. \tag{5}$$

Substituting the values of r_1 and r_2 from (4), expanding and retaining terms of the order $(1/r^3)(q/r)^2$ we obtain

$$\mathbf{F}_\gamma=-\frac{\mathbf{p}_\gamma}{r^3}+\frac{3\mathbf{r}(\mathbf{r}\cdot\mathbf{p}_\gamma)}{r^5}-\frac{12}{r^4}q\mathfrak{y}_\gamma\cos\theta_1+\frac{6\mathbf{r}\mu_\gamma q}{r^5}(5\cos^2\theta_1-1). \tag{6}$$

[4] This assignment of coordinates is opposite to that used in the first paper, in which the center of the α-molecule was the main reference point. The subsequent integrations make it obvious that for the present problem the above choice is more convenient.

[5] E. T. Whittaker and G. N. Watson, *Modern Analysis* (Cambridge University Press, 1935), p. 329.

The field of the α-molecule is given by

$$\mathbf{F}_\alpha = -\frac{\mathbf{p}_\alpha}{r^3}+\frac{3\mathbf{r}(\mathbf{r}\cdot\mathbf{p}_\alpha)}{r^5}-\frac{\mathfrak{y}_\alpha}{r^3}+\frac{3\mathbf{r}(\mathbf{r}\cdot\mathfrak{y}_\alpha)}{r^5}. \quad (7)$$

The polarizations $\mathbf{p}_\alpha$ and $\mathbf{p}_\gamma$ may be expressed in terms of the polarizabilities A and C by

$$\mathbf{p}_\alpha = A\mathbf{F}_\gamma \quad \mathbf{p}_\gamma = C\mathbf{F}_\alpha.$$

With the approximations and the procedure given in the previous paper,[1] the interaction energy of the two molecules becomes

$$E_{\alpha\gamma} = (12/r^4)q\mathfrak{y}_\alpha\cdot\mathfrak{y}_\gamma\cos\theta_1 - (6\mu_\gamma q/r^5)\mathbf{r}\cdot\mathfrak{y}_\alpha(5\cos^2\theta_1-1). \quad (8)$$

Since $[F_{(\gamma)_\delta}]_{Av}$ has no components perpendicular to $\mathfrak{y}_\alpha$, and $F_{(\gamma)_3}=\mathbf{F}_\gamma\cdot\mathfrak{y}_\alpha/\mu_\alpha$ we have

$$[F_{(\gamma)_1}]_{Av}=[F_{(\gamma)_2}]_{Av}=0,$$

$$[F_{(\gamma)_3}]_{Av}=\frac{n_\gamma}{4\pi}\int e^{-E_{\alpha\gamma}/kT}\frac{\mathbf{F}_\gamma\cdot\mathfrak{y}_\alpha}{\mu_\alpha}d\tau.$$

Approximating $\exp(-E_{\alpha\gamma}/kT)$ with $(1-E_{\alpha\gamma}/kT)$, substituting the value of $E_{\alpha\gamma}$ from (8) and evaluating $\mathbf{F}_\gamma\cdot\mathfrak{y}_\alpha$ from (6) yields for the average field of a γ-molecule

$$[F_{(\gamma)_3}]_{Av}=\frac{n_\gamma}{4\pi}\int\left[1+\frac{6\mu_\alpha\mu_\gamma q}{kTr^4}\times\{\cos\epsilon(5\cos^2\theta_1-1)-2\cos\theta_1\cos\theta_2\}\right]\times\left[\frac{C\mu_\alpha}{r^6}(1+3\cos^2\epsilon)+\frac{6\mu_\gamma q}{r^4}\{\cos\epsilon(5\cos^2\theta_1-1) -2\cos\theta_1\cos\theta_2\}\right]r^2drd\omega_1d\omega_2, \quad (9)$$

where

$$\cos\epsilon=\sin\theta_1\sin\theta_2\cos(\phi_1-\phi_2)+\cos\theta_1\cos\theta_2,$$
$$d\omega_1=\sin\theta_1d\theta_1d\phi_1 \quad \text{and} \quad d\omega_2=\sin\theta_2d\theta_2d\phi_2.$$

The limits of integration are given by the scheme

$$r\left|{}^{\infty}_{b(1-e^2\cos^2\theta_1)^{-\frac{1}{2}}}\right.\quad\theta_1\left|{}^{\pi}_{0}\right.\quad\phi_1\left|{}^{2\pi}_{0}\right.\quad\theta_2\left|{}^{\pi}_{0}\right.\quad\phi_2\left|{}^{2\pi}_{0}\right.\quad\psi_2\left|{}^{2\pi}_{0}\right..$$

It is easily shown that

$$\int d\omega_1d\omega_2\{\cos\epsilon(5\cos^2\theta_1-1)-2\cos\theta_1\cos\theta_2\}=0$$

and

$$\int d\omega_1d\omega_2\cos^2\epsilon\{\cos\epsilon(5\cos^2\theta_1-1) -2\cos\theta_1\cos\theta_2\}=0,$$

thus reducing (9) to

$$[F_{(\gamma)_3}]_{Av}=\frac{n_\gamma}{4\pi}\int d\omega_1d\omega_2\int r^2dr\left[\frac{C\mu_\alpha}{r^6}\{1+3\cos^2\epsilon\} +\frac{36\mu_\alpha\mu_\gamma{}^2q^2}{kTr^8}\{\cos\epsilon(5\cos^2\theta_1-1)-2\cos\theta_1\cos\theta_2\}^2\right].$$

In the next step, the integration over r between the limits $r=r_0=b(1-e^2\cos^2\theta_1)^{-\frac{1}{2}}$ and $r=\infty$ is carried out. Thus

$$[F_{(\gamma)_3}]_{Av}=\frac{n_\gamma}{4\pi}\left[\int\frac{C\mu_\alpha}{3b^3}(1-e^2\cos^2\theta_1)^{3/2} \times(1+3\cos^2\epsilon)d\omega_1d\omega_2+\int\frac{36\mu_\alpha\mu_\gamma{}^2q^2}{5kTb^5}(1-e^2\cos^2\theta_1)^{5/2} \times\{\cos\epsilon(5\cos^2\theta_1-1)-2\cos\theta_1\cos\theta_2\}^2d\omega_1d\omega_2\right].$$

Integrating with respect to ϕ_1, ϕ_2 and θ_2 we obtain, finally

$$[F_{(\gamma)_3}]_{Av}=\frac{2\mu_\alpha}{b^3}\cdot\frac{4\pi}{3}n_\gamma\left[\frac{H}{2}C+\frac{9}{5}\cdot J\cdot\frac{\mu_\gamma{}^2}{kT}\cdot\frac{q^2}{b^2}\right], \quad (10)$$

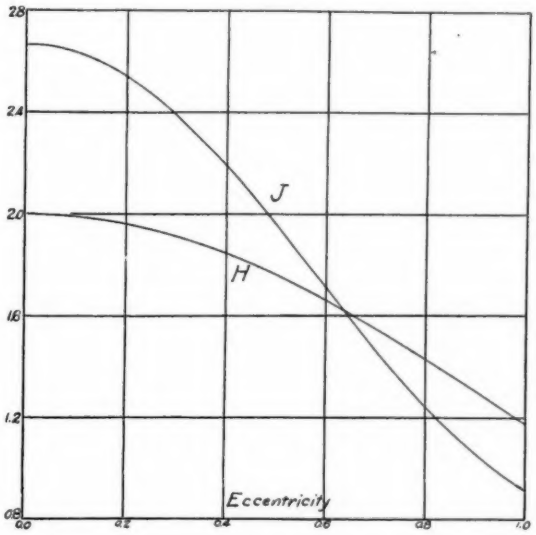

FIG. 2.

where

$$H \equiv \int_0^{\pi} (1-e^2\cos^2\theta_1)^{3/2} \sin\theta_1 d\theta_1,$$

$$J \equiv \int_0^{\pi} (1-e^2\cos^2\theta_1)^{5/2} \times (1-2\cos^2\theta_1+5\cos^4\theta_1)\sin\theta_1 d\theta_1. \quad (11)$$

These may be integrated[6] to give:

$$H = \tfrac{1}{4}(2s^3+3s+3\,e^{-1}\sin^{-1}e),$$

$$J = -s^7\left(\frac{3}{8e^4}+\frac{1}{2e^2}\right)+\left(s^5+\frac{5}{4}s^3+\frac{15}{8}s+\frac{15}{8}\frac{\sin^{-1}e}{e}\right)\left(\frac{1}{3}-\frac{1}{12e^2}+\frac{1}{16e^4}\right),$$

where $s=(1-e^2)^{\frac{1}{2}}$.

The first term in square brackets of Eq. (10) is the same as that of Eq. (1) multiplied into $H/2$. It is the contribution to $[F_{(\gamma)_\delta}]_{Av}$ of the polarizability of the CS_2 molecule. For $e=0$, $H/2=1$ and the two terms become identical. That is, the factor $H/2=H(e)/2$ is the contribution of the ellipticity of the solvent molecule. The ellipticity of the solvent molecules creates, therefore, only a trivial alteration in the form of the field equation. On this account we can understand why the assumption (i) (that the molecules concerned are spherical), used throughout our previous paper,[1] gave formulae in such good agreement with experiment.

The second term in square brackets of (10) is the contribution to the solvent field of the two oppositely directed dipoles of CS_2. It is this quadrupole which is responsible for the apparently anomalous behavior of CS_2.

For convenience the integrals H and J have been evaluated and plotted for various values of e between 0 and 1 (Fig. 2). J was evaluated for values of e between 0 and 0.1 by expansion in powers of e. This reduced J to the form

$$J = \frac{8}{3}-\frac{68}{21}e^2+\frac{37}{21}e^4-\frac{325}{1386}e^6+\cdots.$$

[6] The authors wish to thank Dr. Irving Kaplan, of these laboratories, for his collaboration in evaluating the integrals.

§3.

The variation of optical rotatory power with solvent, $n_\beta=0$, n_α/n_γ small, is given by the equation[1]

$$\Omega = \Omega_1+\Omega^3[F_{(\gamma)_3}]_{Av}, \quad (12)$$

where Ω, the rotivity of the solution, is defined as $[\alpha]/n^2+2$, Ω_1 is the rotivity in the absence of an electrostatic field and Ω^3 is the deformability coefficient. To facilitate a comparison with the data on dipole solvents, the coefficient $2\mu_\alpha/b^3$ is removed from the brackets and the expression (10) for $[F_{(\gamma)_3}]_{Av}$ substituted in (12) to give

$$\Omega = \Omega_1+\Omega^3\frac{2\mu_\alpha}{b^3}\left[n_\gamma\left\{\frac{2\pi}{3}CH+\frac{12\pi}{5}\frac{\mu_\gamma^2}{kT}\left(\frac{q}{b}\right)^2\cdot J\right\}\right]. \quad (13)$$

While the dipole term in Eq. (1) can be evaluated by an independent measurement, namely, that of dielectric constant, the quadrupole term in (10) and (13) cannot. Values of e, the eccentricity of the ellipsoid, and of q/b must be estimated from other data. Since, however, no method is available for localizing the dipole μ_γ, i.e. fixing the value of q, it was thought desirable to reverse the procedure and calculate q.

From the data on l-menthyl methyl naphthalate,[1] $\Omega-\Omega_1$ and $\Omega^3\cdot 2\mu_\alpha/b^3$ can be estimated and thus the expression in square brackets of Eq. (13) calculated. This is, in fact, the value (0.71) of the equivalent volume-polarization necessary to put the CS_2 point on the $M\Omega$ volume polarization curve.[7] The density of l-menthyl methyl naphthalate not being given by Rule,[8] its molecular volume was estimated as 378.0 cc from the molecular volumes of naphthalic acid, methyl alcohol, menthol and water. Assuming spherical molecules and closest packing the molecular radius was calculated to be 4.80A.

The size and shape of the CS_2 molecule were determined by the method of Magat[9] from the zero point volume of the liquid. This volume was obtained by extrapolating Timmerman's equation for the density of CS_2[10] to absolute zero. The volume of the molecule was calculated to be

[7] Reference 1, p. 796, Fig. 3.
[8] H. G. Rule, J. Chem. Soc. 669 (1931).
[9] M. Magat, Zeits. f. physik. Chemie **B16**, 1 (1932).
[10] Taken from J. W. Mellor, *Comprehensive Treatise on Inorganic Chemistry*, Vol. 6 (Longmans, Green and Co., London, 1925), p. 98.

55.55A^3 on the assumption of closely packed spheres. The radius of this sphere bears about the same relationship to radii calculated from gas viscosity and Sutherland's constant, from van der Waals' constant b and from Rankine's collision area that the corresponding radii for the CO_2 molecule[11] do to each other. The estimated volume of the CS_2 molecule can be looked upon, therefore, as being very probable. The internuclear C−S distance was taken from the recent data of Cross and Brockway[12] to be 1.54A and the effective radius of the C atom from the calculations of Magat to be 1.63A. From these data, the effective radius of the S atom was calculated to be 1.87A. This model of three overlapping spheres can be closely approximated by an ellipsoid of revolution with a semi-major axis of 3.41A and semi-minor axis of 1.97A.[13] The ellipsoid of closest approach is defined, therefore, by the axes $a=8.21$A and $b=6.77$A, corresponding to an eccentricity of $e=0.566$.

From Fig. 2 one can determine the values of the H and J integrals as 1.698 and 1.795, respectively. The polarizability, C, is taken as 87.6×10^{-25} from the compilation of data of Wolf and Fuchs[14] and μ_γ as 3.0 debyes from the estimate of Sidgwick.[15] With $k=1.37\times10^{-16}$ and $T=300°$K, q/b was calculated to be 0.116, giving a value of $q=0.78$A. Our calculated position of the dipole is therefore about halfway between the carbon and sulfur nuclei. The very close agreement between this value of q and one-half the C−S distance, namely 0.77, is to be regarded as fortuitous. Because of the many assumptions made to estimate the size of these molecules, any calculated value of q lying between 0.5 and 1.3A would be considered as satisfactory.

The successful treatment of this problem may be looked upon as confirmation of the correctness of the original method. The extension to other types of molecules is limited only by the difficulty in performing certain integrations etc. We note again, with surprise, the good agreement between theory and experiment. This was not foreseen, and its existence indicates the general validity—or perhaps unimportance—of our many auxiliary assumptions.

[11] H. A. Stuart, *Molekülstruktur* (Julius Springer, Berlin, 1934), p. 36, table 2.

[12] P. C. Cross and L. O. Brockway, J. Chem. Phys. **3**, 821 (1935).

[13] It must be recalled that the lower limit of integration of Eq. (9) is not the surface of the CS_2 molecule but the ellipsoid of revolution produced by the center of the spherical α-molecule when rolled over the CS_2 molecule. In this particular case, this ellipsoid differs but slightly from the figures produced by rolling the α-molecule either over the ellipsoidal CS_2 molecule or over the model of three overlapping spheres. Errors due to other approximations are much larger than those due to assuming these three figures equivalent.

[14] Article by K. L. Wolf and O. Fuchs in K. Freudenberg, *Stereochemie* (Franz Deuticke, Leipzig and Wien, 1933), p. 233, table 5.

[15] N. V. Sidgwick, *The Covalent Link in Chemistry* (Cornell University Press, 1933), p. 149.

LETTERS TO THE EDITOR

This section will accept reports of new work, provided these are terse and contain few figures, and especially few halftone cuts. The Editorial Board will not hold itself responsible for opinions expressed by the correspondents. Contributions to this section must reach the office of the Managing Editor not later than the 15th of the month preceding that of the issue in which the letter is to appear. No proof will be sent to the authors. The usual publication charge ($3.00 per page) will not be made and no reprints will be furnished free.

The Energy of Isomerization of Normal Pentane into Tetramethylmethane[1]

In 1935, one of the writers estimated[2] a value for the heat of combustion of gaseous tetramethylmethane by extrapolating the values, then newly obtained in the National Bureau of Standards thermochemical laboratory,[3] for the heats of combustion of methane, ethane (monomethylmethane), propane (dimethylmethane), and isobutane (trimethylmethane). Combination of this value with that for normal pentane yielded a value for the energy of isomerization of gaseous normal pentane into gaseous tetramethylmethane, corresponding to $\Delta H=\Delta E=-4.9\pm1.0$ kilocalories per mole at 25°C. New experimental measurements of the heat of combustion of tetramethylmethane have just been completed and it seems desirable to report the results here briefly, because of the immediate importance to science and industry of the energy content of this molecule. This importance ranges from consideration of the amount of hindrance to rotation of the methyl groups in the molecule to problems in the commercial production of 2,2,4-trimethylpentane, the standard "100 octane number" automotive fuel.

The new measurements have been made according to the regular procedure of this laboratory on a sample of tetramethylmethane kindly made available to us by Professor Frank C. Whitmore of The Pennsylvania State College. The synthesis and purifications were carried out by Mr. E. Rohrmann, and a "best" sample was obtained by fractional distillation by Dr. G. H. Messerly and Professor J. G. Aston. The new experimental value for the heat of combustion of tetramethylmethane, at 25°C and 1 atmosphere, is

$C(CH_3)_4(gas)+8O_2(gas)=5CO_2(gas)+6H_2O(liq.)$
$\Delta H=-3516.41\pm0.94$ NBS international kilojoules per mole.

Combining this value (which becomes 840.58 ± 0.23 kilocalories per mole, using the conventional factor[4] 1/4.1833) with the value previously reported for normal pentane,[3] one obtains for the energy of isomerization of normal pentane into tetramethylmethane, at 25°C,

$n-C_5H_{12}(gas)=C(CH_3)_4(gas)$
$\Delta H=\Delta E=-19.59\pm1.24$ kilojoules, or -4.68 ± 0.30 kilocalories, per mole.

The uncertainty in this energy of isomerization, as given by the earlier estimated value (see above), is thus reduced by over two-thirds. In view of the accord of the former estimated value with that obtained directly from the experimental data, the method of extrapolation used in obtaining the former estimated value appears to be a reliable one.

The new calorimetric measurements on the heat of combustion of tetramethylmethane will be described in detail in a forthcoming paper[5] which will also include new data on 2-methylbutane.

FREDERICK D. ROSSINI
JOHN W. KNOWLTON

National Bureau of Standards,
Washington, D. C.,
January 27, 1938.

[1] Publication approved by the Director of the National Bureau of Standards, United States Department of Commerce.
[2] F. D. Rossini, J. Chem. Phys. **3**, 438 (1935).
[3] F. D. Rossini, Nat. Bur. Stand. J. Research **6**, 37 (1931); **12**, 735 (1934).
[4] F. D. Rossini, Chem. Rev. **18**, 233 (1936).
[5] J. W. Knowlton and F. D. Rossini, Nat. Bur. Stand. J. Research. Forthcoming publication.

Note

In my recent paper[1] I failed to give reference to D. G. Bourgin, "Sound Absorption and Velocity in Mixtures,"[2] which has since come to my attention. With the change in this paper from his earlier f_{ij} symbol to the newer k_{ij}, a symbol exactly equivalent to my $(f_{ij}{}^{\sigma})_k$, Bourgin has eliminated an approximation made in his earlier papers as he explained in Appendix A. I wish to commend this last paper for its clarity and general organization as well as for its completeness.

HAROLD L. SAXTON

Department of Physics,
The Pennsylvania State College,
State College, Pennsylvania,
February 15, 1938.

[1] Saxton, J. Chem. Phys. **6**, 30 (1938).
[2] Bourgin, Phys. Rev. **50**, 355 (1936).

The Absorption Spectrum of Free Hydroxyl Calibrated for a Chemical Test

The absorption spectrum has served as a test for free hydroxyl in reacting gases.[1] It obviously serves as a *qualitative test;* it even serves as a *quantitative test in the relative sense* with the help of a certain comparison of intensities of rotational lines. In order to apply it as a *quantitative chemical test* in the *absolute sense* the intensity of the absorption spectrum must be calibrated against a known concentration of hydroxyl. Such a concentration is produced, according to Bonhoeffer and Reichardt,[2] by water vapor thermally dissociated.

The measurement of the absolute intensity of narrow absorption lines presents a difficult spectroscopic problem. This can be carried through by either one of two methods which differ in the background against which the absorption is observed—either a *continuous* or else a *sharp line* emission spectrum may be used as a background. The *continuous* spectrum as a background requires high resolving power of the spectrograph, because the whole contour of the narrow absorption line must be traced; this can be done only with the largest interference spectrographs. On the other hand, the *sharp line spectrum* as a background ("line absorption") requires only a medium size prism spectrograph because only the *total intensity* of a certain line—with and without the absorbing medium—is measured. Therefore "line absorption" is technically a great deal simpler to measure. However, the simplicity of this method is counterbalanced by a serious difficulty in that line absorption is obviously affected by the broadening of both lines—the emission line forming the background and the absorption line to be measured. The case of equal widths of both lines has been treated by Ladenburg and Reiche.[3] Obviously the case of unequal widths is much more complicated.

Avramenko and Kondratjew,[4] in a recent paper, applied an ingenious method to overcome this difficulty. Dealing with an absorption line at a pressure of 760 mm and an emission line at a pressure of 1.5 mm, they are sure of unequal widths of the two lines. On the basis of evidence obtained from atomic spectra they assume that for all pressures above 1 mm, Doppler broadening is negligible, that instead, the width is determined by "collision broadening" and that such a width is proportional to $p/(T)^{\frac{1}{2}}$. Therefore the calibration at $p=760$ mm and $T=1473°K$ can be applied for other values of p and T as long as this type of broadening prevails. Since they had no high dispersion spectrograph at their disposal they had no way of checking this fundamental assumption.

Unfortunately this method fails under the conditions of actual experiment. How wide the discrepancy is will be evident from the following comparison. Under the conditions of the discharge tube (1.5 mm, 300°K), the pressure broadening ought to be at least twice the Doppler broadening in order to make the theory applicable; that is, a pressure broadening of at least 0.02A. Consequently, in the furnace the pressure broadening as computed by the above relation would amount to at least 4.5A. The present authors had an occasion to measure the pressure broadening of OH under the same conditions and found only about 1/120 of this value; therefore Doppler broadening is not negligible but rather is of the same order of magnitude. Because of the smaller width of these lines the absorption effect is more concentrated, and, as a result, the formulae derived by Avramenko and Kondratjew for "weak absorption" are inapplicable for some of their measurements.

These are the reasons why the results of Avramenko and Kondratjew, obtained with "line absorption," differ widely from results obtained by the authors with absorption on a continuous background. The final result of Avramenko and Kondratjew is a probability of the transition $^2\Pi \rightarrow {}^2\Sigma$ in OH radicals of the same order of magnitude as the probability for the transition $^2P \rightarrow {}^2S$ in Na atoms; on the other hand, the continuous background leads to a figure smaller by a factor of about 1/1000, a surprisingly small value.

Nevertheless the measurements of Avramenko and Kondratjew are of great interest in another interpretation as follows: In their experiments a line from a low pressure discharge was absorbed by water vapor, thermally dissociated. The present authors, applying the high resolving power of Fabry-Pérot plates, have found that in the discharge the broadening is very small even with a current density of 10 amp./cm². Furthermore, with a 21-foot grating they observed for the furnace (at 1 atmos. and 1473°K) a line width of 0.06A (this includes Doppler broadening and pressure broadening); no shift of the line by pressure takes place. Hence one can consider the narrow emission line as a probe which hits just the center of the absorption line and so indicates the maximum of this line (independent of the width of the emission line as long as it remains narrow; this argument involves the assumption that the emission tube is not operated with too high a current density; the paper published gives only the figures 3000 v a.c., 1.5 kw). With our above value of the line-width, the total absorption is derived from a simple integral. This new interpretation of the measurements of Avramenko and Kondratjew leads to a probability of absorption agreeing rather well with our value mentioned above.

We shall publish our results and their application to the measurement of rate constants of certain hydroxyl reactions in more detail.

O. OLDENBERG

Research Laboratory of Physics,
Harvard University,
Cambridge, Massachusetts,

F. F. RIEKE

Department of Physics,
Johns Hopkins University,
Baltimore, Maryland,
February 7, 1938.

[1] O. Oldenberg, J. Chem. Phys. **2**, 713 (1934) and **3**, 266 (1935); A. A. Frost and O. Oldenberg, J. Chem. Phys. **4**, 642 and 781 (1936); V. Kondratjew and M. Ziskin, Acta Physicochimica U.S.S.R. **5**, 301 (1936) and **6**, 307 (1937).
[2] K. F. Bonhoeffer and H. Reichardt, Zeits. f. physik. Chemie **A139**, 75 (1928).
[3] R. Ladenburg and F. Reiche, Ann. d. Physik **42**, 181 (1913).
[4] L. Avramenko and V. Kondratjew, Acta Physicochim. U.S.S.R. **7**, 567 (1937).

Raman Effect in Liquid Ethylene

Because of inconsistencies in the reports of previous investigators (Table I) we have studied the Raman spectrum of liquid ethylene (−120°C). Ten Raman shifts have been measured. Nine of these have been recorded at one time or another in the literature. Our results include two lines found in the gas by Dickinson, Dillon, and Rasetti[1] which had not been checked by subsequent experimenters.[2, 3] Only six of the frequencies can be assigned to fundamental vibrations of the molecule.[3]

The new frequency 1601 cm^{-1} found by us is a faint companion to the strong Raman line 1621 cm^{-1} which has been attributed to parallel vibrations of the carbon atoms with relatively large displacements.[3, 4] The new line is apparently produced by this same type of vibration in those molecules which contain the C^{13} isotope.[5] Calculation checks roughly the separation observed, and the intensity ratio is appropriate.

TABLE I.

Liquid Ethylene			Ethylene Gas		
Glockler Renfrew[8] (1938)	Hemptinne Jungers Delfosse[6] (1937)	Bonner[3] (1936)	Daure[7] (1929)	Bhagavantam[2] (1936)	Dickinson Dillon Rasetti[1] (1929)
942		950			
1339	1341	1341	1340	1343	1342.4
1601					
1621	1621	1619	1620	1626	1623.3
1655		1654		1656	
2871		2880		2880	2880.0
3009	3007	3009	3000	3020	3019.3
3076	3082	3069	3080		
3231					3240.0
3264					3272.0

The weak 942 cm^{-1} line is very diffuse; also diffuse is the somewhat stronger line 3076 cm^{-1}. A faint "shadow" accompanies the strong 3009 cm^{-1} frequency; however, microphotometer tracings failed to show a separate line. All other lines are well defined, though in some cases they are very weak.

The 3-prism Steinheil spectrograph used in this laboratory gives a dispersion of 8A/mm at 4916A. Exposures of 12 hours brought out all lines. No filters were used. The strongest Raman frequencies were excited by Hg lines 4047, 4078, and 4358; the weak lines by 4047 and 4358, except for the Raman shift 1655 cm^{-1} which falls behind the Hg "triplet" when excited by 4047.

Ethylene (99.95 percent) manufactured for anaesthesia was used.

GEORGE GLOCKLER
M. M. RENFREW

University of Minnesota,
Minneapolis, Minnesota,
February, 1938.

[1] R. G. Dickinson, R. T. Dillon and F. Rasetti, Phys. Rev. **34**, 582 (1929).
[2] S. Bhagvantam, Nature **138**, 1096 (1936).
[3] L. G. Bonner, J. Am. Chem. Soc. **58**, 34 (1936).
[4] H. W. Thompson and J. W. Linnett, J. Chem. Soc. 1376 (1937).
[5] S. Bhagavantam, Proc. Ind. Acad. Sci. **2A**, 86 (1935).
[6] M. Hemptinne, J. C. Jungers and J. M. Delfosse, Nature **140**, 323 (1937).
[7] P. Daure, Ann. de physique **12**, 375 (1929).
[8] M. M. Renfrew, duPont Fellow (1937–38).

Abstracts* of Papers Presented Before Meeting of Section C—Chemistry American Association for the Advancement of Science

INDIANAPOLIS, INDIANA, DECEMBER 28–30, 1937

Symposium on the Application of Surface Chemistry to Biology

1. Overturning and Anchoring of Monolayers. IRVING LANGMUIR, *General Electric Company, Schenectady, N. Y.* (30 min.) Address of the retiring vice president of Section C of the A.A.A.S.—Monolayers of many substances spread on water can be deposited upon suitably prepared plates by a process of dipping. On the down trip an *A*-layer is deposited, which should be expected to have its hydrophilic side out. On the other hand, if the plate is immersed in clean water, a monolayer is spread on the surface, and the plate is withdrawn; a *B*-layer is deposited during the up trip, which should have its hydrophobic surface turned out. The method of formation of the *A*- and *B*-layers suggests that they should have very different properties, especially that the first should be wettable by water and the second not wettable. However, with most substances studied no appreciable differences of contact angle are observed. Similarly the chemical reactivity of the surface and many other properties fail to show striking differences, although slight differences are often observed. It appears therefore that many monolayers are able to turn over or to exchange their hydrophilic and hydrophobic parts when brought into contact with substances that have specific affinity for either of these groups. It is possible in many cases so to "condition" the surface of the prepared plate before depositing a monolayer that the latter is no longer able to overturn, and in this way monolayers from a single substance may be prepared having a wide range of properties, depending on the degree of anchoring of active groups by the underlying conditioned surface.

2. Some Aspects of Surface Chemistry Fundamental for Biology. WILLIAM D. HARKINS, *University of Chicago, Chicago, Ill.* (30 min.)—For the development of surface chemistry as fundamental for biology it is essential to devise simple apparatus which may be used by biologists to obtain accurate results. From this point of view there have recently been developed: (1) A simple and accurate film balance for the determination of the surface pressure-area relations of monolayers. (2) A slit viscosimeter for the determination of the viscosity of liquid monolayers of high fluidity. (3) Several surface ring viscosimeters for liquid and plastic solid films. Interesting and remarkable changes in viscosity occur in monolayers as the pressure or temperature is changed, and especially when an acid film is changed to a salt film. The two-dimensional solubility of a non-polar oil in a polar-non-polar monolayer is found to be highly dependent on the pressure. At low pressure a pentadecylic acid film will dissolve, for example 32 percent of a non-volatile non-polar oil. The relations of two-dimensional solubility give new information of value concerning the nature of expanded films. Films of acids are found to be highly compressed, and to have their compressibility greatly influenced by salt formation. In earlier work, which followed that of Clowes, it was found that the interfacial energy between an oil could be greatly influenced by uni- and bivalent metal ions. Thus the interfacial tension was reduced to about one twenty-thousandth its initial value by salt formation and the influence of salts. Salts, presumably by the effects of metal ions, are found to lower greatly the surface tension of soap solutions, and the effect increases with the valence of the ion. With paraffin ion soaps the effects of *p*H are very marked. The ion effect seems to be related to the absence or presence of micelles in the solution. The energy of a liquid edge is found to be about 2×10^{-6} erg per cm, which is very low, but nevertheless the existence of this energy greatly reduces the number of cells in the animal body which exhibit edges. The surface energy values for a number of solid liquid systems have recently been determined.

3. A Study of the Arrangement of Organic Molecules in Unimolecular and Multimolecular Layers. L. H. GERMER, *Bell Telephone Laboratories, New York, N. Y.* (30 min.)—As far as I am aware, the methods of electron diffraction have not been applied to any organic substance of immediate biological interest. We have, however, recently investigated by electron diffraction the arrangement of molecules in unimolecular layers of stearic acid and of barium stearate, and in multimolecular layers of the same substances. The results of these studies are of intrinsic interest and represent an advance toward fundamental understanding of the nature of "oiliness" and of boundary lubrication. Although applications to biology are not so obvious, it seems likely that similar experimental methods will ultimately be successful in determining the structures of some unimolecular biological films. The experiments consist of scattering electrons from unimolecular and from multimolecular

* Upon request, the American Institute of Physics preprinted these abstracts in the form of a program for distribution to those attending the meeting. In the hope and belief that this has been a useful service, the *Journal of Chemical Physics* is glad now to publish them for the further service of all interested in the scientific borderland to which this journal is dedicated.

layers deposited upon polished metal surfaces. Scattered electrons record diffraction patterns upon photographic plates; from these the arrangements of the molecules can be deduced. Barium stearate molecules form a hexagonal structure with the molecular axes normal to the surface upon which the molecules rest. In a film of several layers stearic acid molecules are arranged, on the other hand, with their axes inclined by 57° to the supporting surface, which is the monoclinic angle characteristic of the crystalline structure of alpha stearic acid. The most interesting part of the observations is the fact that, although a film of several layers of stearic acid gives diffraction patterns characteristic of the inclined molecules of the acid, a single layer of acid molecules produces a pattern which is entirely different; this pattern is like that produced by a single barium stearate layer. We believe this means that the molecules in a single layer of stearic acid combine at once with a metal surface to form stearate, but that subsequent layers placed on top of the first remain uncombined.

4. Interaction Between Built-up Films and Solutions of Physiologically Active Substances. HARRY SOBOTKA, *Mount Sinai Hospital, New York.* (30 min.)—Monomolecular layers may be situated at the boundary in any system consisting of two phases, the various possibilities to be briefly discussed. "Mono-layers" on a liquid-gas interface, i.e. monolayers spread on the surface of a liquid, have been successfully studied in recent years. Their properties, on the one hand their analogy to the behavior of three-dimensional aggregates, the common applicability of laws governing intermolecular forces, and on the other hand the special properties due to the dorsiventrally asymmetrical orientation in such films, form the fundament of what one may call two-dimensional chemistry. The study of mechanical and electrical properties as well as of the chemical reactions with substances dissolved in the liquid phase and of the incidental diffusion and penetration phenomena, harbors numerous preparative and microanalytical possibilities. The application of these principles has been essentially widened by Langmuir and Blodgett's studies of built-up films. The new technique of building films of a known number of monolayers on prepared slides opens new avenues for research in organic and biological chemistry. Reactions of built-up films submerged in fluids and solutions permit the study of interaction in systems like sterols with saponins, bile acids with lipids, enzymes with their substrates, and antigens with their antibodies. Many systems of biological importance include proteins. These may, in some instances, be built up from monolayers spread on water, or otherwise by adsorption from solution on heavy-metal conditioned slides, or, finally, by specific adsorption on slides with specific reaction partners. The knowledge gained from these experiments—by optical methods for the estimation of thickness, of contact angles, of diffusion and penetration, skeletonization and other typical operations—as to molecular dimensions, angles of orientation, structural features, other physical properties and chemical reactivity—can be interestingly correlated with facts established by x-ray spectroscopy, electron diffraction, ultracentrifugation etc. A new tool has been won for the elucidation of structure and reactivity of many classes of substances, especially in the field of immunology, enzymology and in the structural investigation of proteins and other megamolecules.

5. Surface Chemistry in Relation to Problems of Cell Division. G. H. A. CLOWES, *Eli Lilly and Co., Indianapolis, Indiana.* (30 min.)—The researches in surface chemistry carried out in the course of the last few years by Langmuir and Blodgett, Rideal, Adam, Sobotka, and others, particularly those dealing with the properties of films of fatty acids, proteins, and sterols, have been considered extensively in relation to the problem of the nature and mode of function of the external cell membrane which controls the passage of incoming foodstuffs and other chemical agents and outgoing waste products. There is a further application of the principles of surface chemistry to biology to which relatively little attention has so far been given, namely, the application of such principles to the study of effects produced by reagents which act inside the living cell. We propose to present data regarding the intracellular effects exerted by a series of nitro- and halophenols on cell respiration, cell division and ciliary motion. These substances affect respiration and cell division at extraordinary dilutions, which suggests that they react at one or more intracellular interfaces rather than in any homogeneous phase. These data will then be discussed with a view to ascertaining (a) how far surface effects are significant in bringing about the experimental results in question, and (b) to what extent the experiments on living cells are paralleled by experiments conducted with simple physical systems of the type used by Langmuir and his associates.

Symposium on Recent Advances in Chemical Physics

6. The Separation of Isotopes. HAROLD C. UREY, *Columbia University, New York.* (30 min.)—Early attempts to separate isotopes made use of the differences in the coefficients of diffusion of molecules of different molecular weights. These methods demonstrated that the mean atomic weights could be changed. The recent work of Hertz has developed an excellent cascade method for the concentration of isotopes by diffusion methods. It will produce high concentrations of rare isotopes, though the apparatus in its present state of development is limited to a rather small rate of transport of the order of magnitude of 1 cc of gas per 24 hours of operation in the case of such rare isotopes as the heavier ones of oxygen, nitrogen, and carbon. The distillation and chemical exchange reaction methods have been applied to the oxygen, hydrogen, nitrogen and carbon isotopes. Appreciable increases in concentration have been secured by these means, the total transports in these cases being approximately one hundred times those of

the Hertz method, but without the production of such high concentrations. Closely related to the distillation and chemical exchange reaction methods in which a liquid and a gaseous phase are used is the Lewis method using different solubilities of isotopes of the elements in two phases. This has been used to concentrate the rarer isotope of lithium. The Beams centrifugal method is an interesting and probably important competitor of these methods. A review will be given of the theory of these methods and their success to date.

7. Recent Investigations of Molecules and Condensed States with Deuterium. F. G. BRICKWEDDE, *National Bureau of Standards, Washington, D. C.* (30 min.)—The first investigations of the properties of condensed states using deuterium emphasized the importance of the zero-point lattice energy. More recent investigations are revealing the importance of the change in the intramolecular energy of molecules upon condensation. The first investigations of the spectra of simple compounds of deuterium showed that, except for small corrections, the binding forces of H and D atoms are the same. With this result, the vibrational and rotational spectra of polyatomic molecules are now being analyzed by investigating the change produced in these spectra by substituting D atoms for H atoms in the molecules. Thus deuterium is proving useful in the investigation of interatomic forces and structures of polyatomic molecules.

8. The Electron Diffraction Investigation of the Structure of Gas Molecules. J. Y. BEACH AND LINUS PAULING, *California Institute of Technology, Pasadena, Cal.* (30 min.)—The first electron diffraction investigation of the structure of gas molecules was that of the carbon tetrachloride molecule by Wierl in 1930. Wierl then applied the method to about forty molecules, and since then investigators in about half a dozen laboratories have reported the structures of roughly 200 molecules. The experiment consists essentially of having a well-defined monochromatic beam of electrons intersect a jet of the gas to be investigated. The scattered electrons are recorded on a photographic plate. The method of interpretation usually employed is the simplified visual method, first used by Wierl. Calculations of the complete electron scattering formula and correlations with experimental curves have been made. For three years after the method was first used there remained a discrepancy of about 4 percent between several interatomic distances determined in this way and those reported from x-ray diffraction by gas molecules, and doubt was thrown on the reliability of the electron diffraction results. It has been verified by several experimenters, however, that it is the x-ray values which were in error. The most fertile field of application of this technique is the investigation of the structures of molecules which are too heavy and too complex to be amenable to spectroscopic study. Many important questions of molecular structure have been answered. The planar structure for benzene and the tetrahedral character of the carbon atom have been verified. Other examples are the determinations of the linear structure of the azide group, the planar structure for formic acid dimer, and the identification of stereoisomers. From the structure determinations made by electron diffraction and other methods a large number of interatomic distances are known. It has been found that similar bonds in different compounds have constant interatomic distances. These results can be expressed by a table of covalent radii for the atoms involved. Deviations of observed interatomic distances in certain types of compounds from the value expected from adding radii are attributed to resonance of the molecule among several electronic structures.

9. Dipole Moments. CHARLES P. SMYTH, *Princeton University, Princeton, N. J.* (30 min.)—Halfway through the twenty-five years which have elapsed since Debye published his theory of molecular dipoles, approximate values of dipole moments calculated from dielectric constant measurements were used to determine molecular structures. Water and hydrogen sulfide were shown to be triangular molecules and ammonia pyramidal, while support was obtained for the theory of the tetrahedral carbon atom. While more extensive dielectric constant measurements and quantum mechanical calculations confirmed more definitely the correctness of the Debye theory, molecular beam experiments gave further confirmation through approximate moment values in agreement with those obtained from dielectric constants. The plane forms of the ethylene, benzene, and naphthalene molecules were determined as were other geometrical forms previously left in doubt by x-ray analysis but subsequently established by x-ray or electron diffraction measurements. Improved experimental technique led to more accurate moment values, which showed that the solvent might alter the apparent moment obtained in solution by more than 10 percent. As this solvent effect has been shown to depend largely upon induction between the molecules, it is evident that more exact knowledge of the structure of liquids and more precise moment measurements are necessary for its complete understanding. The phenomenon of resonance accounts largely for the difference in moment between corresponding alkyl and aryl compounds, the orienting effect of a single substituent on a benzene ring depending upon the sign of this difference. The moment values show in a semiquantitative fashion the existence of resonance in many molecules from the small carbon monoxide and nitrous oxide molecules to the large ethylene, acetylene and benzene derivatives. The recent exact determinations of atomic positions in molecules by electron diffraction measurements has made possible the calculation of new or more accurate values for the moments associated with the bonds between the atoms. These moments correspond closely to the differences in electronegativity of the atoms. The variation with temperature of the moments of molecules containing two polar groups capable of rotational oscillation has been used to study the mutual potential energies of the groups. Similarly, the variation with temperature of the dielectric constants of solids consisting of polar molecules is being used to determine the rotation or non-rotation of the molecules and to show the smallness of the difference between the molecular conditions in the liquid and in the high temperature solid states of some substances. The variation

with frequency of the dielectric constants of solutions is being used to determine the approximate weights of very large molecules.

10. Chemical Thermodynamics. MERLE RANDALL, *University of California, Berkeley, Cal.* (30 min.)—The rapid utilization of the data of chemical thermodynamics demands not only the maximum simplification and standardization of method but also a ready accessibility of correlated data, presented in such a way that its reliability can be estimated. The data of thermodynamics being the result of experimental measurements form a related mass of data, each measurement having some bearing upon the accuracy of all preceding measurements and conversely. It is quite necessary to analyze each set of experimental measurements in order to determine which values of the several fundamental constants were used in presenting the data, and it is often necessary to adjust the published values in order to combine them with other data. The importance of low temperature calorimetric data for assisting in the extrapolation of equilibrium measurements at high temperatures to low temperatures is stressed. Likewise the utilization of diffraction patterns, absorption, line and Raman spectra are discussed. Entropy, heat capacity, and the free energy based upon spectroscopic and diffraction data are peculiarly useful as they give values for the gases in their standard state.

11. Recent Development in Band Spectroscopy of Polyatomic Molecules. H. SPONER, *Duke University, Durham, N. C.* (30 min.)—The complexity of band spectra of polyatomic molecules makes their analysis extremely difficult. Yet, some progress is steadily made. Typical examples are the gradual clarification of the benzene spectrum and the increasing number of Rydberg series found in polyatomic spectra. Besides trying to analyze a spectrum completely, there are other methods of approaching an understanding of polyatomic spectra which confine themselves to less detailed results. They make use of more general features of the spectrum as its continuity or discontinuity, the spectral region, occurrence of predissociation, symmetry properties of the states and the molecules, electronic configurations and so on. The explanation of color of organic compounds belongs to this category. Another example is the interpretation of the continuous nature of the absorption spectra of tetrahalides. In a still more general way even the mere existence of band spectra of polyatomic molecules can serve for an understanding of chemical problems. It is known that many molecules show fluorescence spectra in solutions. It is discussed that this is possible in spite of the many collisions of the excited particles and why, furthermore, fluorescent substances are advantageous for the initiation of chemical reactions. Finally a few remarks are added about the importance of spectroscopic investigation of radicals.

12. Infrared Spectra in Chemistry. OLIVER R. WULF, *Bureau of Chemistry and Soils, Washington, D. C.* (30 min.)—An analysis of the infrared spectra of simple molecules leads to a knowledge of the molecular geometry and of the forces holding the atoms together. However, the number of molecules other than diatomic whose spectra have been successfully analyzed is small, being confined to a few of the simplest polyatomic molecules. Chemistry, however, is largely concerned with complex molecules. Moreover, to attempt the above-mentioned analysis the spectrum of the substance in the gas phase is required. But for the many complex molecules which cannot be obtained in the gas phase it is necessary to work with their spectra in the condensed phase. In this condition rotational spectral structure is obliterated, leaving only a more or less modified vibrational spectrum. Aside from some important considerations of rather narrow scope relating to the infrared spectra of crystals, this limits the measurements to the liquid phase. The strong influence of neighboring molecules combined with the desirability of observing absorption processes under as nearly constant environment as possible tends to restrict much of the material of chemical interest to solutions. The infrared spectrum of a complex molecule in solution frequently consists of rather sharp peaks of absorption which are found to be characteristic of the presence in the molecule of particular groups such as the NH_2, the CO, and the OH. The identification and quantitative estimation of such groups making use of such spectra aid in studying chemical constitution, equilibrium, and reaction. It is, moreover, observed that the absorption characteristic of a particular group is often altered by the structure of the rest of the molecule, especially by the character of adjacent groups. As a consequence infrared spectra also yield information regarding the structure of complex molecules. Molecular association, isomeric forms and hydrogen bonding have been among the subjects studied.

13. Recent Developments and Applications of the Raman Effect. JAMES H. HIBBEN, *Carnegie Institution of Washington, Washington, D. C.* (30 min.)—Raman spectra are physical manifestations which may be exactly measured. The reasons for their existence are now fully understood. These are intimately connected with interatomic forces in the molecule, atomic arrangement in space in the molecule, and certain rules—developed from the point of view of theoretical physics—which explain why under certain circumstances such lines should exist. From the physical standpoint both the existence of Raman lines and their non-existence are of importance, and consequently to this end this spectroscopic method has made no small contribution. However, in addition to contributing to purely theoretical advances Raman spectra have added greatly to the knowledge of chemistry and chemical physics. Without a reasonable knowledge of probable molecular structure neither physics as applied to chemistry nor chemistry itself can advance beyond an hypothetical basis.

The major contributions of Raman spectra investigations, apart from those which have a more or less purely physical significance, are those which have been devoted to a delineation of molecular constitution. Many other physical and chemical methods have been used to determine the structure of organic compounds, the constitution of liquids, and the behavior of pure substances and compounds in

different stages of aggregation. From the point of view of Raman spectra, however, many of these interpretations have been found to be inexact. On the other hand, many have been substantiated.

It is the purpose of this communication to outline some typical examples from organic and inorganic chemistry wherein Raman spectra have aided in the interpretation of physical behavior and chemical constitution. This has resulted in a better understanding of science as applied to chemistry, physics, geology and biochemistry.

14. Theoretical Considerations Concerning the Rates of Chemical Reactions. ALBERT SHERMAN, *University of Cincinnati, Cincinnati, Ohio.* (30 min.)—The determination of molecular structure is being actively pursued by a variety of experimental methods, including infra-red, Raman, and band spectra, electron diffraction, and dipole moment measurements. One of the most important reasons why the chemist is desirous of obtaining this information is that the chemical reactivity of atoms and molecules is dependent upon their structure. The nature of this dependence is brought out in the subsequent material. The limitations of the Arrhenius equation are discussed and semi-empirical attempts to modify the equation are considered. The application of quantum mechanics to the calculation of activation energies of chemical reactions is presented and the usefulness of such computations in the interpretation and prediction of experimental data is demonstrated by considering specific cases, some of which are the reactions of the halogens with the halogen derivatives of methane, the addition of the halogens to unsaturated hydrocarbons, the decomposition of some halogen derivatives of the hydrocarbons, the reaction of water vapor with some organic molecules, isotopic exchange reactions, and the rearrangement of ergosterol to calciferol.

Theoretical considerations, including both thermodynamical and statistical mechanical methods, of treating the absolute rate of chemical reactions by postulating an intermediate activated complex are set forth. Mathematical applications of the theory to numerous cases are considered, including isotopic exhange reactions, reactions between hydrogen and the halogens, and trimolecular reactions. The Arrhenius equation turns out to be a special case of a more general equation.

Contributed Papers

15. The Kinetics of Oxygen Exchange Reactions. MILDRED COHN AND HAROLD C. UREY, *Columbia University, New York, N. Y.*—The existence and the approximate rates of exchange reactions between oxygen in water and some typical organic compounds have been investigated with the use of water differing from ordinary water in isotopic composition of oxygen. The course of reaction was followed by measuring the change in isotopic composition of the water with a mass spectrometer. Several waters ranging from 0.080 percent to 0.950 percent O^{18} (normal concentration 0.200 percent O^{18}) were used. It was found that, in general, the oxygen of hydroxyl groups and carboxyl groups (except chloracetic acids) does not exchange, but the oxygen of the carbonyl group in both acetone and acetaldehyde does exchange with water, the latter more readily than the former. A detailed kinetic study of the reaction between acetone and water revealed that the reaction was catalyzed by hydrogen ions, hydroxyl ions, and salicylic acid molecules, but not by salicylate ions. The catalytic coefficients of the hydrogen ion and salicylic acid molecules for a bimolecular reaction between water and acetone in a 10 percent water-acetone medium, were 116.5 and 0.0683 $(m/l)^{-1}$ min.$^{-1}$, respectively. The difference between these rates and the rates of enolization of acetone shows that the exchange of the oxygen does not proceed through the enolic form, although it has been demonstrated that the exchange with hydrogen does. Furthermore, the rate of ionization of acetone cannot be slower than the rate of oxygen interchange.

16. Electromotive Force of Weston Normal Cells Containing Deuterium Oxide. GEORGE W. VINAL AND LANGHORNE H. BRICKWEDDE, *National Bureau of Standards, Washington, D. C.*—Saturated Weston normal cells in which D_2O is substituted for some or all of the H_2O may be expected to show a small difference in electromotive force from cells made with normal H_2O. In the hydration of the cadmium sulphate formed by the primary reaction and the removal from the saturated solution of the cadmium sulphate which must also be hydrated, the change in free energy accompanying this part of the reaction can be expected to depend on the D_2O content of the solution. Twelve cells alike in all respects except the isotopic content of the water were prepared. The electrolyte for all cells was 0.028 N acid. Four samples of water containing 0.018 (normal water), 1.036, 3.121 and 6.848 mole percent D_2O were saturated with $CdSO_4 \cdot 8/3H_2O$. The electromotive forces of the cells at 20°.00C are as follows:

D_2O Content of original sample mole percent	Electromotive force at 20°.00 International volts
Normal water	1.018272_1
1.036	1.018269_8
3.121	1.018266_5
6.848	1.018258_0

Each of the above results is the mean of values for 3 cells, which deviated individually from the mean of their respective groups by not more than 0.8 microvolt. The temperature coefficient between 20° and 28°C was found to be the same for all groups.

17. Experimental Determinations of Activation Energies in the Decomposition of Alkyl Halides. PRESTON VELTMAN AND FARRINGTON DANIELS, *University of Wisconsin.*—Extreme precautions are necessary in the experimental determination of activation energies. An example is given showing how the deposit left on the walls by the products of a reaction affect the rate of a second reaction carried out

in the same flask and could lead to very erroneous results in the calculation of the activation energy. An all-glass apparatus is described in which it is possible to follow the rates of decomposition of organic vapors at high temperatures in successive experiments. As many as sixteen successive experiments can be made in the same flask without admitting air or changing the character of the walls. Careful measurements have been made at different temperatures on the rate of thermal decomposition of ethyl bromide, propyl bromide and several alkyl bromides, chlorides, and iodides. The object has been to determine accurately the energies of activation and to compare them with values calculated from theoretical considerations. Only when accurate experimental values are available is it possible to evaluate critically the theoretical calculations of activation energies.

18. Absolute Reaction Rates from Statistical Mechanics; and the Entropy of Activation. ALLEN E. STEARN, *University of Missouri.*—The statistical mechanical method of Darwin and Fowler, as applied to absolute reaction rates by Eyring, has yielded calculated rate values in agreement with experiment for gaseous reactions even in the case of negative Arrhenius activation energy. With its aid it has also been possible to account theoretically for a steric factor of about 10^{-4} in a particular case studied. When thrown into the quasi-thermodynamic formulation of Eyring or of Evans and Polanyi the rate of a slow reaction in solution with a large negative activation energy was quantitatively accounted for by the large loss of entropy on activation. It has been thought worth while to attempt a rather comprehensive survey of the data on reaction rates from this point of view, in somewhat the same manner as that by Hinshelwood and by Moelwyn-Hughes from the point of view of classical collision theory. The latter theory has no place for reactions with negative temperature coefficients, and the energy factor bears the principal burden of rate determination. Entropy of activation is completely ignored though it is frequently a very important factor. It is hoped that the investigation will yield some inferential information, which may be formulated in at least empirical rules, regarding certain properties of the activated complex.

19. The Structures of the Hydrides of Boron. S. H. BAUER, *Pennsylvania State College, State College, Pa.*—The hydrides of boron have presented an interesting puzzle to chemists. Electron diffraction investigations of four hydrides and of several derivatives for the first time permitted the establishing of the configurations of these compounds. The structures and interatomic distances are tabulated below.

B_2H_6	ethane-like	B–B = 1.86±0.04	B–H = 1.27±0.03
B_4H_{10}	butane-like	1.84±0.04	1.28±0.03
B_5H_{11}	pentane or isopentane-like	1.81±0.03	1.26±0.03
B_5H_9	methyl cyclobutane-like (planar)	1.76±0.02	1.17±0.04
H_3BCO	as written, linear B–C–O	B–C = 1.57±0.03 C–O = 1.13±0.03	1.20±0.03
$H_3BN(CH_3)_3$	neopentane-like	B–N = 1.63±0.15 N–C = 1.53±0.06	
$B_3N_3H_6$	benzene-like	B–N = 1.44±0.02	
B_2NH_7	probably like dimethylamine	B–N = 1.56±0.03	1.20±?
Radius sum (extrapolated)		B–B = 1.78	B–H = 1.21
BH (spectroscopic)			1.226

Attention is called to the following interesting observations: (1) All the chain-like hydrides have internuclear separations greater than would be expected if the bonds were of the pure covalent type. (2) B_5H_9 differs markedly both with respect to its structure and interatomic distances from the above. If this is representative of the more stable hydrides, the observed chemical differences are evidently due to fundamental differences in structure. As a consequence of these studies, a set of statements were formulated which helps explain the constitution of the hydrides of boron. The importance of further study of these compounds both by diffraction and spectral technics is stressed.

20. The Application of Electrodialysis to the Study of Copper Fungicides. A. A. NIKITIN, *Research Dept., Tennessee Copper Company, Copperhill, Tenn.*—A study was made to correlate the chemical composition to the behavior of the copper compounds when used as fungicides. Electrodialysis methods as used in the study of soils were adapted to this purpose. From the character of a deposit, variation of current and temperature, certain deductions can be made concerning the behavior of the copper compounds for agricultural purposes. The rate of decomposition is related to the character and composition of the compound. This rate may be evaluated by observation of the change of *p*H in the cells, the time required for discoloration of the deposit and the change in the character of the dispersed phase. By the use of electrodialysis it is possible to determine the effect of various acid radicles on the chemical behavior. The degree of discoloration of the deposit on the diaphragm has been found to be indicative of the character and composition. Furthermore the adhesiveness and spreading properties of a fungicide can be, in most cases, estimated from the degree of adherence of the deposit to the diaphragm. It seems that electrodialysis helps to establish the facts which are of importance in understanding the action of copper fungicides.

21. The Effect of Hydroxyl Groups on the Apparent Diene Values of Vegetable Oils and Fats. W. G. BICKFORD, F. G. DOLLEAR, AND K. S. MARKLEY, *U. S. Regional Soybean Industrial Products Laboratory, Urbana, Illinois.*—The "Diene Synthesis" (addition of α, β-unsaturated carbonyl compounds to conjugate dienes) of Diels and Alder has been applied recently as a quantitative measure of the extent of conjugation present in fats. Two methods have been developed for this purpose; one by Kaufmann, Baltes, and Büter[1] and the other by Ellis and Jones.[2] Moreover, Kaufmann and co-workers have assumed that a diene value is a qualitative indication of the presence of conjugation in fats which are now not known to contain conjugate systems. Evidence is presented to show that the latter assumption may not be warranted especially in the presence of hydroxylated compounds. It has also been observed that the Ellis and Jones method is particularly susceptible to the influence of the hydroxyl group, although the method gives a correct value for diene in the absence of interfering compounds. Typical results obtained on fats and pure synthetic compounds are given below.

	Acetyl Value	Kaufmann D. NO.	Ellis MAV
Anthracene (calc'd diene = 142.5)		141.1	140.5
Castor oil	166	3.2	10.2
Acetylated castor oil		0.2	1.0
Soybean oil	6.7	0.8	1.8
α-monopalmitin		6.0	20.0
Methyl 12-hydroxystearate		3.8	25.0

[1] Berichte **70**, 903 (1937).
[2] Analyst **61**, 812 (1936).

22. The Influence of Particle Size in the Use of Colloidal Gold in Clinical Tests on Spinal Fluid. P. K. GLASOE AND C. H. SORUM, *University of Wisconsin, Madison, Wis.*—Extensive clinical tests carried out with samples of pathological spinal fluid obtained from the Wisconsin General Hospital, Madison, Wisconsin, have demonstrated that, to be suitable for use in the so-called "Lange" spinal fluid test gold sols must be made up of micelles of quite definite size and stability. If the particles are too small the resulting sol is too stable and does not give the proper precipitation range. If the particles are too large the sol precipitates too easily. A gold sol of optimum stability and particle size serves as a dependable tool for the diagnosis of a number of diseases, such as paresis, meningitis, syphilis and encephalitis, which produce a change in the composition of the spinal fluid. Gold sols of optimum particle size and stability can be prepared at room temperature by the reduction, with formaldehyde, of alkaline solutions of gold chloride to which gold nuclei have been added. The nuclear solutions are prepared by the reduction of alkaline solutions of gold chloride with resorcinol or with mixtures of resorcinol and formaldehyde. The size of the nuclei in these nuclear solutions varies with the concentration of resorcinol used, decreasing as the concentration increases The use of nuclear solutions eliminates, largely, the effect of slight variations in the purity of water used in the preparation of gold sols since it substitutes a large and definite number of nuclei for the variable number that foreign substances in the water may produce. Furthermore, it permits of the rapid preparation of good gold sols at room temperature. The influence of the size of the colloid particles in the utility of gold sols in the Lange test suggests that the mechanism of this test involves a proper balance between the protective agents and the precipitating agents, both present in pathological spinal fluid.

23. Equilibria in the Thyroid Protein Found by Ultracentrifugal Sedimentation. HAROLD P. LUNDGREN,* *Laboratory of Physical Chemistry, Upsala University.*—Thyroglobulin, the protein of the thyroid gland which is directly concerned with its hormonal activity, is being studied in the Svedberg ultracentrifuge. In concentrated solutions dialyzed electrolyte-free an equilibrium has been found to be slowly established with another component, α-thyroglobulin. The latter sediments more slowly than the original protein. The amount of α-thyroglobulin present at equilibrium is a function of the initial protein concentration and the electrolyte concentration. On dilution of the concentrated solution a new equilibrium is rapidly set up with a series of slower sedimenting components which like α-thyroglobulin disappear into the original protein on addition of sufficient electrolyte. Conditions have been found where thyroglobulin can be made to associate into a definite component having a sedimentation constant about 10× the original molecule which corresponds to a molecular weight of 17,000,000 as compared to 700,000 for normal thyroglobulin.

Studies were carried out on the effect of various small molecules on the dissociation of the protein. These were among the first experiments on this present popular subject at the Upsala Laboratory. Phenoles, glycine, tyrosine, and thyroxine were among those found to cause dissociation of thyroglobulin. The effect is specific.

References:
1. H. P. Lundgren, Nature **138**, 122 (1936).
2. H. P. Lundgren, Proceedings of the Scandinavian Scientific Society, Helsingfors, August 1936.

* Now associated with the Laboratory of Colloid Chemistry, University of Wisconsin.

24. Determination of Intermolecular Forces from Joule-Thomson Coefficients. J. O. HIRSCHFELDER, R. BARTLETT EWELL, AND J. R. ROEBUCK, *University of Wisconsin.*—The chemistry of solutions depends on molecular interactions. The simplest case of solutions occurs in the gas phase. Here the accurate experimental data of Roebuck and Osterberg on the Joule-Thomson coefficient provide an excellent source of information. The Joule-Thomson coefficient at zero pressure, μ_0, is related to the usual second virial coefficient, B, in the following manner:

$$\mu_0 = \frac{T^2}{R[R+C_v^0]}\frac{d}{dT}\left(\frac{B}{T^2}\right). \quad (1)$$

Here T is the absolute temperature, R is the gas constant, and C_v^0 is the specific heat for large constant volume. Statistical considerations show that

$$\mu_0[R+C_v^0] = -2\pi N\int^{\infty} r^2\left(1-e^{-E(r)/kT} + \frac{E(r)}{kT}e^{-E(r)/kT}\right)dr \equiv A, \quad (2)$$

where $E(r)$ is the energy of interaction of two molecules separated a distance r. Taking $E(r)$ in the functional form $E(r) = b/r^n - a/r^6$, the above expression for μ_0 is integrated with the aid of formulae obtained by Lennard-Jones in his analysis of the second virial coefficients. The constants a, b, and n are then determined by comparison with the experimental data of Roebuck and Osterberg. The variation of the Joule-Thomson coefficients with pressure involves the third and fourth virial coefficients in an important manner. For mixtures of gases, μ_0 should satisfy the relation

$$[R+N_1(C_v^0)_1+N_2(C_v^0)_2]\mu_0 = N_1^2A_1+N_2^2A_2+2N_1N_2A_{12}, \quad (3)$$

where N_1 and N_2 are the mole fractions of components 1 and 2; $(C_v^0)_1$ and $(C_v^0)_2$ are the specific heats for the corresponding pure components; and A_1, A_2, and A_{12} are integrals of interaction of two molecules of species 1 and 1, 2 and 2, and 1 and 2 corresponding to the A in formula (2). The experimental μ for mixtures of gases are being analyzed to determine the law of force between unlike molecules.

25. Partial Purification of a Vitamin-like Substance Which Stimulates Sexual Reproduction in Certain Fungi. V. G. LILLY AND L. H. LEONIAN, *Department of Plant Pathology & Forestry, West Virginia University.*—Leonian[1] found that peas contained a substance which induced sexually formed spores in many Oomycetes. The partial purification of this substance is now reported. Pea flour was extracted with 90 percent ethanol in a metal Soxhlet. The alcohol was removed from the crude extract which was then dissolved in peroxide-free ether and acetone added to precipitate phospholipoids. The acetone-ether solution contained the active substance. After removal of the solvent the extract was saponified by the method of Olcott and Mattill.[2] The nonsaponified material was extracted with peroxide-free ether, and the solvent removed. The preparation at this stage was a red oil which contained pigments, sterols, and the active substance. The sterols were largely removed by cooling a hot alcoholic solution of the material and filtering. At this point the active concentrate represented 0.4 percent of the original pea flour. The concentrate was then distilled at 0.1 mm, and the material boiling below 180°C was redistilled at 0.1 mm. The 110–135°C fraction was most active. This fraction was chromatographed on a column of activated alumina (Hydralo). Two bands formed; the upper was brown and the lower red. The column was sectioned and eluted with peroxide-free ether. The red band and the colorless region immediately below it contained most of the active material. Upon elution of the colorless region of the column a pale yellow viscous oily liquid was obtained; this exhibited maximum potency. The material at this stage of purification was insoluble in water but soluble in the common organic solvents. Long boiling with alkalies apparently did not affect the potency. The activity is partially destroyed in boiling with mineral acids. Benzoylation and acetylation reduced the potency. Bromine destroyed the activity. This material is not vitamin E as shown by animal experiments. Also the boiling point is too low.[3]

Potency was tested by dissolving a sample in a minimum amount of boiling ethanol and adding to 0.1 percent agar solution. The agar acted as a dispersing agent. Agar alone is without effect in inducing sexual reproduction in fungi. The most active preparation tested caused a response at a concentration of 0.1 gamma per milliliter. This substance is specific in its action on Oomycetes, but not all Oomycetes responded to it. Five species of *Pythium* out of twenty-three tested failed to respond whereas all species of *Phytophthoras* gave positive response. This substance was not found to be toxic for any Oomycetes tested. On the other hand no stimulating effect was found with any species of Zygomycetes, Ascomycetes, or Basidiomycetes tested, and in some cases it even proved toxic.

[1] Am. J. Bot. **3**, 188–190 (1936).
[2] J. Am. Chem. Soc. **58**, 1627–1630 (1936).
[3] Olcott and Mattill, J. Biol. Chem. **104**, 423–435 (1934).

AUTHOR INDEX

Bauer, S. H.—No. 19
Beach, J. Y. and Linus Pauling—No. 8
Bickford, W. G., F. G. Dollear and K. S. Markley—No. 21
Brickwedde, F. G.—No. 7
Brickwedde, Langhorne H.—see Vinal, George W.

Clowes, G. H. A.—No. 5
Cohn, Mildred and Harold C. Urey—No. 15

Daniels, Farrington—see Veltman, Preston
Dollear, F. G.—see Bickford, W. G.

Ewell, R. Bartlett—see Hirschfelder, J. O.

Germer, L. H.—No. 3
Glasoe, P. K. and C. H. Sorum—No. 22

Harkins, William D.—No. 2
Hibben, James H.—No. 13
Hirschfelder, J. O., R. Bartlett Ewell and J. R. Roebuck—No. 24

Langmuir, Irving—No. 1
Leonian, L. H.—see Lilly, V. G.
Lilly, V. G. and L. H. Leonian—No. 25
Lundgren, Harold P.—No. 23

Markley, K. S.—see Bickford, W. G.

Nikitin, A. A.—No. 20

Pauling, Linus—see Beach, J. Y.

Randall, Merle—No. 10
Roebuck, J. R.—see Hirschfelder, J. O.

Sherman, Albert—No. 14
Smyth, Charles P.—No. 9
Sobotka, Harry—No. 4
Sorum, C. H.—see Glasoe, P. K.
Sponer, H.—No. 11
Stearn, Allen E.—No. 18

Urey, Harold C.—see Cohn, Mildred
———No. 6

Veltman, Preston and Farrington Daniels—No. 17
Vinal, George W. and Langhorne H. Brickwedde—No. 16

Wulf, Oliver R.—No. 12